Collective excitations in nuclei: The isoscalar and isovector electric giant resonances and spin-isospin charge-exchange modes

Muhsin N. Harakeh

KVI-CART, University of Groningen, the Netherlands

XVI International Meeting on
"Selected Topics in Nuclear and Atomic Physics"
Fiera di Primiero, Italy
2-6 October 2017

Vibrations of a liquid drop in weightlessness

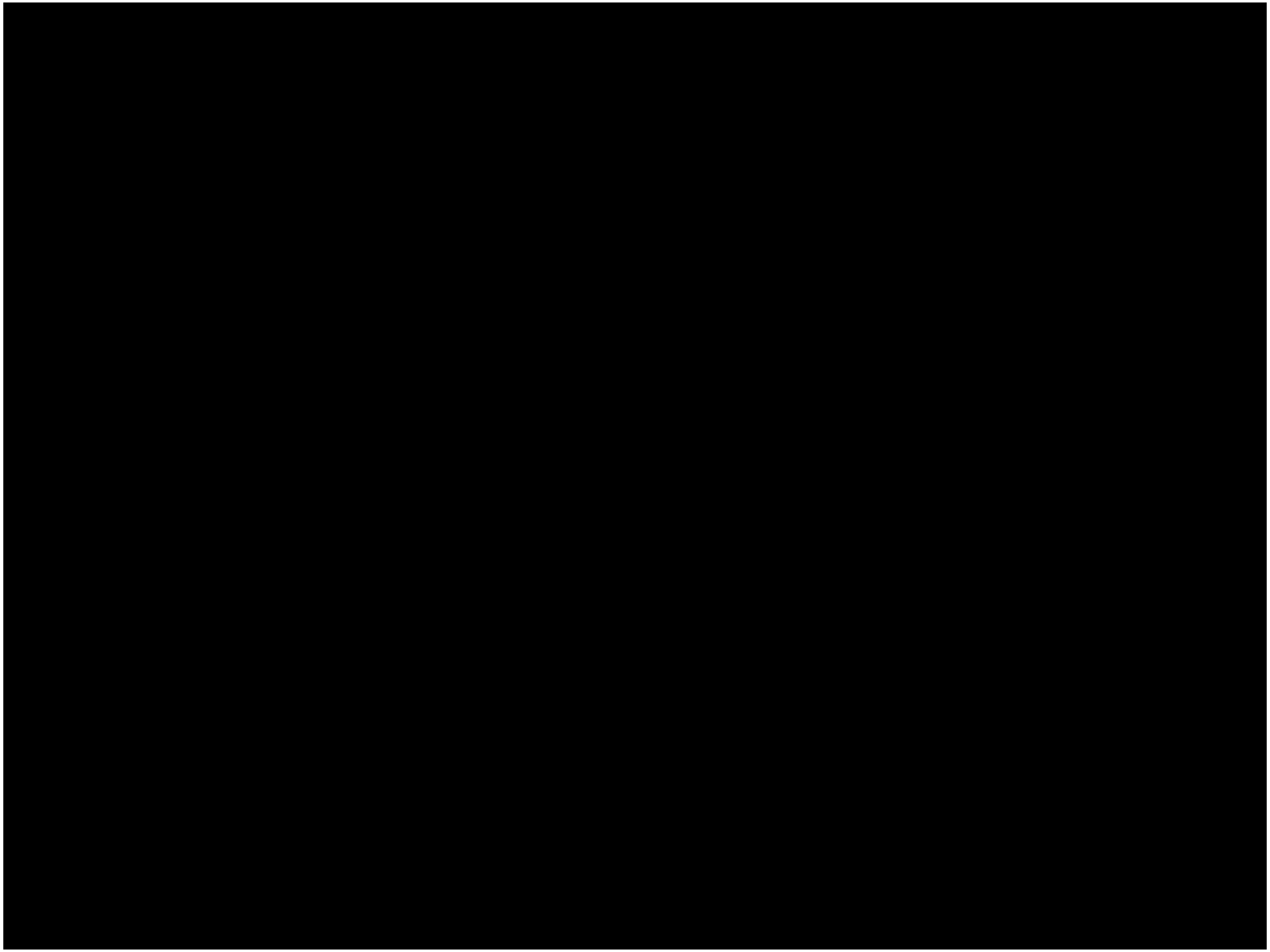

In the following:

IS = Iso-Scalar

IV = Iso-Vector

S = Spin

G = Giant

M = Monopole

D = Dipole

Q = Quadrupole

O = Octupole

e.g., ISGMR = Isoscalar giant monopole resonance

ISGDR = Isoscalar giant dipole resonance

IVGDR = Isovector giant dipole resonance

IVSGMR= Isovector spin giant monopole resonance

IVSGDR = Isovector spin giant dipole resonance

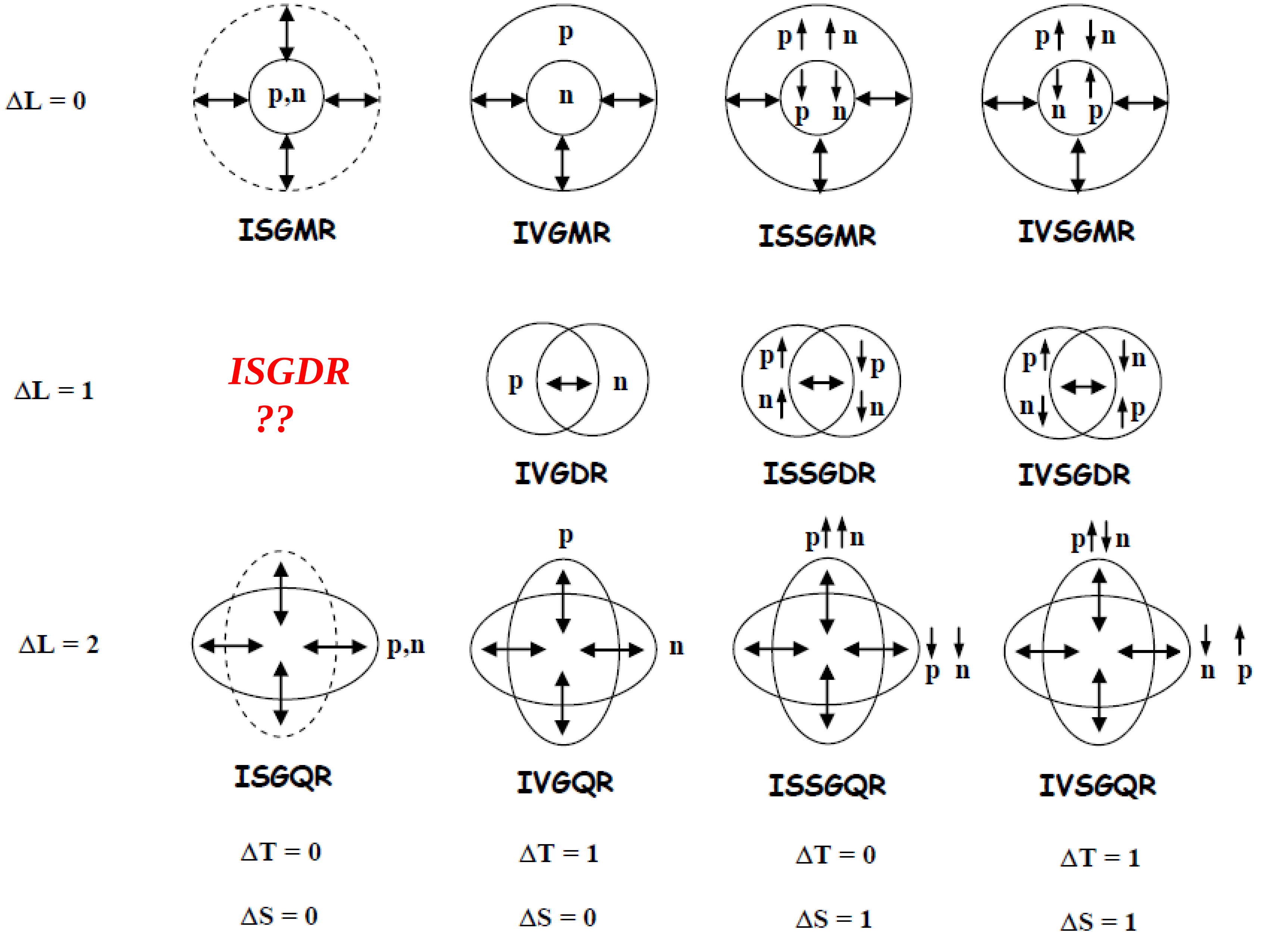
ΔL = 0
p,n
ISGMR
p
n
IVGMR
p n
p n
ISSGMR
p n
n p
IVSGMR
ΔL = 1
ISGDR
??
p
n
IVGDR
p
p
n
n
ISSGDR
p
n
n
p
IVSGDR
ΔL = 2
p,n
ISGQR
p
n
IVGQR
p n
p n
ISSGQR
p n
n p
IVSGQR
ΔT = 0
ΔS = 0
ΔT = 1
ΔS = 0
ΔT = 0
ΔS = 1
ΔT = 1
ΔS = 1

The Collective Response of the Nucleus: Giant Resonances

Compression modes

Isoscalar (In phase)
$\Delta T = 0$

Isovector (Out of phase)
$\Delta T = 1$

Monopole
$\Delta L = 0$
(GMR)

Dipole
$\Delta L = 1$
(GDR)

Quadrupole
$\Delta L = 2$
(GQR)

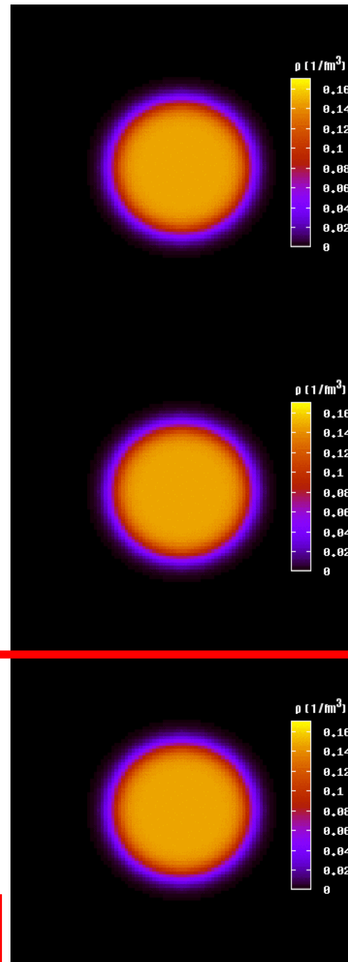

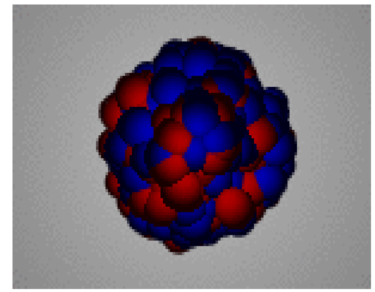

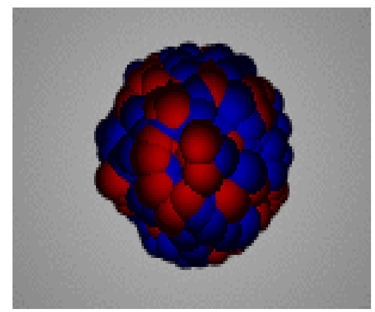

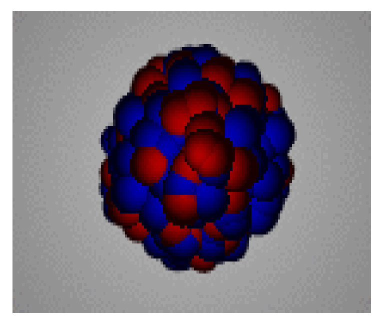

M. Itoh

Operators and Microscopic Structure

Microscopic picture: GRs are coherent (1p-1h) excitations induced by single-particle operators.

- **Excitation energy depends on**

  ***i*) multipole *L* ($L\hbar\omega$, since radial operator $\propto r^L$; except for ISGMR and ISGDR, $2\hbar\omega$ & $3\hbar\omega$, respectively),**

  ***ii*) strength of effective interaction and**

  ***iii*) collectivity.**

- **Exhaust appreciable % of EWSR**
- **Acquire a width due to coupling to continuum and to underlying 2p-2h configurations.**

Microscopic structure of ISGMR & ISGDR

Transition operators:

$$O^{L=0} = \sum_i r_i^0 Y_0^0 + \frac{1}{2}\sum_i r_i^2 Y_0^0 + \ \ldots$$

Constant   Overtone

2ħω **excitation**

$$O^{L=1} = \sum_i r_i^1 Y_0^1 + \frac{1}{2}\sum_i r_i^3 Y_0^1 + \ \ldots$$

Spurious c.o.m. motion   Overtone

3ħω **excitation (overtone of c.o.m. motion)**

Nucleus → **Many-body system with a finite size**

Vibrations → **Multipole expansion with r, Y_{lm}, τ, σ**

	$\Delta S=0, \Delta T=0$	$\Delta S=0, \Delta T=1$	$\Delta S=0, \Delta T=1$	$\Delta S=1, \Delta T=1$	$\Delta S=1, \Delta T=1$
L=0: Monopole	ISGMR r^2Y_0	IAS τY_0	IVGMR $\tau r^2 Y_0$	GTR $\tau\sigma Y_0$	IVSGMR $\tau\sigma r^2 Y_0$
L=1: Dipole	ISGDR $(r^3 - 5/3\langle r^2\rangle r)Y_1$		IVGDR $\tau r Y_1$		IVSGDR $\tau\sigma r Y_1$
L=2: Quadrupole	ISGQR r^2Y_2		IVGQR $\tau r^2 Y_2$		IVSGQR $\tau\sigma r^2 Y_2$
L=3: Octupole	LEOR, HEOR r^3Y_3				

Dropped $\Delta S=1, \Delta T=0$ operators because excitations are very weak

IVGDR

$\tau r Y_1$

$\Delta N = 1$ **E1 (IVGDR)**

$\Delta N = 2$ **E2 (ISGQR)**

&

$\Delta N = 0$ **E0 (ISGMR)**

ISGMR $r^2 Y_0$

ISGQR $r^2 Y_2$

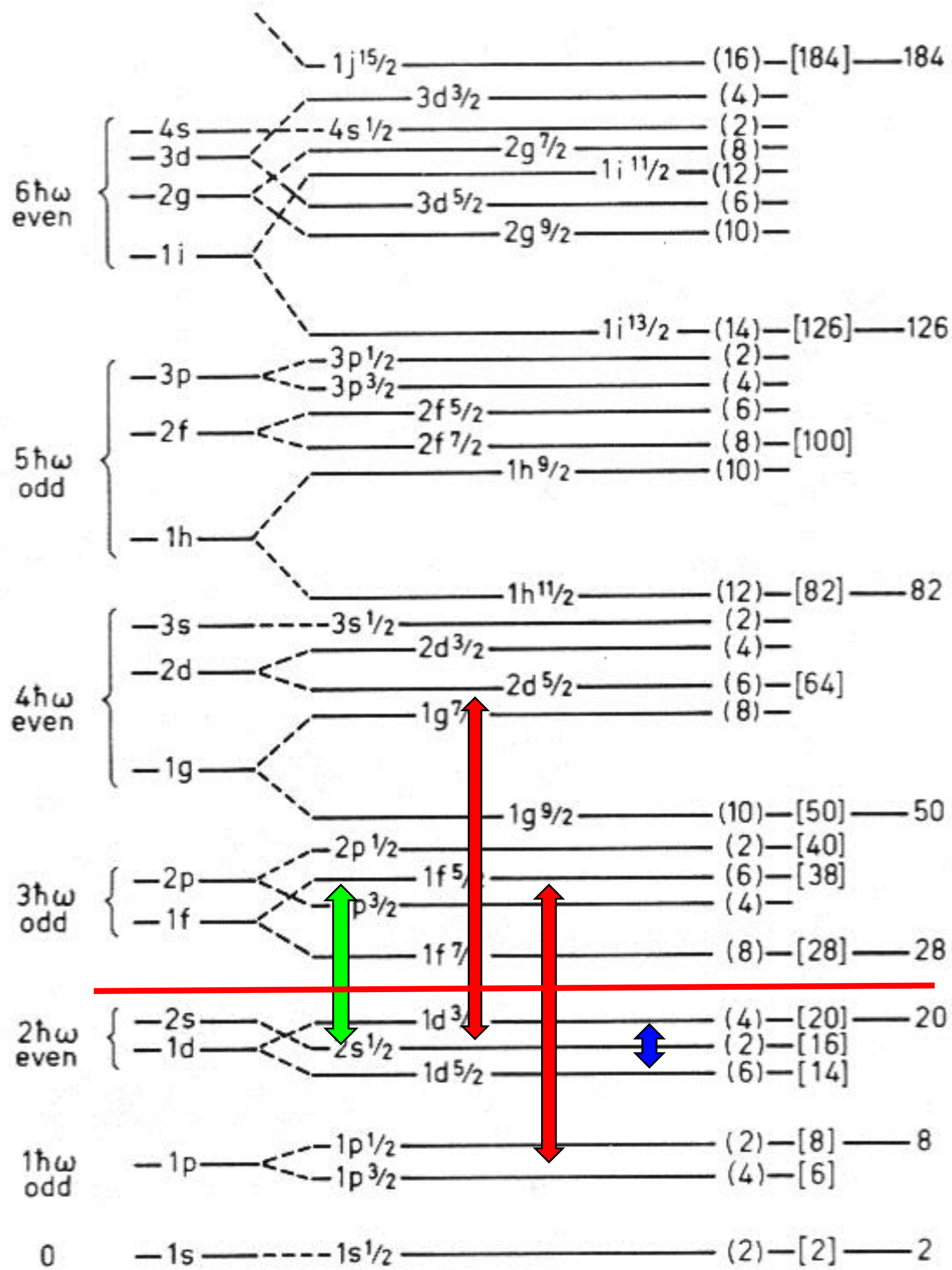

Decay of giant resonances

- **Width of resonance**

  $\Gamma, \Gamma^{\uparrow}, \ \Gamma^{\downarrow} \ (\Gamma^{\downarrow\uparrow}, \Gamma^{\downarrow\downarrow})$

  - $\Gamma^{\uparrow}$**: direct or escape width**
  - $\Gamma^{\downarrow}$**: spreading width**

  $\Gamma^{\downarrow\uparrow}$**: pre-equilibrium,** $\Gamma^{\downarrow\downarrow}$**: compound**

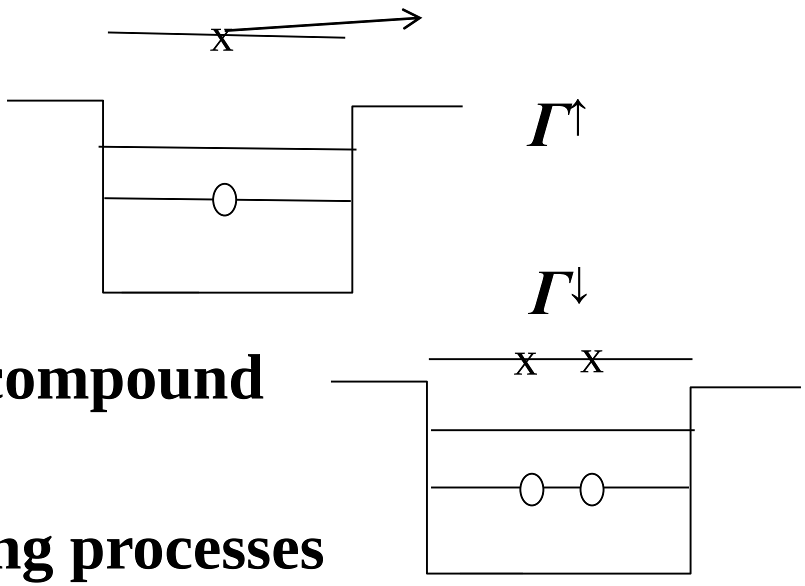

- **Decay measurements**

  ⇒ Direct reflection of damping processes

  Allows detailed comparison with theoretical calculations

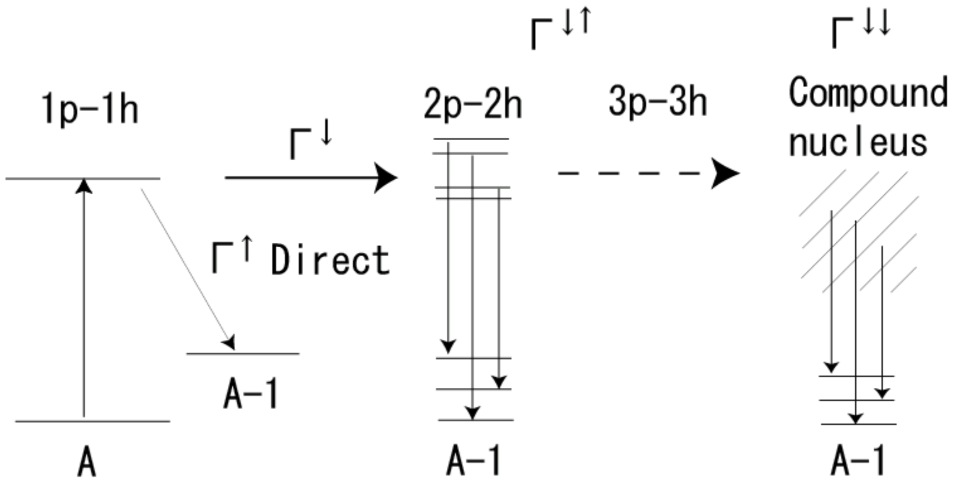

Energy-Weighted Sum Rules

Intermezzo: Sum rules

Consider the most general electric multipole operator (Bohr & Mottelson 69), neglecting the current term:

$$\mathcal{M}(E\lambda,\mu) = \frac{(2\lambda+1)!!}{q^{\lambda}(\lambda+1)}\int \rho(\vec{r})\frac{\partial}{\partial r}\big(r j_{\lambda}(qr)\big)Y_{\lambda\mu}(\hat{r})d\tau$$

$$j_{\lambda}(qr) = \frac{(qr)^{\lambda}}{(2\lambda+1)!!}\left(1-\frac{1}{2}\frac{(qr)^{2}}{(2\lambda+3)}+\cdots\right)$$

Bessel function

This leads in 1st order (long-wave length limit, i.e. *qr* ≪ 1):

$$\mathcal{M}(E\lambda,\mu) = \frac{(2\lambda+1)!!}{q^{\lambda}(\lambda+1)}\int \rho(\vec{r})\frac{\partial}{\partial r}\left(\frac{r(qr)^{\lambda}}{(2\lambda+1)!!}\right)Y_{\lambda\mu}(\hat{r})d\tau$$

$$\mathcal{M}(E\lambda,\mu) = \int \rho(\vec{r})r^{\lambda}\,Y_{\lambda\mu}(\hat{r})d\tau$$

Using $\rho(\vec{r}) = \sum_{k} e\left(\frac{1}{2}-t_{zk}\right)\delta(\vec{r}-\vec{r}_k)$

we get:

$$\mathcal{M}(E\lambda,\mu) = \sum_k e\left(\frac{1}{2} - t_{zk}\right) r_k^\lambda Y_{\lambda\mu}(\Omega_k)$$

$$\mathcal{M}(E\lambda,\mu) = \frac{1}{2} e \sum_k r_k^\lambda Y_{\lambda\mu}(\Omega_k) - e \sum_k t_{zk}\, r_k^\lambda Y_{\lambda\mu}(\Omega_k)$$

For the isoscalar *E0* and *E1*, 1st order leads to a constant and c.o.m. coordinate, respectively. Expanding to 2nd order (taking only dependence on *r*) we get:

$$\mathcal{M}(E0) = \frac{1}{4} e \sum_k r_k^2 - \frac{1}{2} e \sum_k t_{zk} r_k^2$$

Isoscalar **Isovector**

$$\mathcal{M}(E1,\mu) = \frac{1}{4} e \sum_k r_k^3 Y_{1\mu}(\Omega_k)$$

Isovector term neglected

Thomas Reiche Kuhn (TRK) sum rule is originally obtained for an atomic system assuming an electric field directed along z-axis:

$$S_e(E1) = \sum_f \left(E_f - E_i\right) |\langle f | \sum_k z_k | i \rangle|^2$$

The total absorption cross section is in the long-wave length limit:

$$\int_0^{\infty} \sigma(E_\gamma) dE_\gamma = \frac{4\pi^2 e^2}{\hbar c} \sum_f \left(E_f - E_i\right) |\langle f | \sum_k z_k | i \rangle|^2$$

For a Hermitian operator and using closure relation

($\sum_f |f >< f| = 1$), we obtain:

$$\int_0^{\infty} \sigma(E_\gamma) dE_\gamma = \frac{4\pi^2 e^2}{\hbar c} \frac{1}{2} \langle i \left| \left[\sum_k z_k, \left[H, \sum_k z_k \right] \right] \right| i \rangle$$

Consider only kinetic term of Hamiltonian:

$$\int_0^\infty \sigma(E_\gamma)dE_\gamma = \frac{4\pi^2 e^2}{\hbar c}\frac{1}{2}\left\langle i \middle| \left[\sum_k z_k, \left[\frac{p_z^2}{2m_e}, \sum_k z_k\right]\right] \middle| i \right\rangle$$

$$\int_0^\infty \sigma(E_\gamma)dE_\gamma = \frac{4\pi^2 e^2}{\hbar c}\frac{\hbar^2 I}{2m_e}$$

I is number of electrons. For a nucleus (see later):

$$e_{eff}^2 I = Z e_{peff}^2 + N e_{neff}^2 = \frac{NZ}{A} e^2$$

Therefore:

$$\int_0^\infty \sigma(E_\gamma)dE_\gamma = \frac{2\pi^2 e^2 \hbar}{mc}\frac{NZ}{A} = 60\frac{NZ}{A}\ MeV\ mb$$

This is the TRK sum rule for a nucleus.

$$B(E\lambda, J_i \to J_f) = \sum_{\mu M_f} \left|\langle \Psi_f | \mathcal{M}(E\lambda, \mu) | \Psi_i \rangle\right|^2$$

$$B(E\lambda, J_i \to J_f) = \sum_{\mu M_f} \langle J_i M_i \lambda\mu | J_f M_f \rangle^2 \left|\langle \Psi_f \| \mathcal{M}(E\lambda) \| \Psi_i \rangle\right|^2$$

$$B(E\lambda, J_i \to J_f) = \frac{2J_f + 1}{2J_i + 1} \left|\langle \Psi_f \| \mathcal{M}(E\lambda) \| \Psi_i \rangle\right|^2$$

$$S_\lambda(E\lambda) = \sum_f (E_f - E_i) |\langle f | \mathcal{M}(E\lambda, \mu) | i \rangle|^2$$

$$\Rightarrow S_\lambda(E\lambda) = \frac{1}{2} \left|\langle i \left| [\mathcal{M}(E\lambda, \mu), [H, \mathcal{M}(E\lambda, \mu)]] \right| i \rangle\right|$$

Introducing for $\mathcal{M}(E\lambda, \mu)$ the isoscalar *E0*, *E1* and $E\lambda$ operators, and using a similar procedure as for TRK sum rule (using Hermitian property and closure relation), we obtain the isoscalar *E0*, *E1* and $E\lambda$ energy-weighted sum rules (EWSR).

$$P_{0\mu} = \frac{1}{2}\sum_i r_i^2$$

$$\sum_n (E_n - E_0) B(E0, 0 \to n) = S_0 = \frac{\hbar^2}{2m} A < r^2 >$$

$$P_{1\mu} = \frac{1}{2}\sum_i r_i^3 Y_{1\mu}(\hat{r}_i)$$

$$\sum_n (E_n - E_0) B(E1, 0 \to n) = S_1 = \frac{\hbar^2}{8\pi m}\frac{3}{4} A[11 < r^4 > - \frac{25}{3} < r^2 >^2 - 10\varepsilon < r^2 >]$$

$$\varepsilon = (\frac{4}{E_2} + \frac{5}{E_0})\frac{\hbar^2}{3mA}$$

$$Q_{\lambda\mu} = \sum_i r_i^\lambda Y_{\lambda\mu}(\hat{r}_i)$$

$$\sum_n (E_n - E_0) B(E\lambda, 0 \to n) = S_\lambda = \frac{\hbar^2}{8\pi m}\lambda(2\lambda+1)^2 A < r^{2\lambda-2} >$$

Isovector E1 operator

$$\mathcal{M}(E1) = \sum_{k=1}^{A} e\left(\frac{1}{2} - t_{zk}\right)\vec{r}_k^{\,int}$$

$$\vec{r}_k = \vec{R} + \vec{r}_k^{\,int} \quad where\ \vec{R} = \sum\nolimits_k \vec{r}_k/A$$

$$\mathcal{M}(E1) = e\sum_{k=1}^{A}\left(\frac{1}{2} - t_{zk}\right)(\vec{r}_k - \vec{R})$$

$$\mathcal{M}(E1) = -e\sum_{k=1}^{A} t_{zk}\,(\vec{r}_k - \vec{R})$$

$$\mathcal{M}(E1) = e\sum_{k=1}^{A}\left(\frac{N-Z}{2A} - t_{zk}\right)\vec{r}_k$$

⇒ Effective charges for neutrons and protons

$$e_D = e\left(\frac{N-Z}{2A} - t_{zk}\right) = \begin{cases} \frac{N}{A}e & for\ proton \\ -\frac{Z}{A}e & for\ neutron \end{cases}$$

$$\sum_n (E_n - E_0) B(E\lambda, 0 \to n) = S_\lambda = \frac{\hbar^2}{8\pi m} \lambda(2\lambda+1)^2 A \langle r^{2\lambda-2} \rangle$$

For isovector *E1*, λ=1 and *A* becomes $Ze^2_{peff} + Ne^2_{neff}$, which leads to:

$$\sum_n (E_n - E_0) B(E1{,}0 \to n) = \frac{\hbar^2}{8\pi m} 9 \left[Z \left(\frac{N}{A} \right)^2 e^2 \right.$$

IVGDR

Consider isovector electric dipole excitations.

How does a nucleus respond to an external perturbation, e.g., real photons?

⇒ Photo-absorption cross section
γ-rays from bremsstrahlung or positron capture in flight

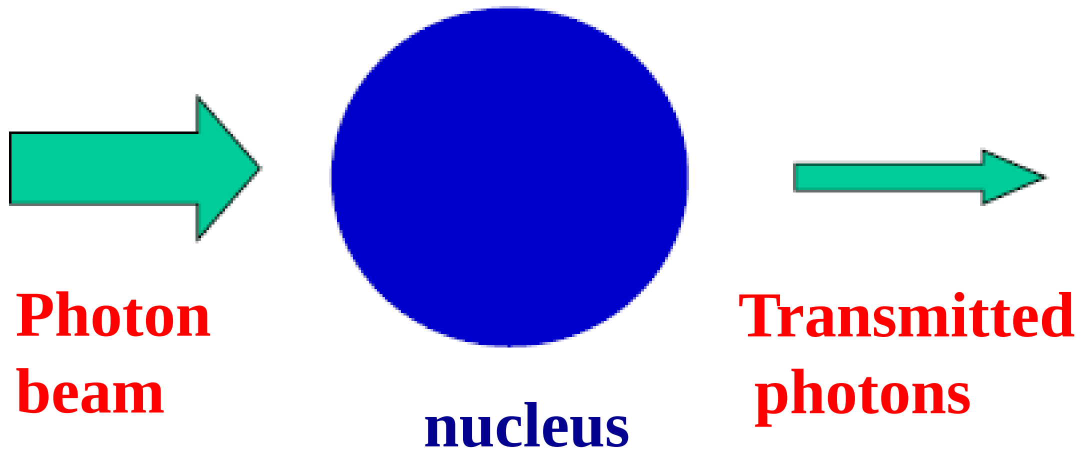

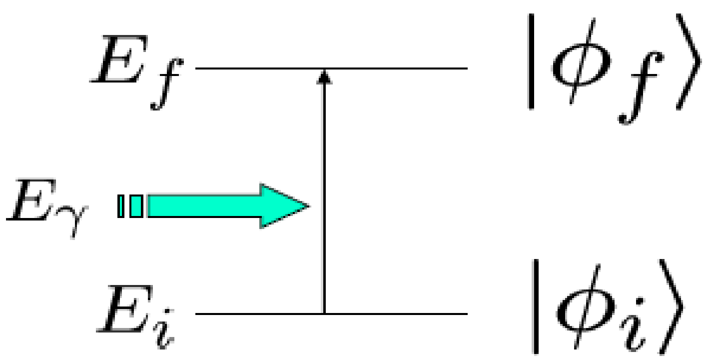

The state is strongly excited when

$$E_f - E_i = E_\gamma$$

Nuclear Collective response
Giant Resonances

Isovector Electric Giant Resonances

Isovector

Photo-neutron cross sections

Monopole (IVGMR)

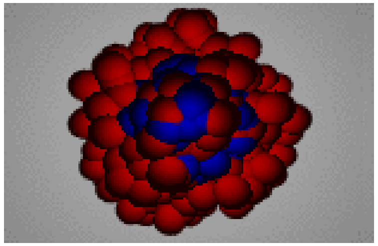

Dipole (IVGDR)

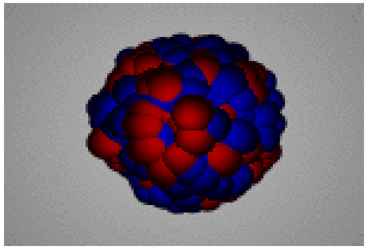

Quadrupole (IVGQR)

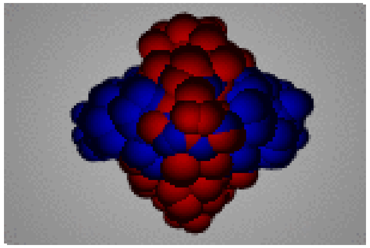

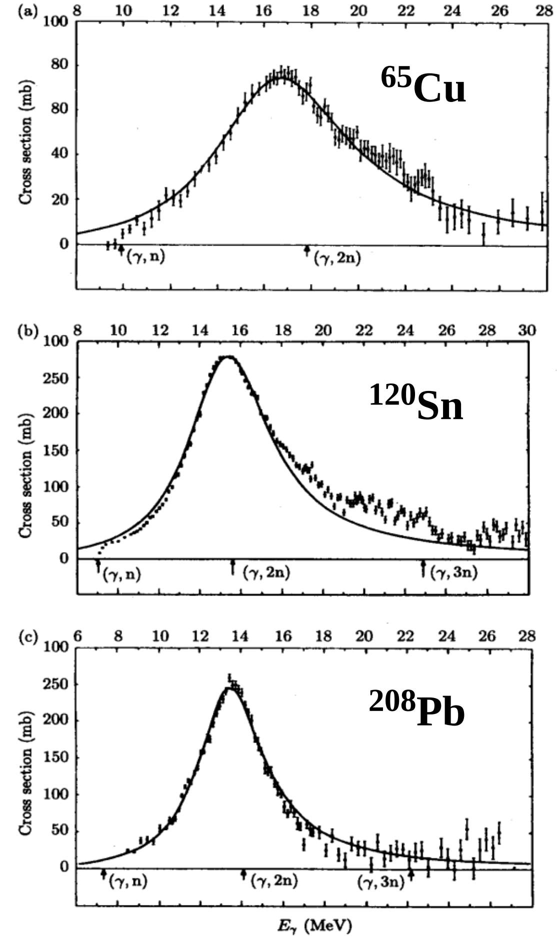

Berman and Fultz, Rev. Mod. Phys. 47 (1975) 713

Isovector Giant Dipole Resonances: Photo-neutron cross section

Spherical and nearly spherical nuclei

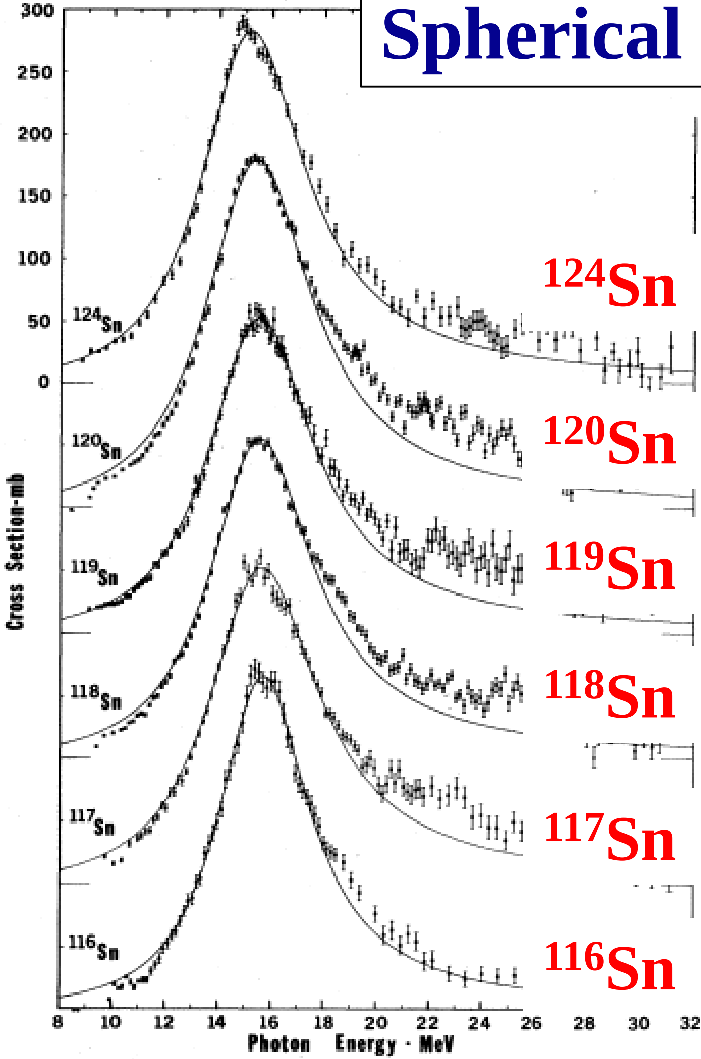

$$\omega \propto \frac{1}{R} \propto A^{-\frac{1}{3}}$$

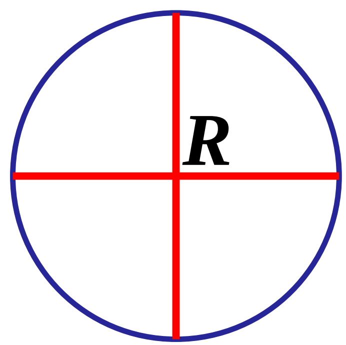

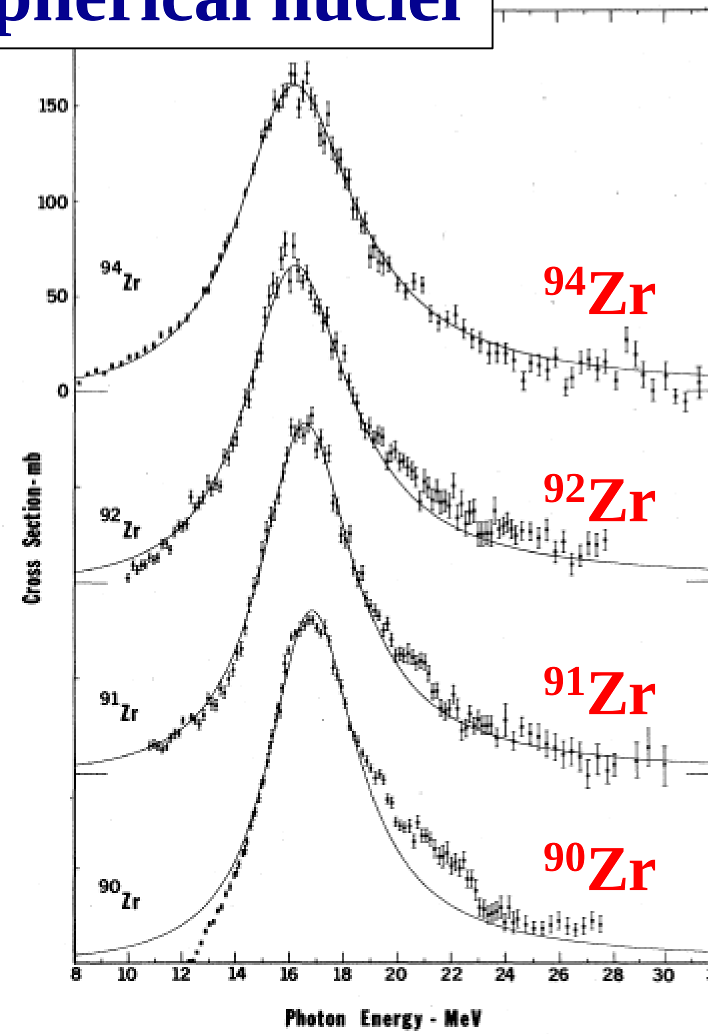

B. L. Berman and S. C. Fultz, Rev. Mod. Phys. 47 (1975) 713

Measurement of the giant dipole resonance with mono-energetic photons

B.L. Berman and S.C. Fultz
Rev. Mod. Phys. 47 (1975) 713

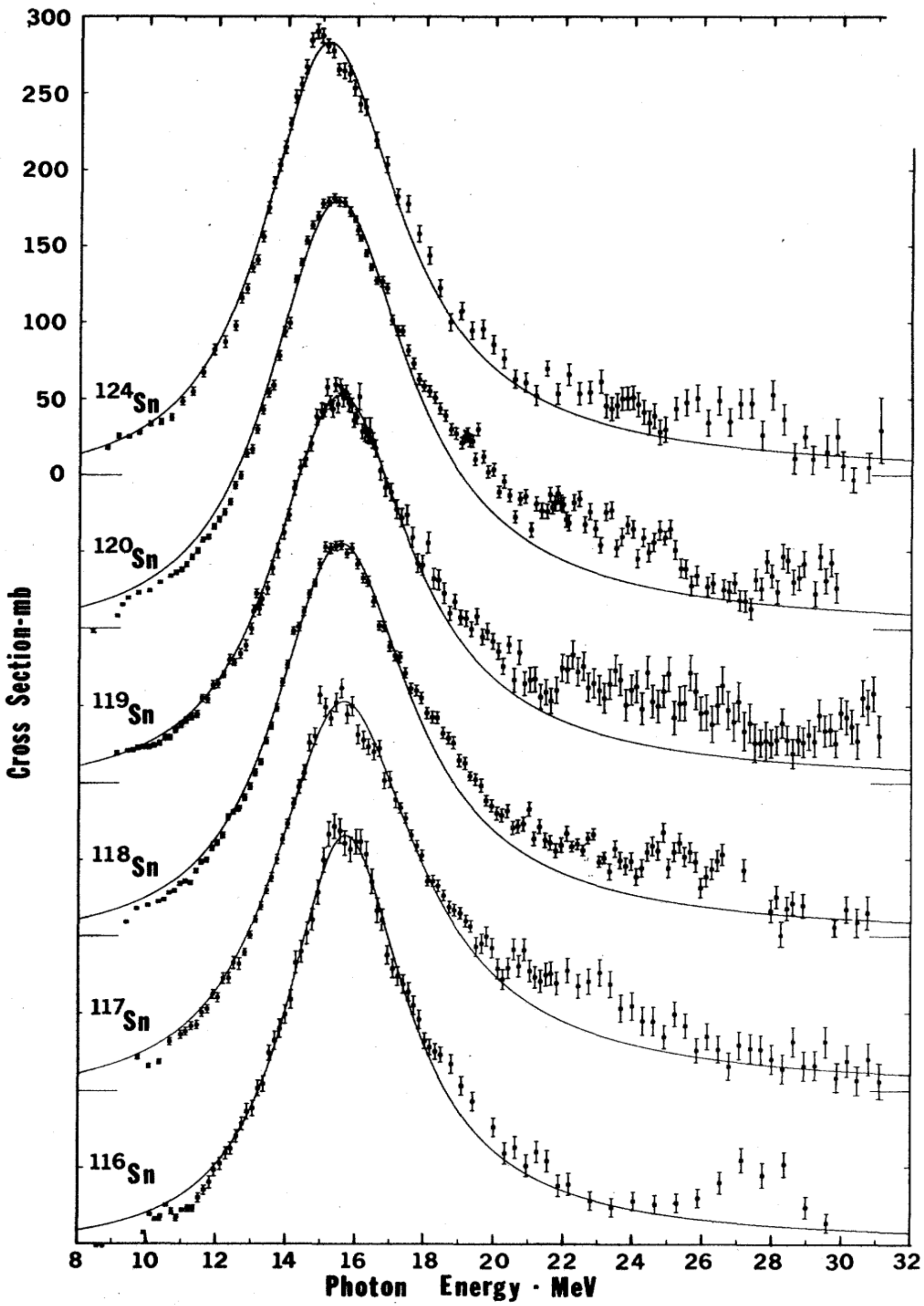

Nucleus	Centroid (MeV)	Width (MeV)
^{116}Sn	15.68	4.19
^{117}Sn	15.66	5.02
^{118}Sn	15.59	4.77
^{119}Sn	15.53	4.81
^{120}Sn	15.40	4.89
^{124}Sn	15.19	4.81

Photo-neutron cross section in deformed nuclei:

Deformed Nucleus

$$R(\theta,\phi)=R_0(1+\beta_2 Y_{20}(\theta,\phi))$$

β_2 (^{150}Nd) = 0.285(3)

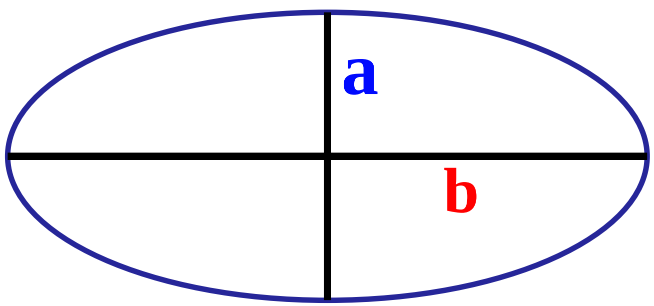

Excitation energies:

$E_2/E_1 = 0.911\eta + 0.089$

Where $\eta = b/a$

$S_1/S_2 = 1/2$

B. L. Berman and S. C. Fultz, Rev. Mod. Phys. 47, 713 (1975)

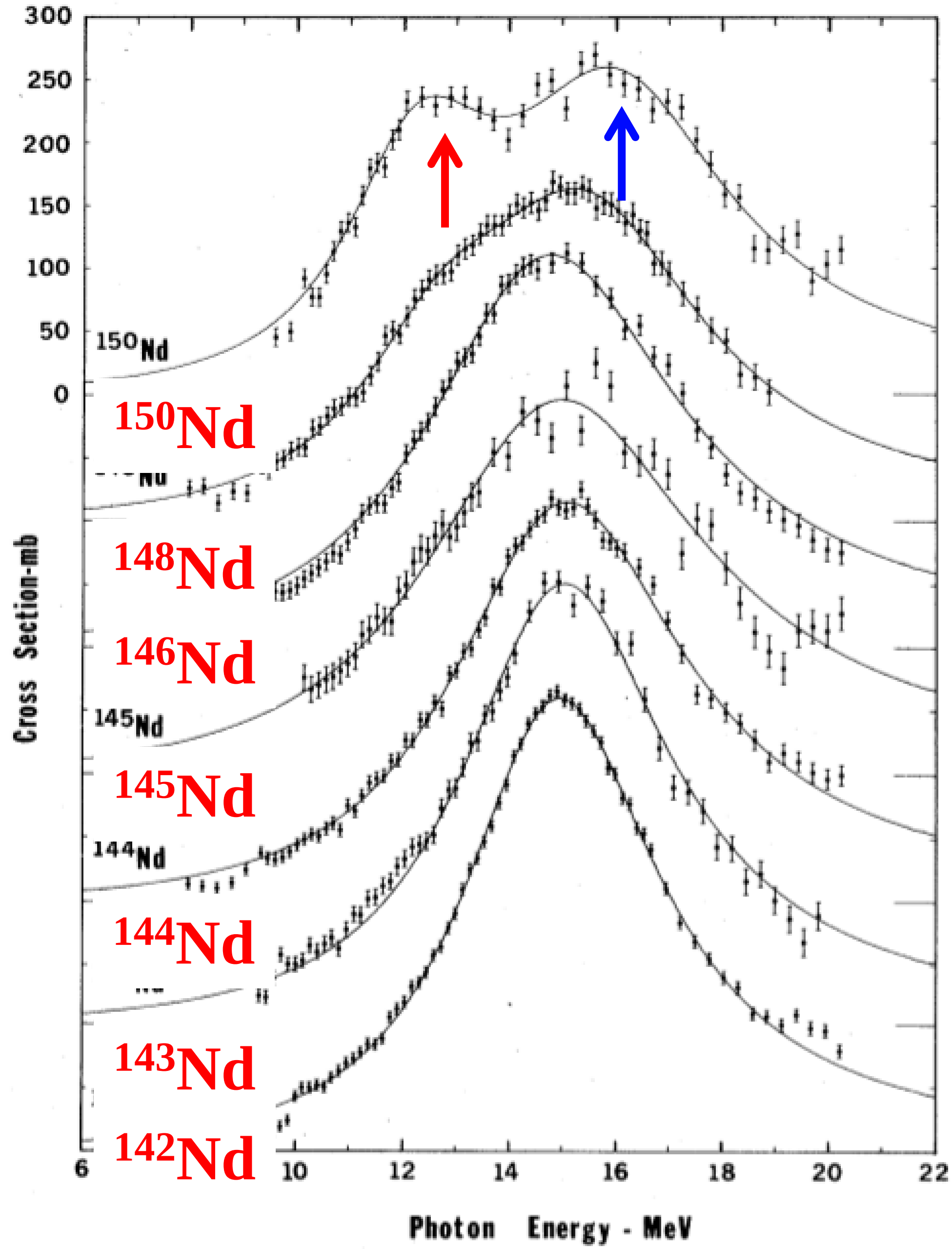

Experimental Tool: Electromagnetic excitation at high energies

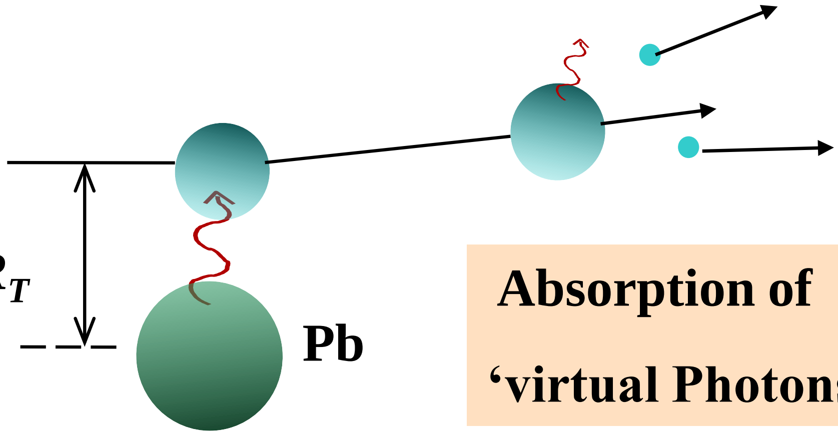

$b > R_P + R_T$

Absorption of 'virtual Photons'

Semi-classical theory:

$$d\sigma_{e.m.} / dE = N_\gamma(E)\, s_\gamma(E)$$

$$\sigma_{e.m.} \sim Z^2$$

adiabatic cut-off:

$$E_{\max} = \frac{\hbar}{\tau} = \frac{\hbar c \gamma \beta}{b}$$

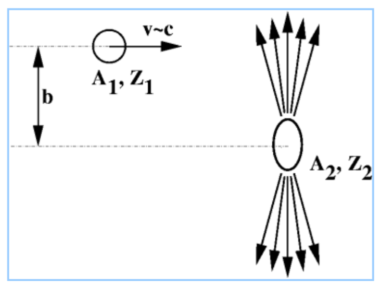

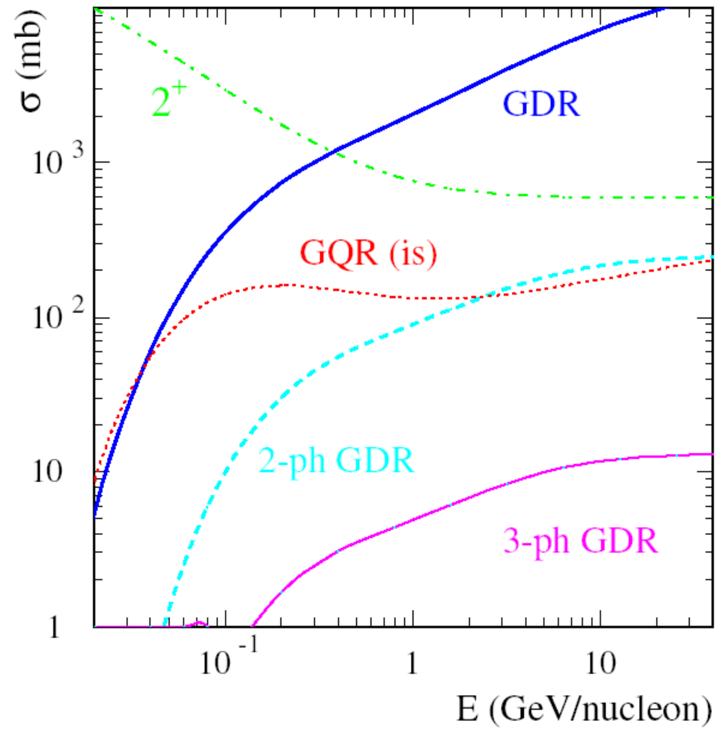

High velocities v/c ≈ 0.6-0.9
⇒ High-frequency Fourier components
$E_{\gamma,max} \approx$ **25 MeV (@ 1 GeV/u)**

Determination of 'photon energy' (excitation energy) via a kinematically complete measurement of the momenta of all outgoing particles (invariant mass)

Experimental Scheme: The LAND reaction setup @GSI

Mixed beam

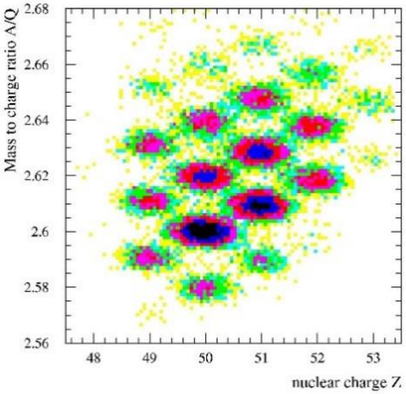

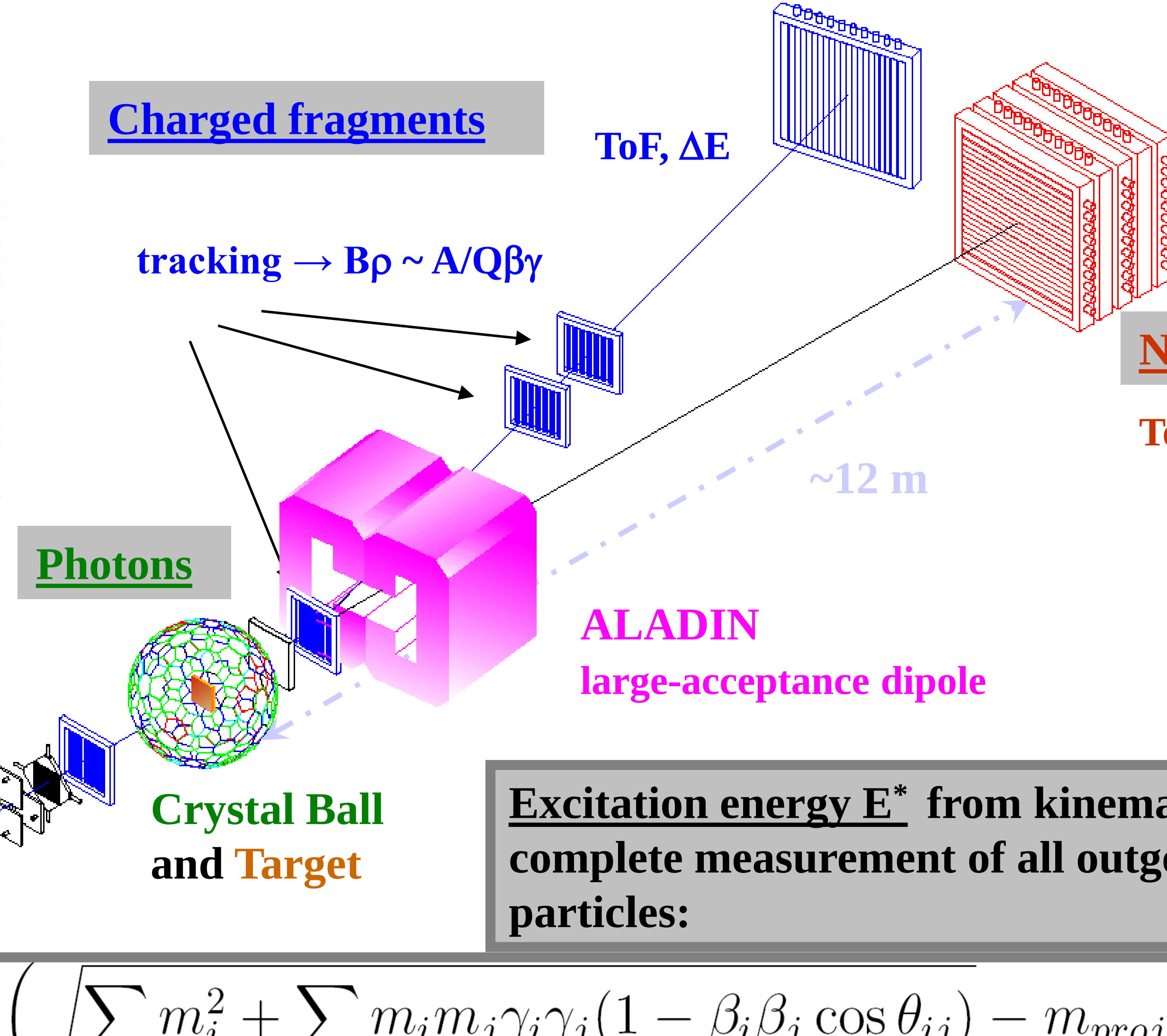

Excitation energy E^* from kinematically complete measurement of all outgoing particles:

$$E^* = \left(\sqrt{\sum_i m_i^2 + \sum_{i \neq j} m_i m_j \gamma_i \gamma_j (1 - \beta_i \beta_j \cos\theta_{ij})} - m_{proj}\right) c^2 + E_\gamma$$

Dipole Strength Distribution of n-Rich Nuclei

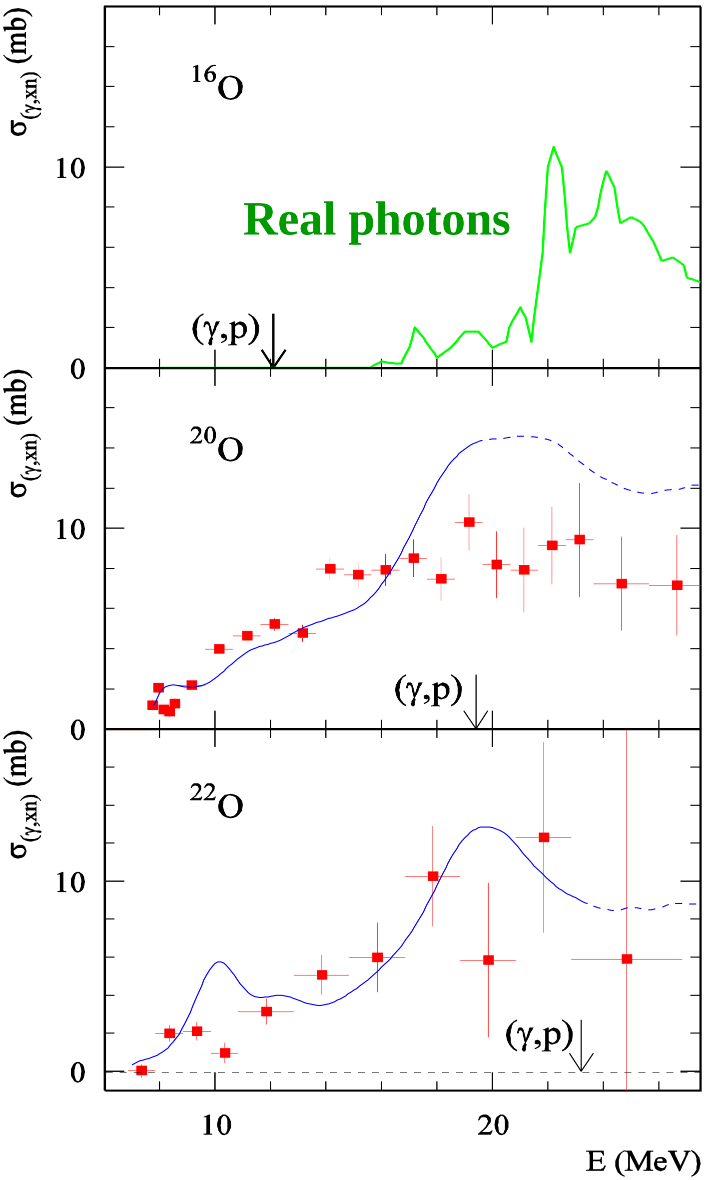

^{A}O (~ 500 MeV/u) + Pb → ^{A-x}O + γ + xn

N-Z=0

N-Z=4

N-Z=6

⇒ Photo-neutron cross sections from virtual photons

⇒ Low-lying dipole strength

⇒ Fragmentation of GDR strength

? Collective soft mode ?

— Large-scale shell model calculation

H. Sagawa, T. Suzuki, Phys. Rev. C 59 (1999) 3116

Data: LAND-FRS@GSI

A. Leistenschneider *et al.*, Phys. Rev. Lett. 86 (2001) 5442

Dipole strength distributions in neutron-rich Sn isotopes

Electromagnetic-excitation cross section

Photo-neutron cross section

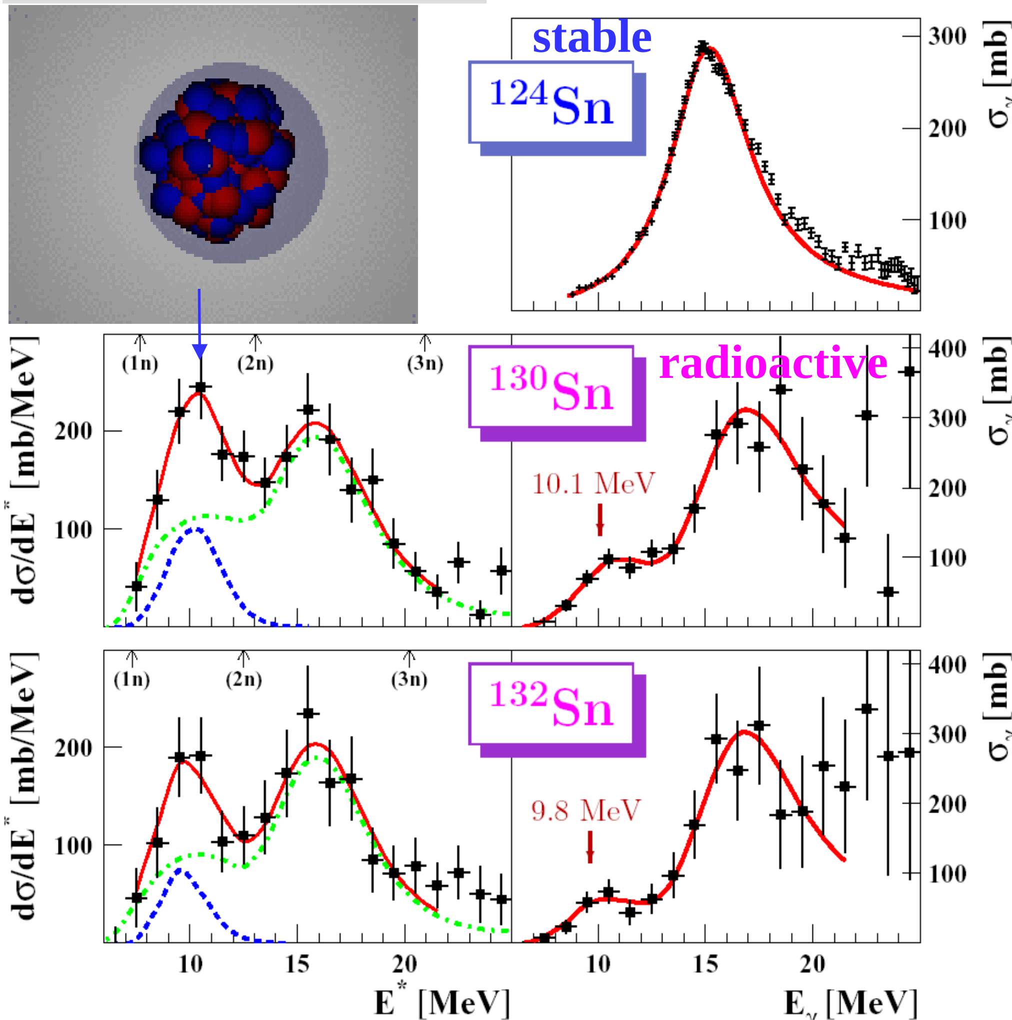

A	PDR		GDR		
	E_{centr} [MeV]	sum-rule fraction [%]	E_{centr} [MeV]	Γ [MeV]	sum-rule fraction [%]
^{124}Sn	-	-	15.3	4.8	116
^{130}Sn	10.1 (0.7)	7.0 (3.0)	15.9 (0.5)	4.8 (1.8)	145 (19)
^{132}Sn	9.8 (0.7)	4.0 (3.1)	16.1 (0.8)	4.7 (2.2)	125 (32)

PDR

- located at 10 MeV
- exhausts a few % TRK sum rule
- in agreement with theory

GDR

- no deviation from systematics

P. Adrich *et al.*, PRL 95 (2005) 132501

Dipole strength distributions in ^{68}Ni

Simultaneous fit of spectra with 8 individual energy bins as free fit parameters:
„deconvolution"

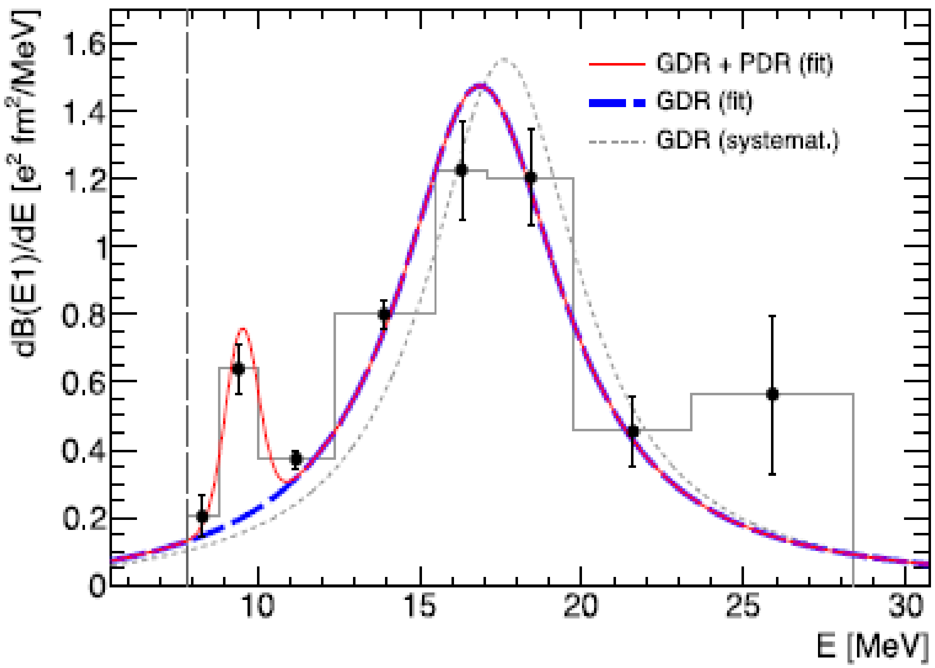

^{68}Ni 600 MeV/u
γ detection only

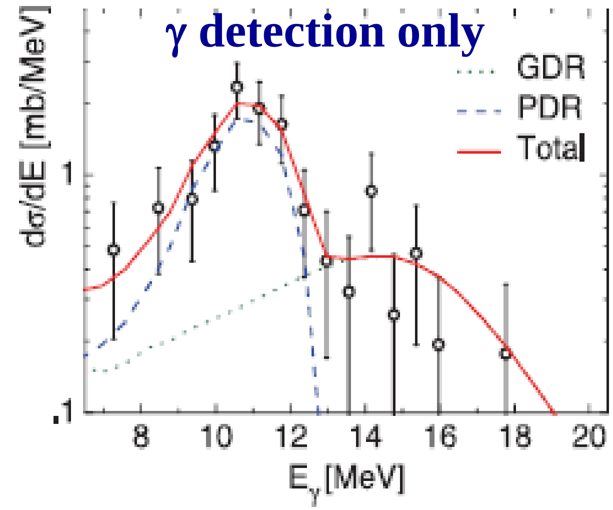

O. Wieland et al., PRL 102, 092502 (2009)

			This work	Lit.	Ref.
	E_m	[MeV]	17.1(2)	17.84	
GDR	Γ	[MeV]	6.1(5)	5.69	[30]
	S_{EWSR}	[%]	98(7)	100	
	E_m	[MeV]	9.55(17)	11	
PDR	σ	[MeV]	0.51(13)	< 1	[13, 25]
	S_{EWSR}	[%]	2.8(5)	5.0(1.5)	

Direct gamma-decay
branching ratio
$\Gamma_0/\Gamma = 7(2)\%$

D. Rossi et al., Phys. Rev. Lett. 111 (2013) 242503

Distribution of isovector dipole strength for the three closed-(sub)shell nickel isotopes ^{56}Ni, ^{68}Ni, and ^{78}Ni calculated in HF-plus-RPA using the FSUGold interaction parameter set.

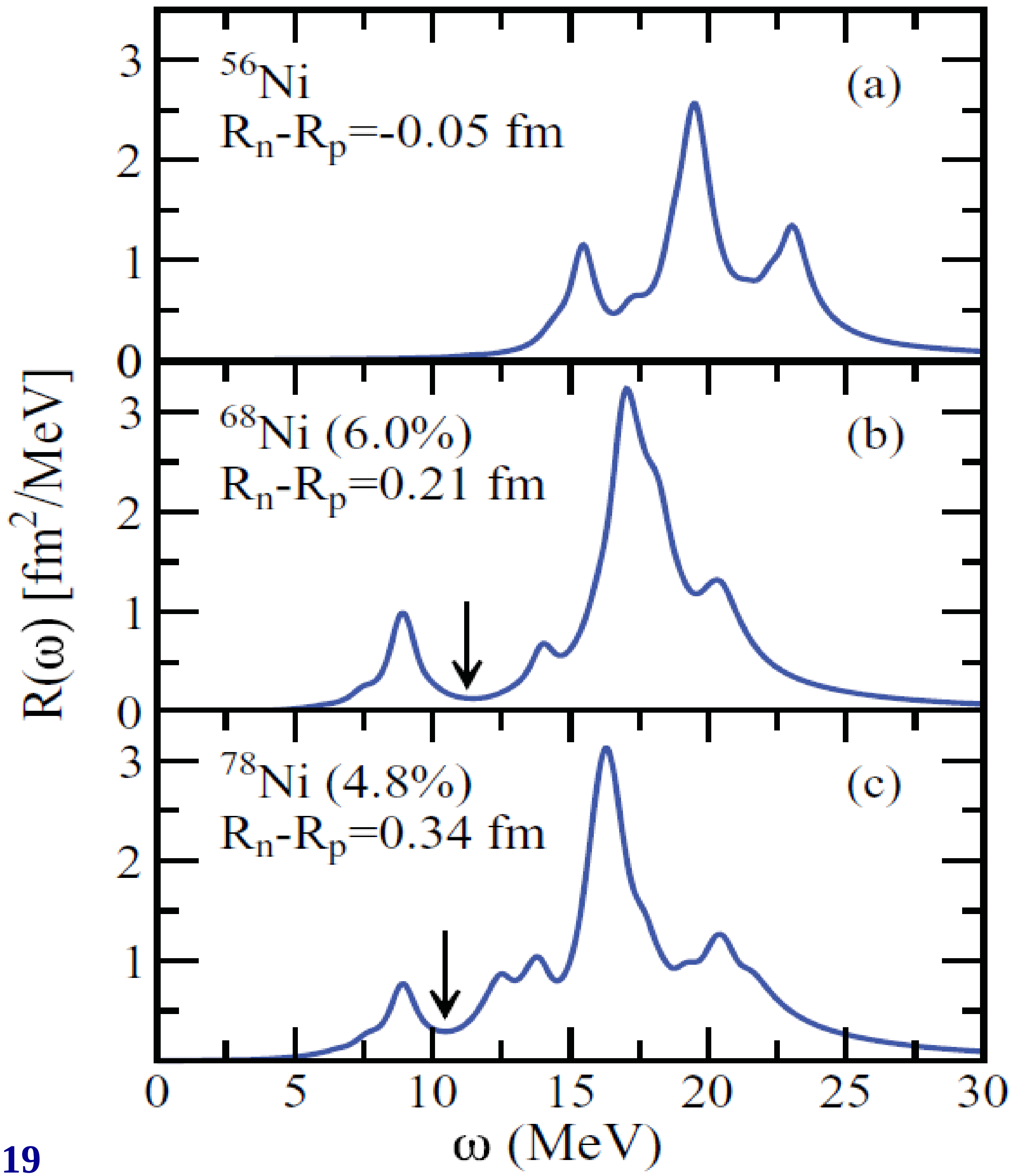

J. Piekarewicz, PRC 83 (2011) 034319

Experiments at RCNP, Osaka University

- **(*p*,*p′*) reaction at 295 MeV**
  - **High-resolution spectrometer “Grand Raiden”**

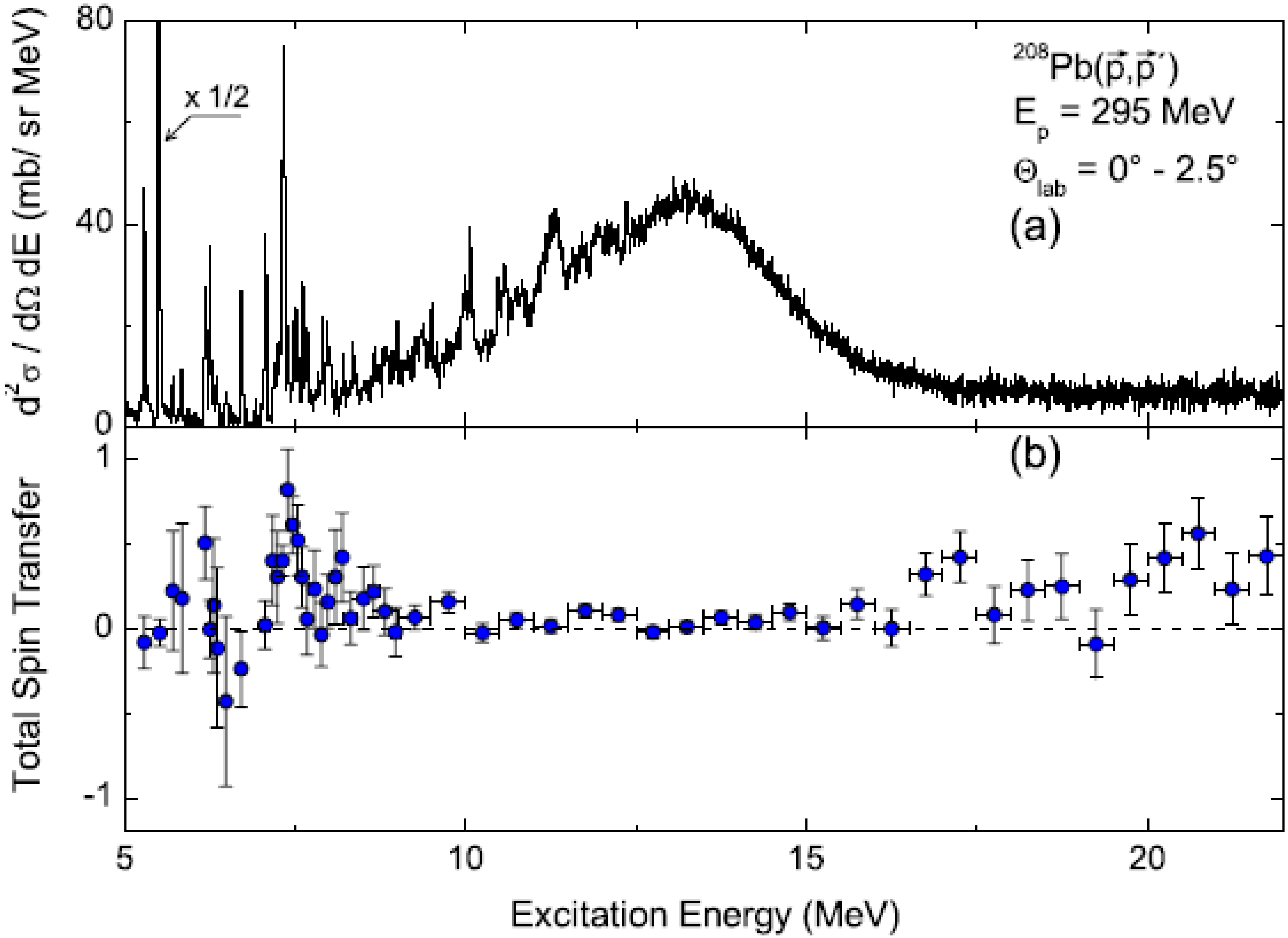

A. Tamii *et al*., Phys. Rev. Lett. 107 (2011) 062502

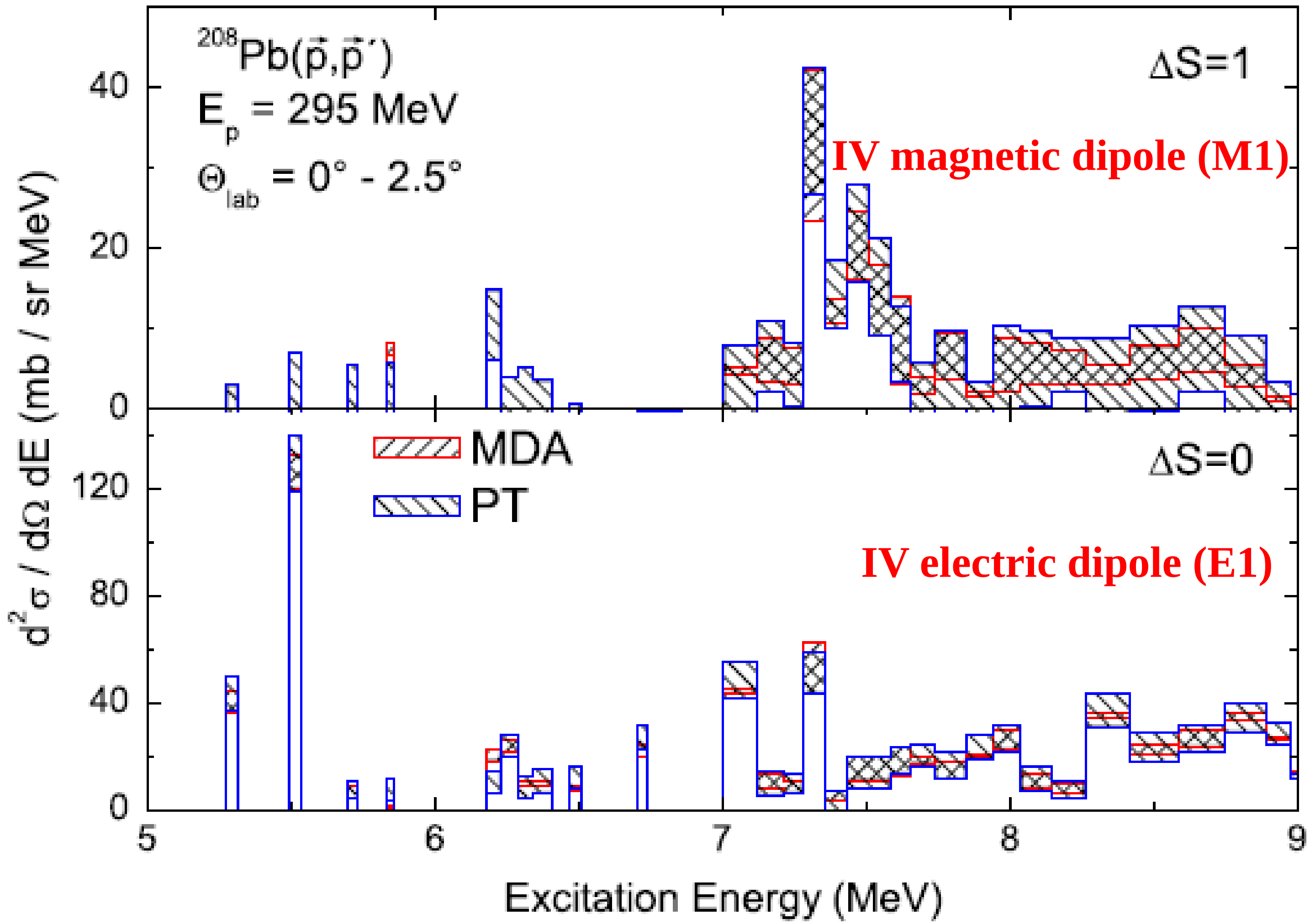

MDA = Multipole-Decomposition Analysis

PT = Polarisation Transfer

A. Tamii *et al*., Phys. Rev. Lett. 107 (2011) 062502

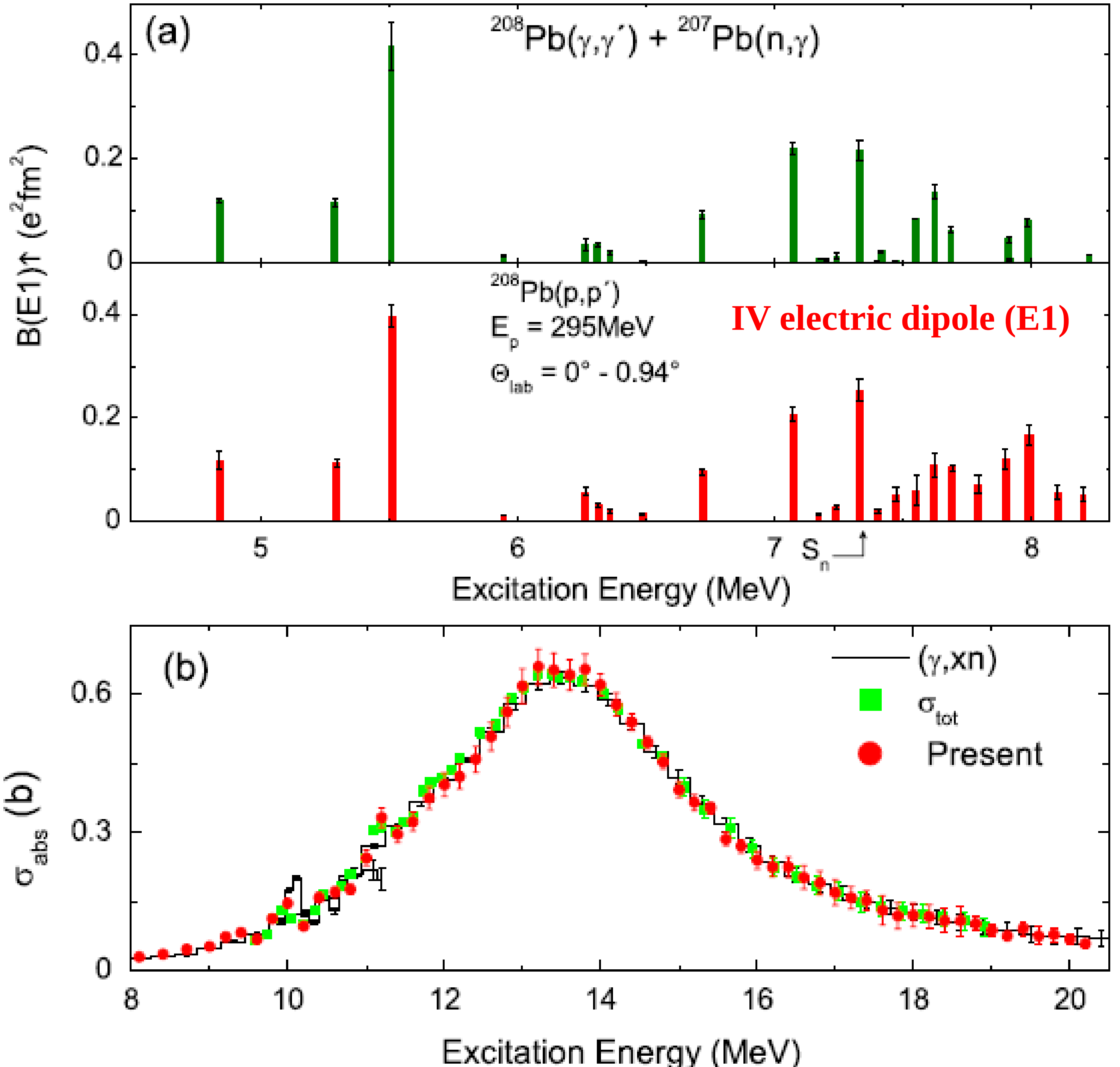

(a)
^{208}Pb(γ,γ′) + ^{207}Pb(n,γ)
B(E1)↑ (e^2fm^2)
0.4
0.2
0
^{208}Pb(p,p′)
E_p = 295MeV
Θ_{lab} = 0° - 0.94°
IV electric dipole (E1)
5
6
7
S_n
8
Excitation Energy (MeV)
(b)
(γ,xn)
σ_{tot}
Present
σ_{abs} (b)
0.6
0.3
0
8
10
12
14
16
18
20
Excitation Energy (MeV)

0°-1.8° inelastic proton scattering spectrum shows in addition to IVGDR low-lying E1 and M1 structures.

Peaks with (*) have been selected for multipole-decomposition analysis.

3.75°-5.25° inelastic proton scattering spectrum is almost structure-less.

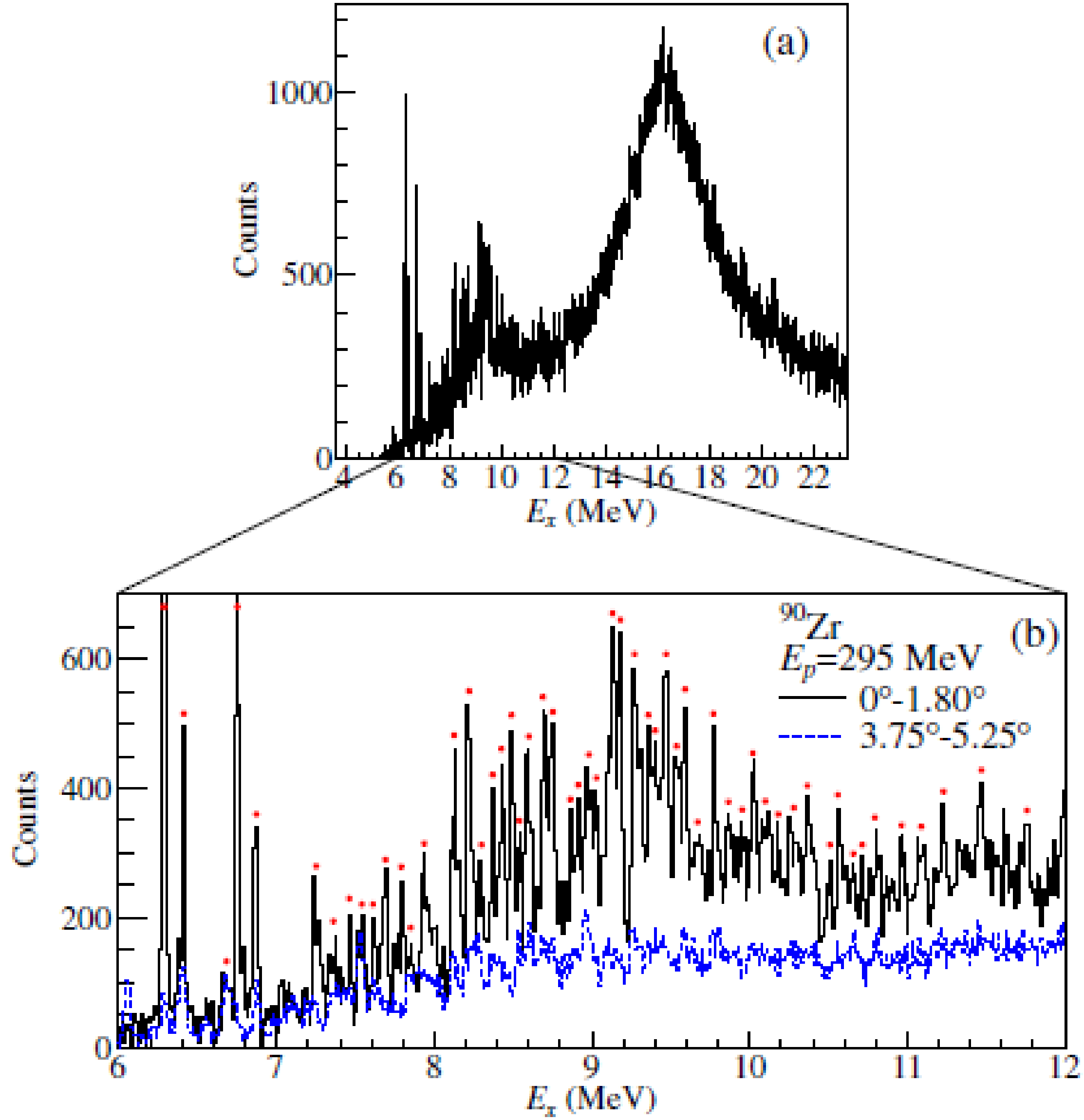

C. Iwamoto *et al.*, Phys. Rev. Lett. 108 (2012) 262501

E1 (dash-dotted line)

M1 (solid line)

E2 (dashed line)

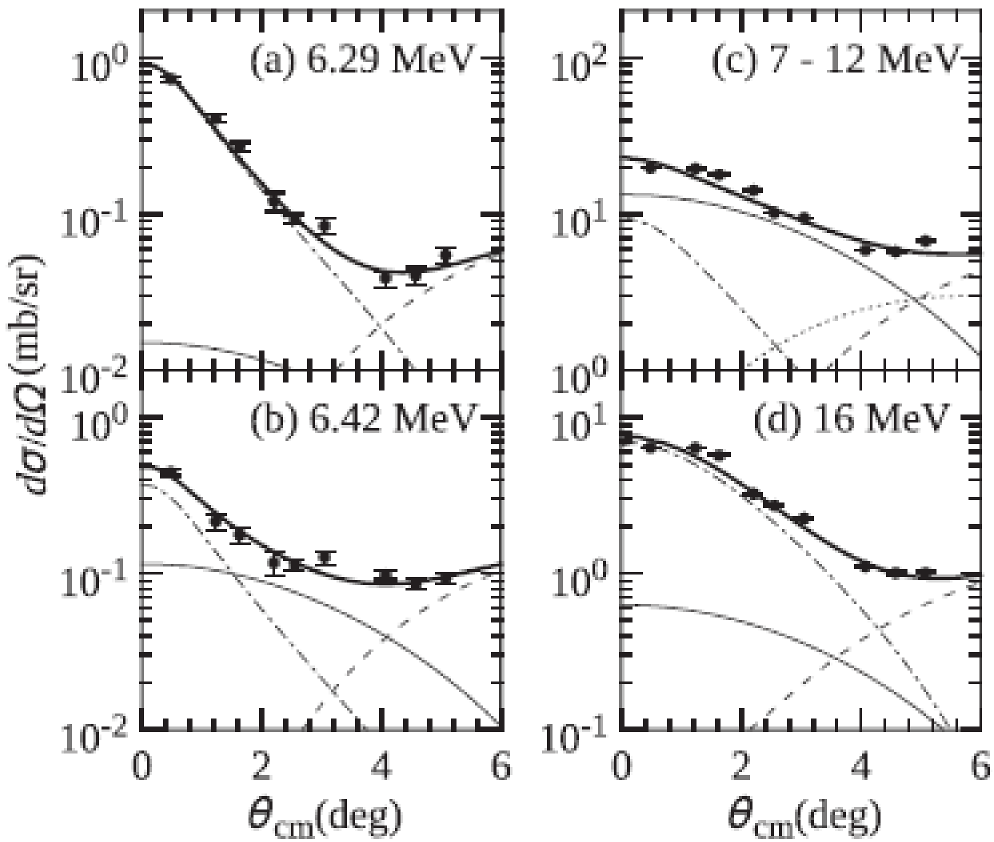

C. Iwamoto *et al.*, Phys. Rev. Lett. 108 (2012) 262501

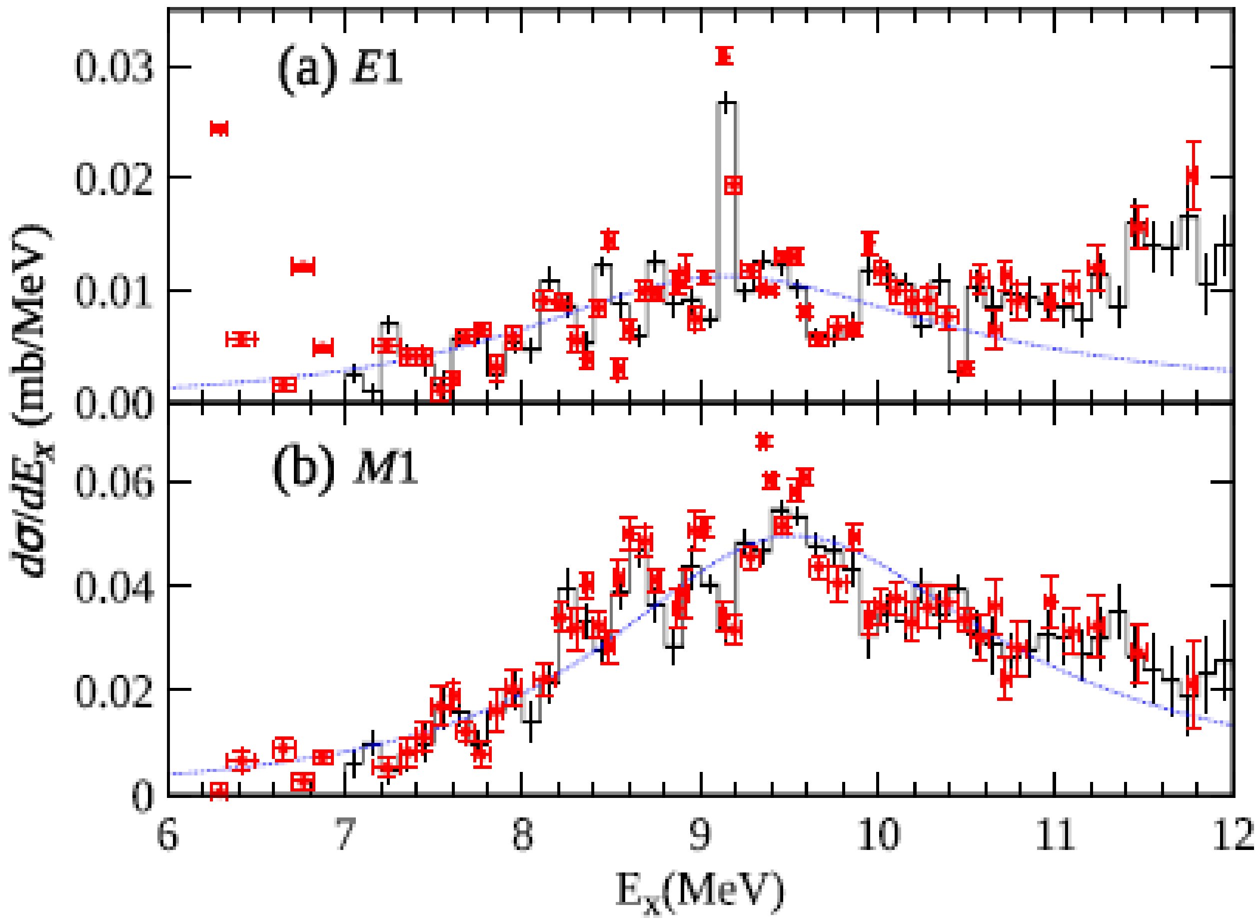

Histograms MDA of 100 keV bins and red circles with errors are of selected peaks.

C. Iwamoto *et al.*, Phys. Rev. Lett. 108 (2012) 262501

Decay of IVGDR built on excited states

Schematic picture of statistical decay of IVGDR built on excited states in ^{114}Sn

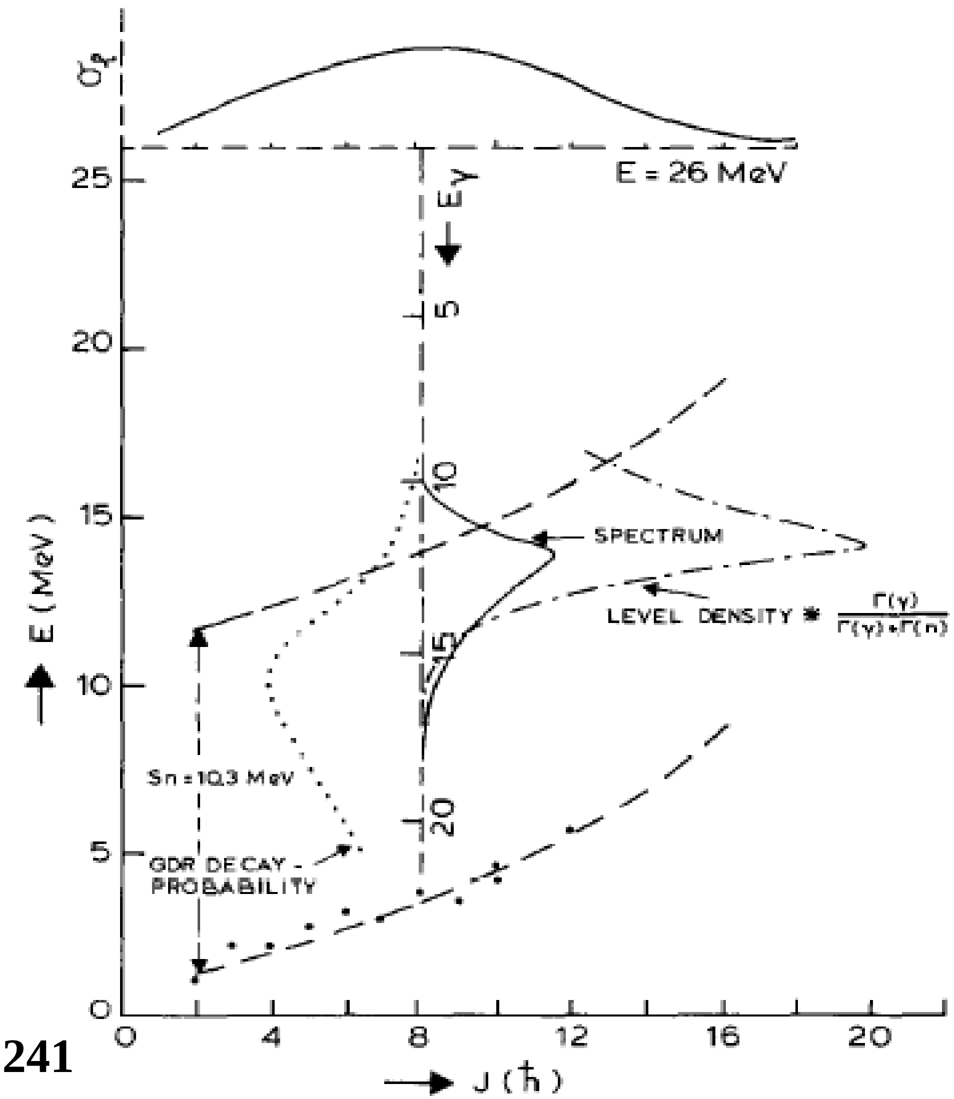

A. Stolk *et al.*, Nucl. Phys. A505 (1989) 241

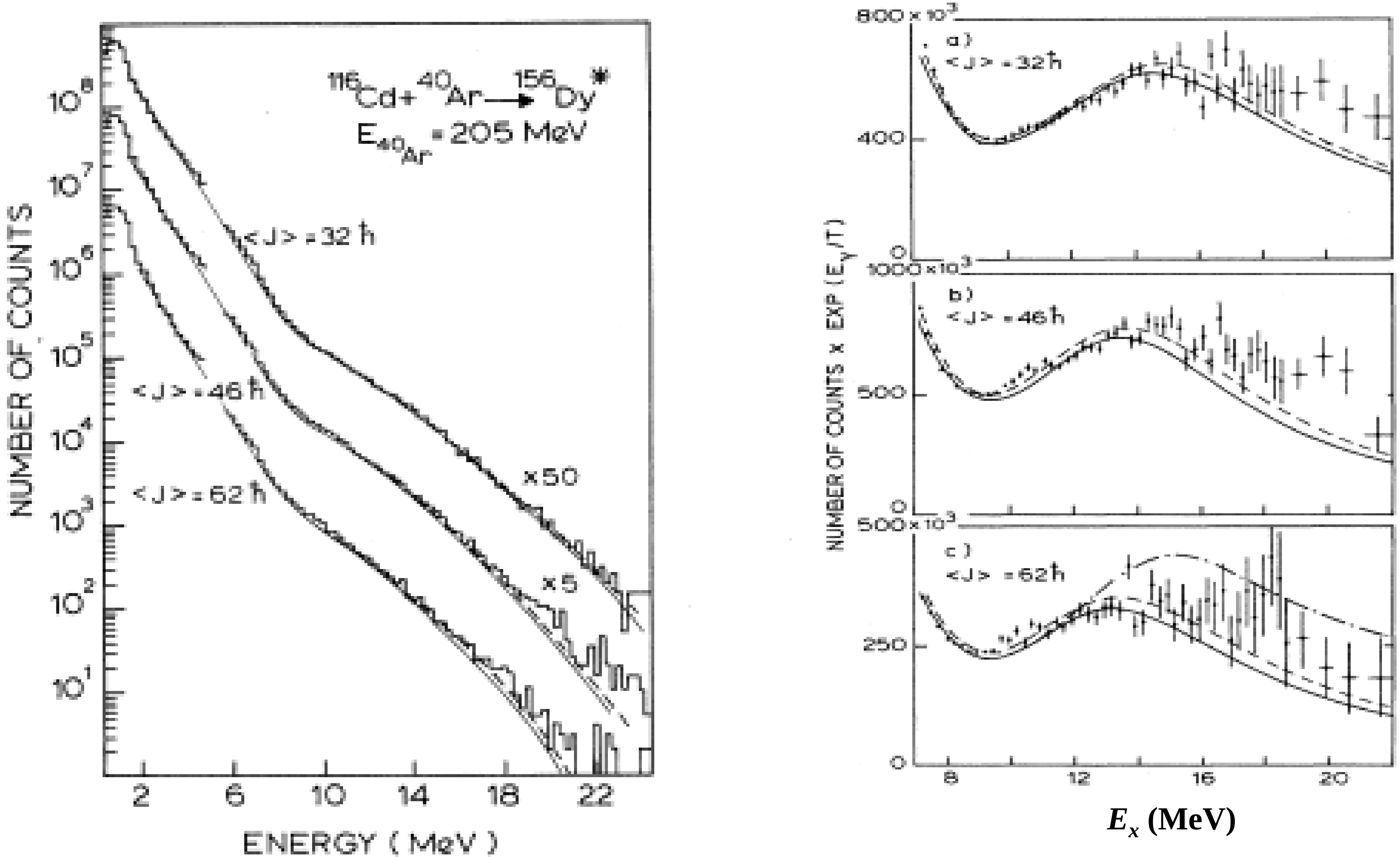

Left: Statistical decay of IVGDR in ^{156}Dy selected on different angular momentum bins. Curves fits CASCADE calculations with dashed curve increased by 5%. Right: Same as left linearized by multiplying with $e^{E\gamma/T_{eff}}$

A. Stolk *et al.*, Phys. Rev. C40 (1989) R2454

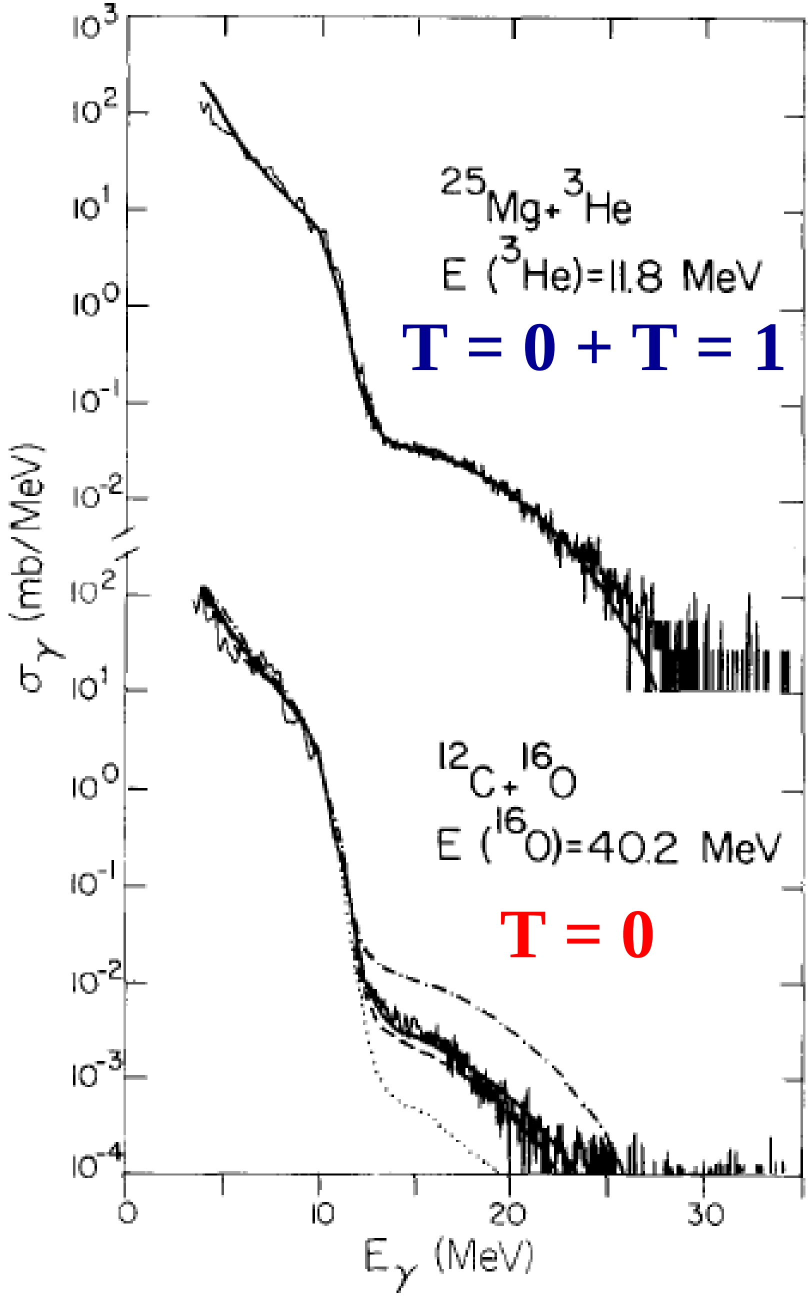

Role of isospin in the statistical decay of the IVGDR built on excited states

Clebsch-Gordon coefficient for isospin coupling
<0010|00>=0

Dotted: pure ISGQR
Dashed: pure isospin
Dash-dotted: complete isospin mixing
Solid: isospin mixing (~ 5%)

M.N. Harakeh *et al*., Phys. Lett. B176 (1986) 297

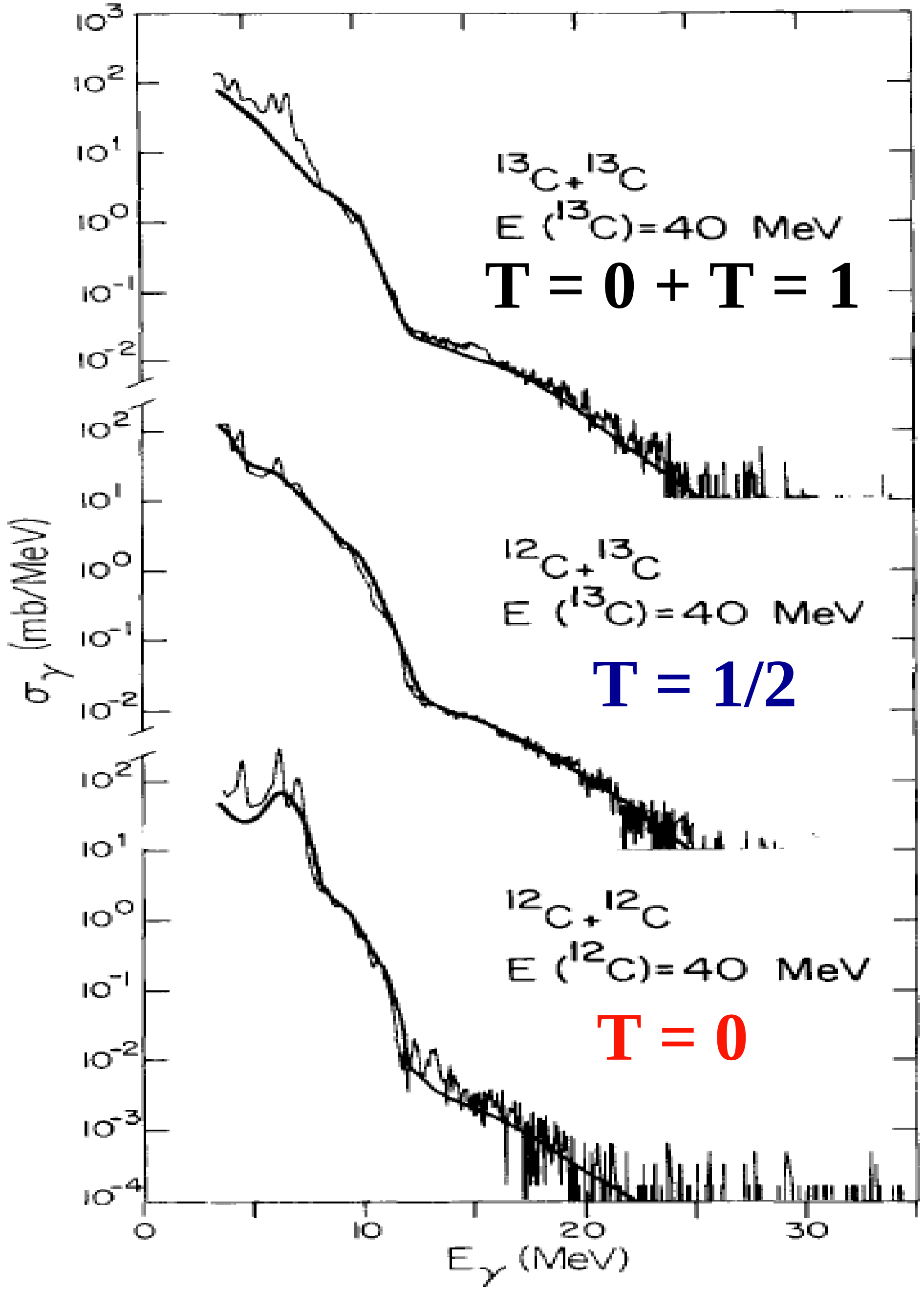

$^{13}C + ^{13}C$
$E(^{13}C) = 40$ MeV
T = 0 + T = 1
$^{12}C + ^{13}C$
$E(^{13}C) = 40$ MeV
T = 1/2
$^{12}C + ^{12}C$
$E(^{12}C) = 40$ MeV
T = 0
σ_γ (mb/MeV)
E_γ (MeV)

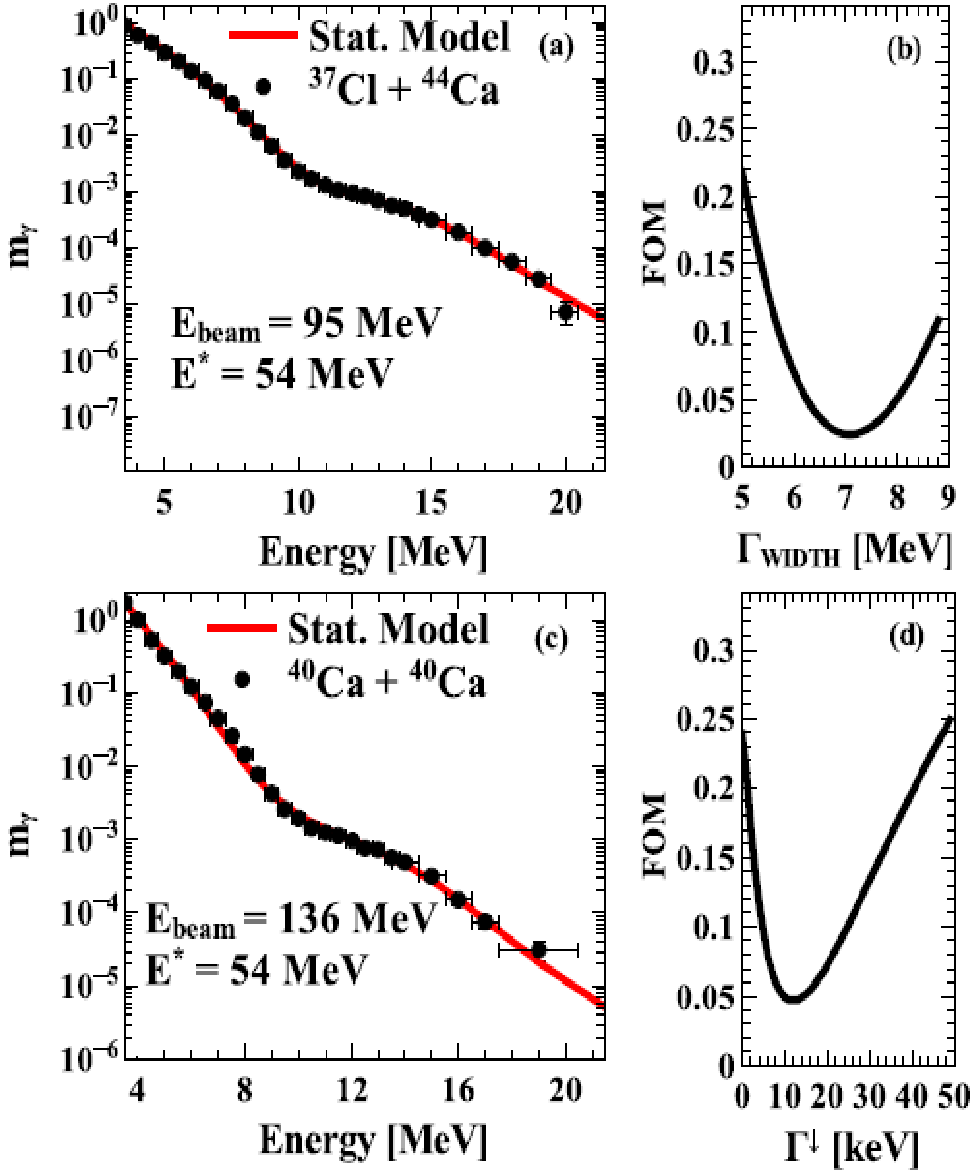

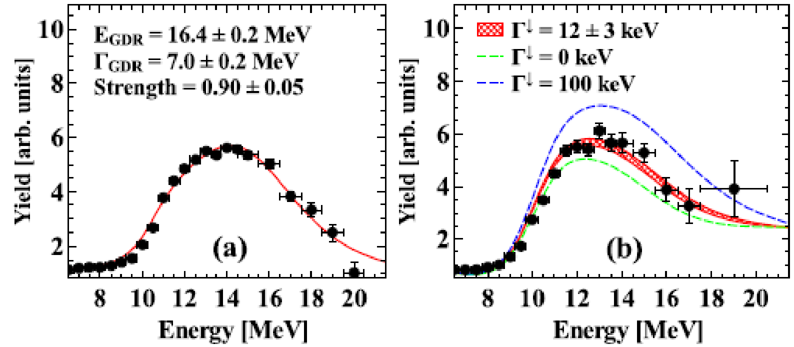

$$T = \sqrt{(E^* - E_{GDR} - E_{rot})/a}$$

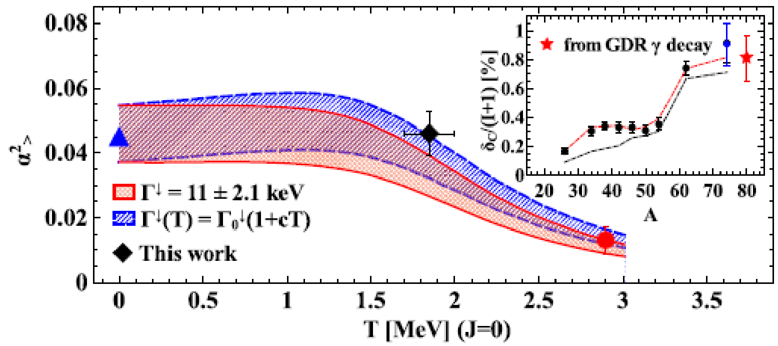

Role of isospin in the statistical decay of the IVGDR built on excited states

- **S. Ceruti *et al.*, PRL 115 (2015) 222502**
- **A. Corsi *et al.*, PRC 84 (2011) 041304 (R)**

Compression Modes
ISGMR & ISGDR

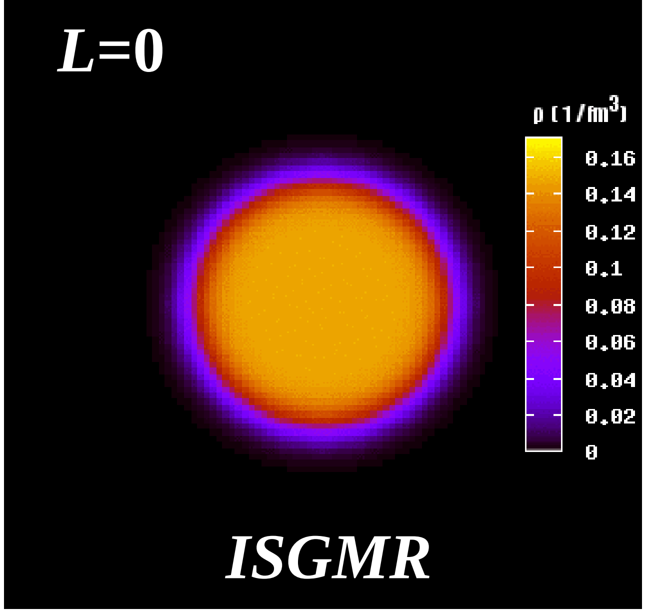
L=0
ρ (1/fm3)
0.16
0.14
0.12
0.1
0.08
0.06
0.04
0.02
0
ISGMR

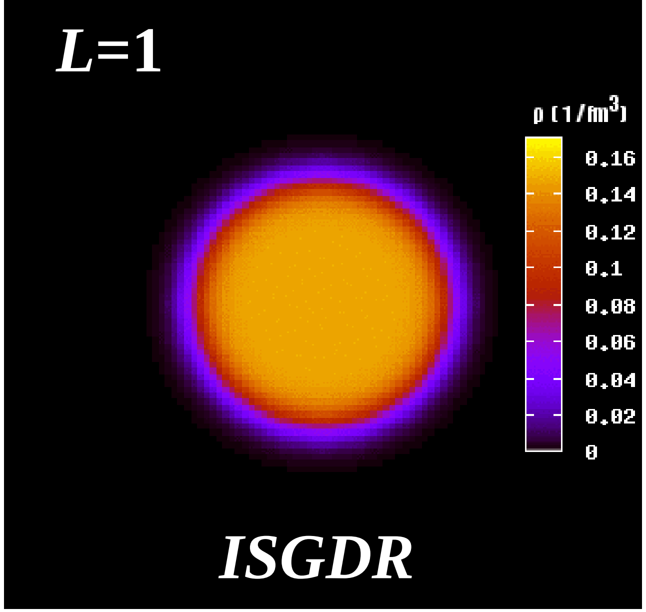
L=1
ρ (1/fm3)
0.16
0.14
0.12
0.1
0.08
0.06
0.04
0.02
0
ISGDR

M. Itoh

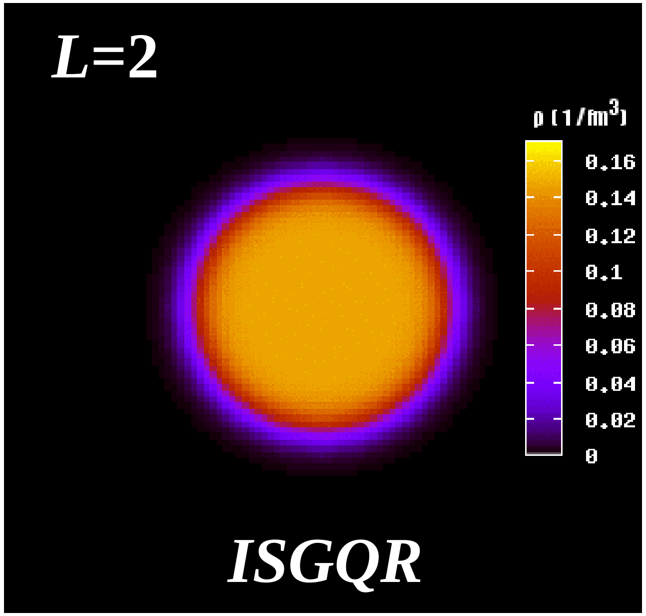
L=2
ρ (1/fm3)
0.16
0.14
0.12
0.1
0.08
0.06
0.04
0.02
0
ISGQR

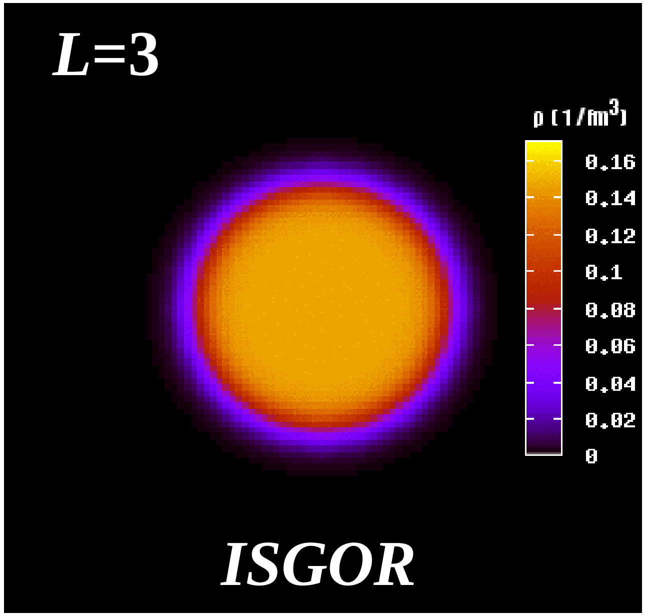
L=3
ρ (1/fm3)
0.16
0.14
0.12
0.1
0.08
0.06
0.04
0.02
0
ISGOR

In fluid mechanics, compressibility is a measure of the relative volume change of a fluid as a response to a pressure change.

$$\beta = -\frac{1}{V}\frac{\partial V}{\partial P}$$

where P is pressure, V is volume.

Incompressibility or bulk modulus (K) is a measure of a substance's resistance to uniform compression and can be formally defined:

$$K = -V\frac{\partial P}{\partial V}$$

For the equation of state of symmetric nuclear matter at saturation nuclear density:

$$\left[\frac{d(E/A)}{d\rho}\right]_{\rho=\rho_0} = 0$$

and one can derive the incompressibility of nuclear matter:

$$K_{nm} = \left[9\rho^2 \frac{d^2(E/A)}{d\rho^2}\right]_{\rho=\rho_0}$$

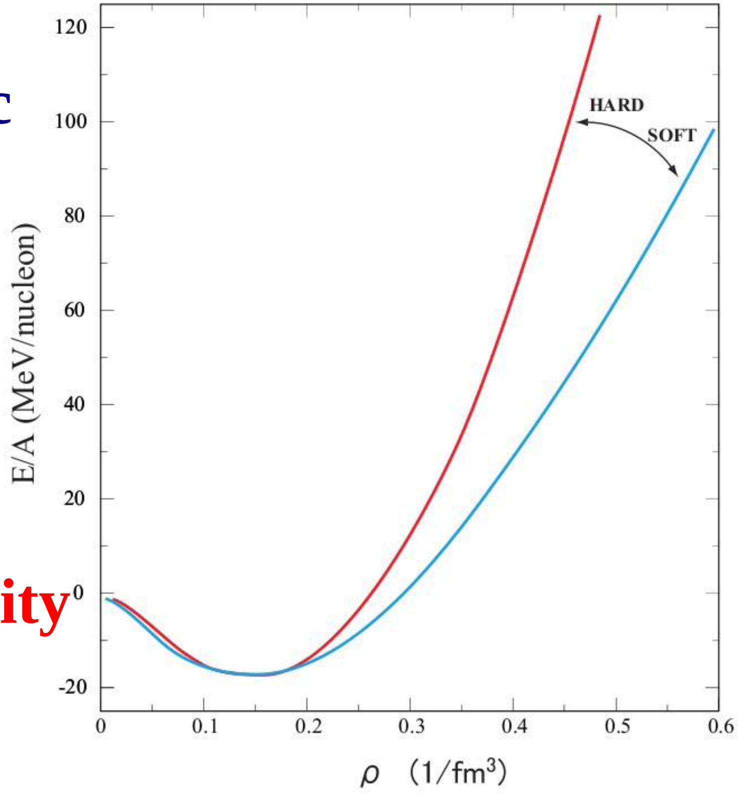

***E/A*: binding energy per nucleon**

***ρ* : nuclear density**

***ρ₀* : nuclear density at saturation**

J.P. Blaizot, Phys. Rep. 64 (1980) 171

Equation of state (EOS) of nuclear matter

More complex than for infinite neutral liquids
Neutrons and protons with different interactions
Coulomb interaction of protons

1. **Governs the collapse and explosion of giant stars (supernovae)**

2. **Governs formation of neutron stars (mass, radius, crust)**

3. **Governs collisions of heavy ions.**

4. **Important ingredient in the study of nuclear properties.**

Isoscalar Excitation Modes of Nuclei

Hydrodynamic models/Giant Resonances

Coherent vibrations of nucleonic fluids in a nucleus.

Compression modes: ISGMR, ISGDR

In Constrained and Scaling Models:

$$E_{ISGMR} = \hbar\sqrt{\frac{K_A}{m\langle r^2\rangle}}$$

$$E_{ISGDR} = \hbar\sqrt{\frac{7}{3}\frac{K_A + \frac{27}{25}\varepsilon_F}{m\langle r^2\rangle}}$$

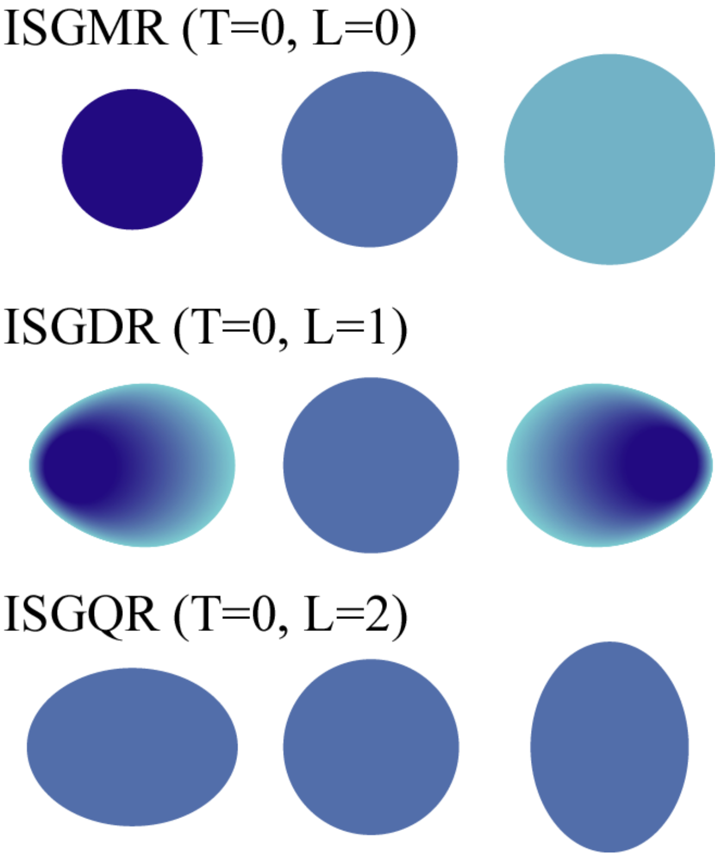

ε_F is the Fermi energy and the nucleus incompressibility:

$$\rightarrow \; K_A = \left[r^2 (d^2(E/A)/dr^2) \right]_{r=R_0}$$

J.P. Blaizot, Phys. Rep. 64 (1980) 171

Giant resonances

- **Macroscopic properties: E_x, Γ, %EWSR**
- **Isoscalar giant resonances; compression modes**

  ISGMR, ISGDR ⇒ Incompressibility, symmetry energy

$$K_A = K_{vol} + K_{surf}A^{-1/3} + K_{sym}((N-Z)/A)^2 + K_{Coul}Z^2A^{-4/3}$$

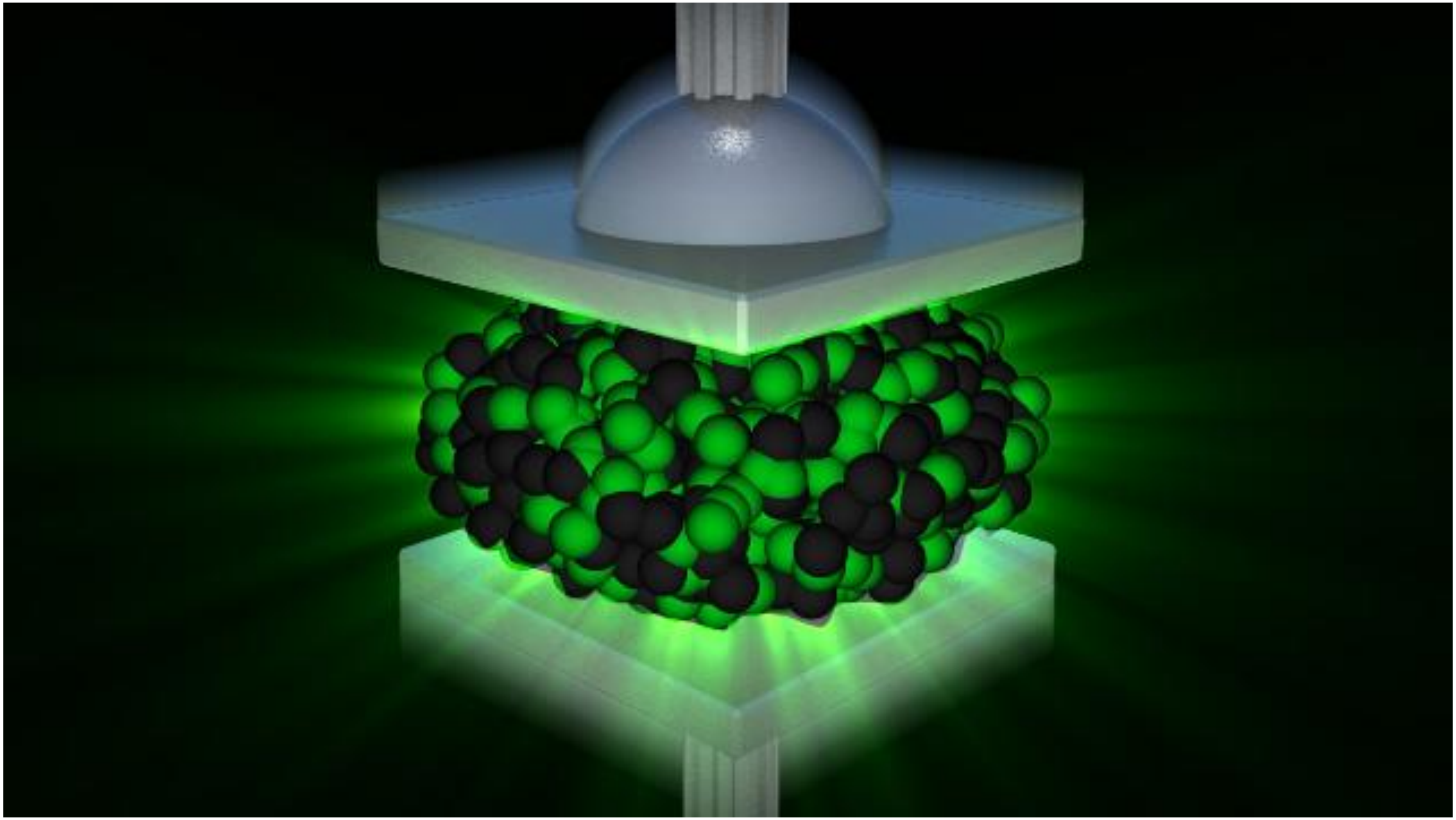

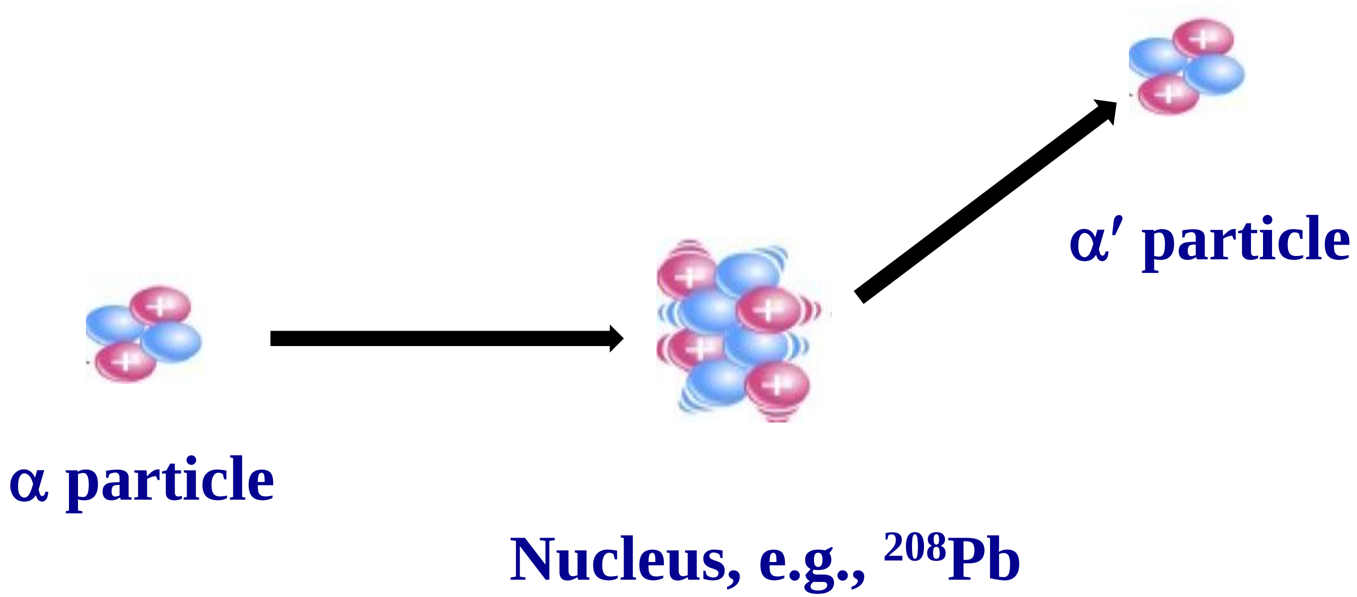

Inelastic α scattering

ISGQR, ISGMR

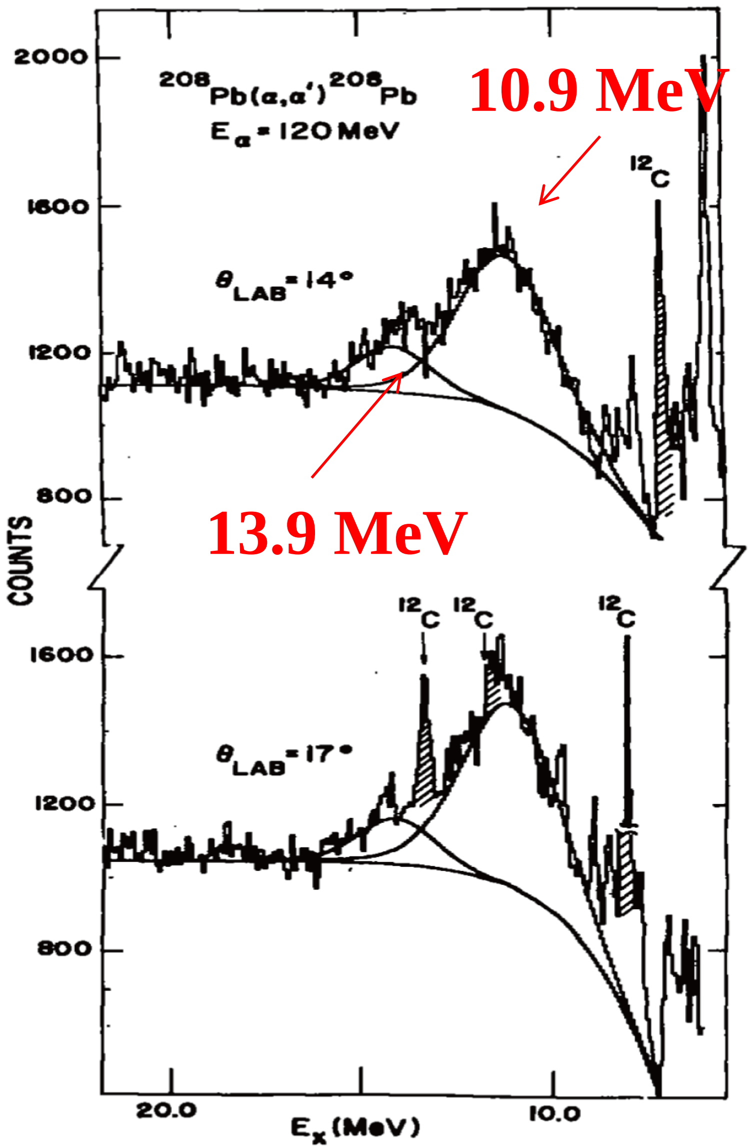

⇐ ^{208}Pb(α,α′) at E_α=120 MeV

Large instrumental background and nuclear continuum!

M. N. Harakeh *et al.*, Phys. Rev. Lett. 38 (1977) 676

ISGMR $L = 0$

ISGDR $L = 1$

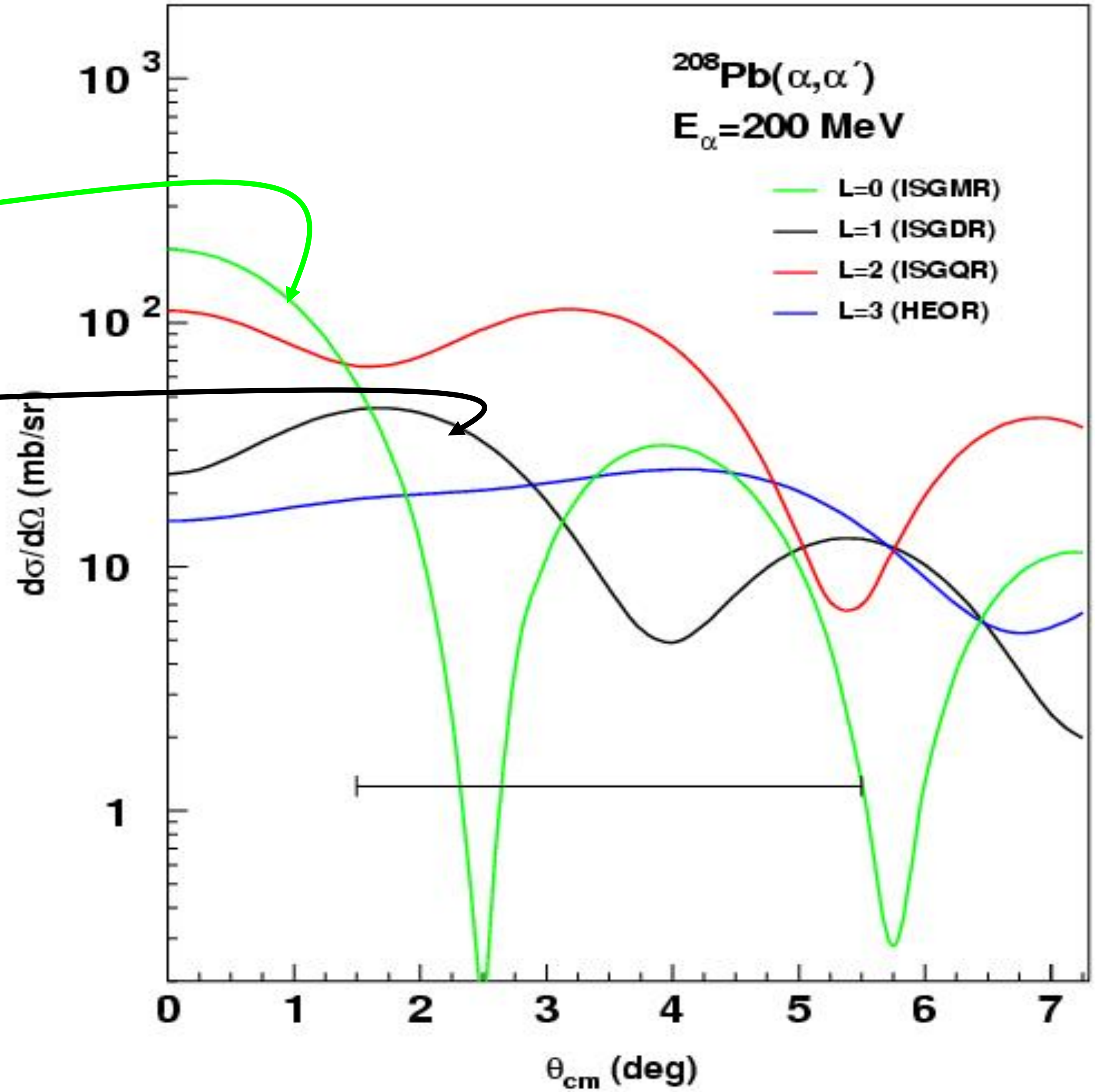

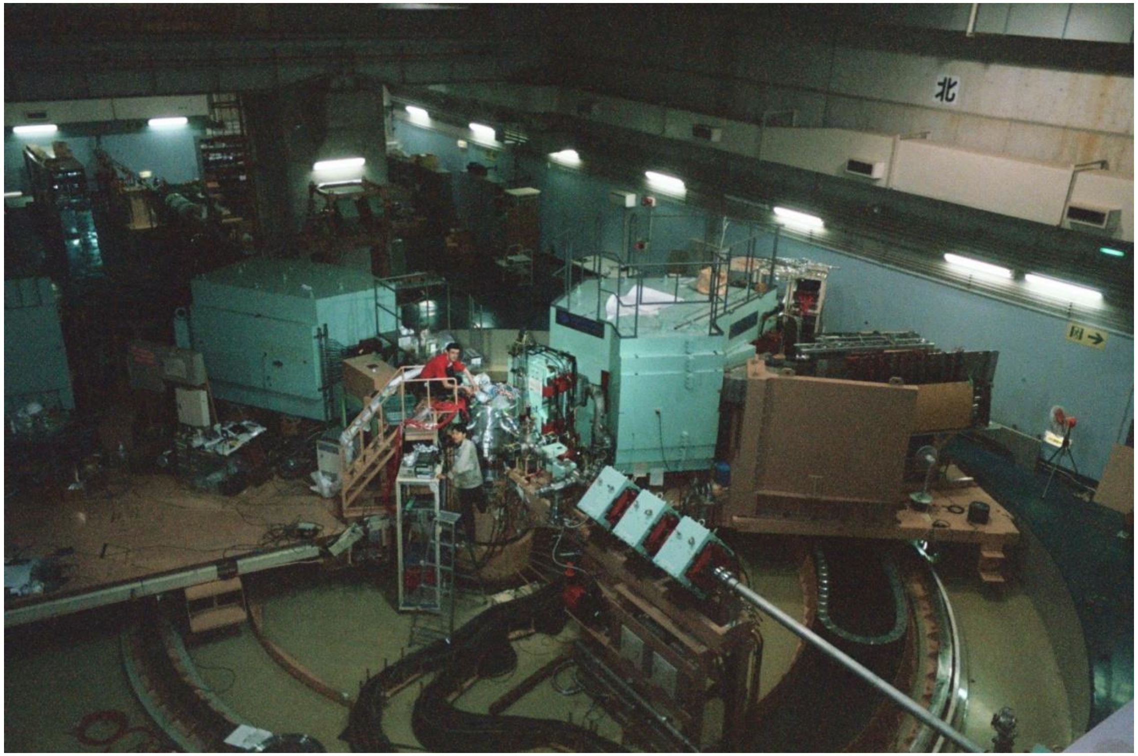

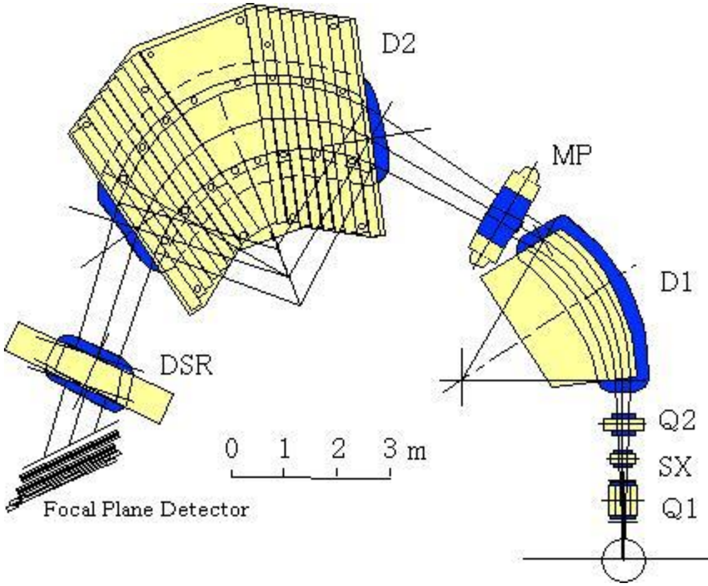

Grand Raiden@ RCNP

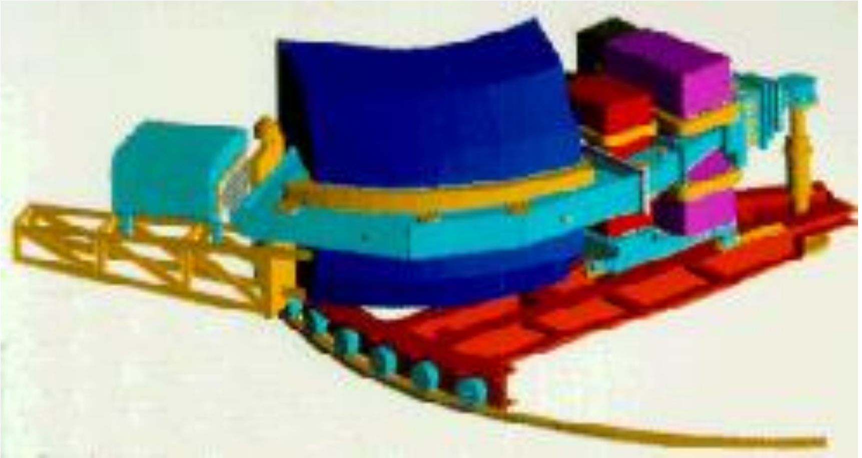

BBS@KVI

(p,p') at E_p~ 300
(α,α') at E_α~ 400 & 200 MeV at RCNP & KVI, respectively

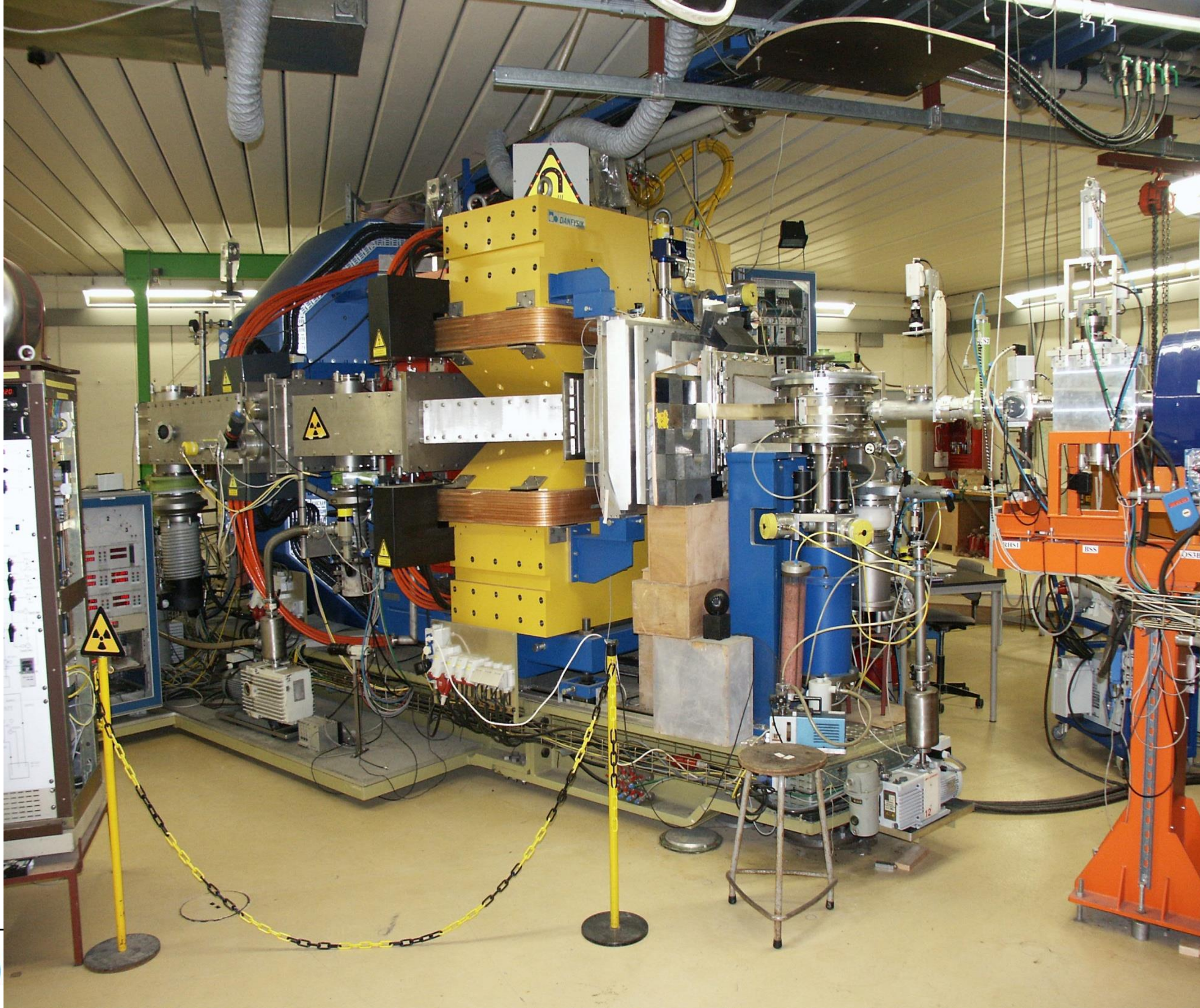
DANFYSIK

Si-ball
16 Si-detectors at
10 cm from the target
total solid angle: 1 sr

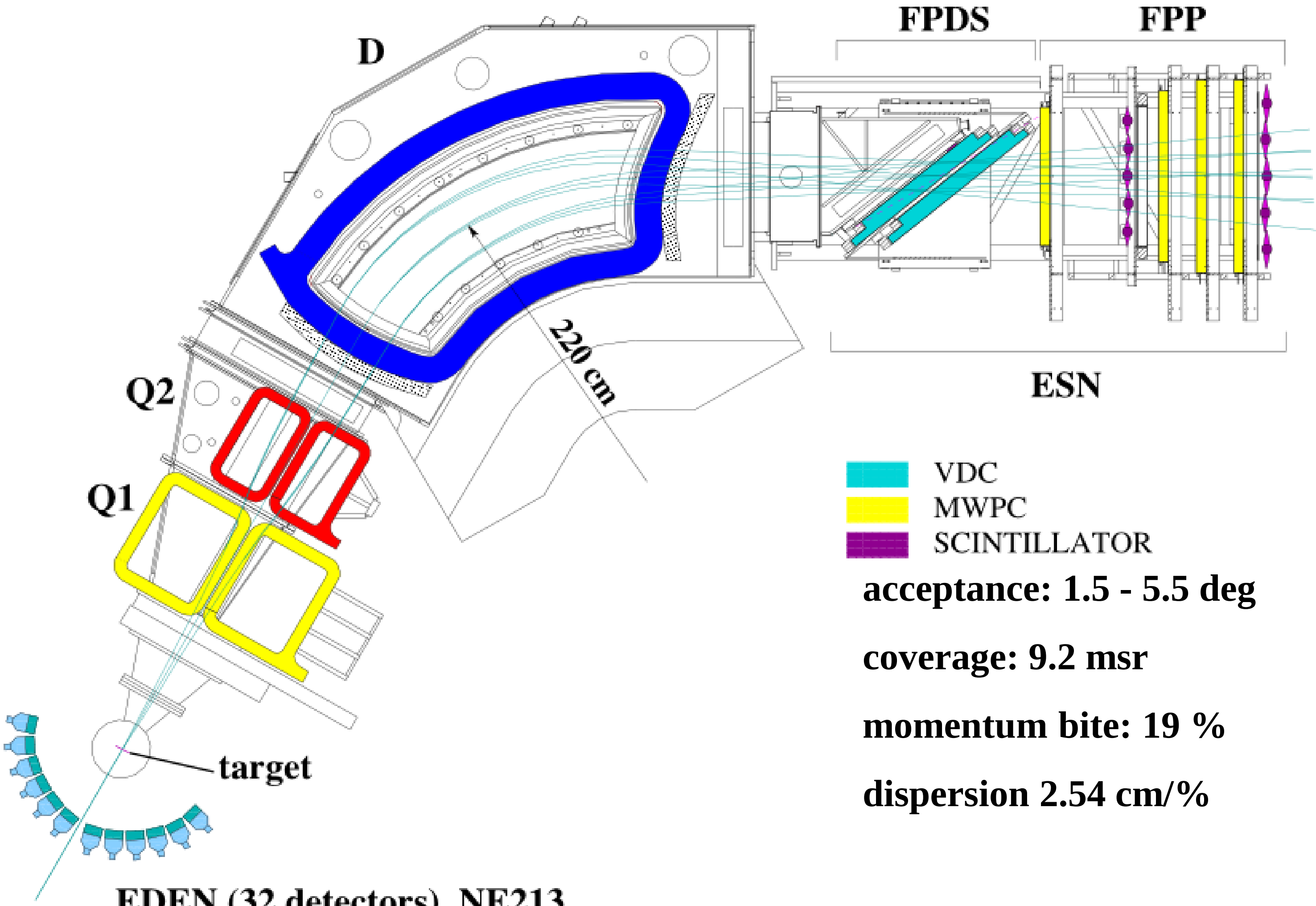

acceptance: 1.5 - 5.5 deg

coverage: 9.2 msr

momentum bite: 19 %

dispersion 2.54 cm/%

total solid angle: 0.37 sr

KVI Big-Bite Spectrometer (BBS)

ISGQR at 10.9 MeV

ISGMR at 13.9 MeV

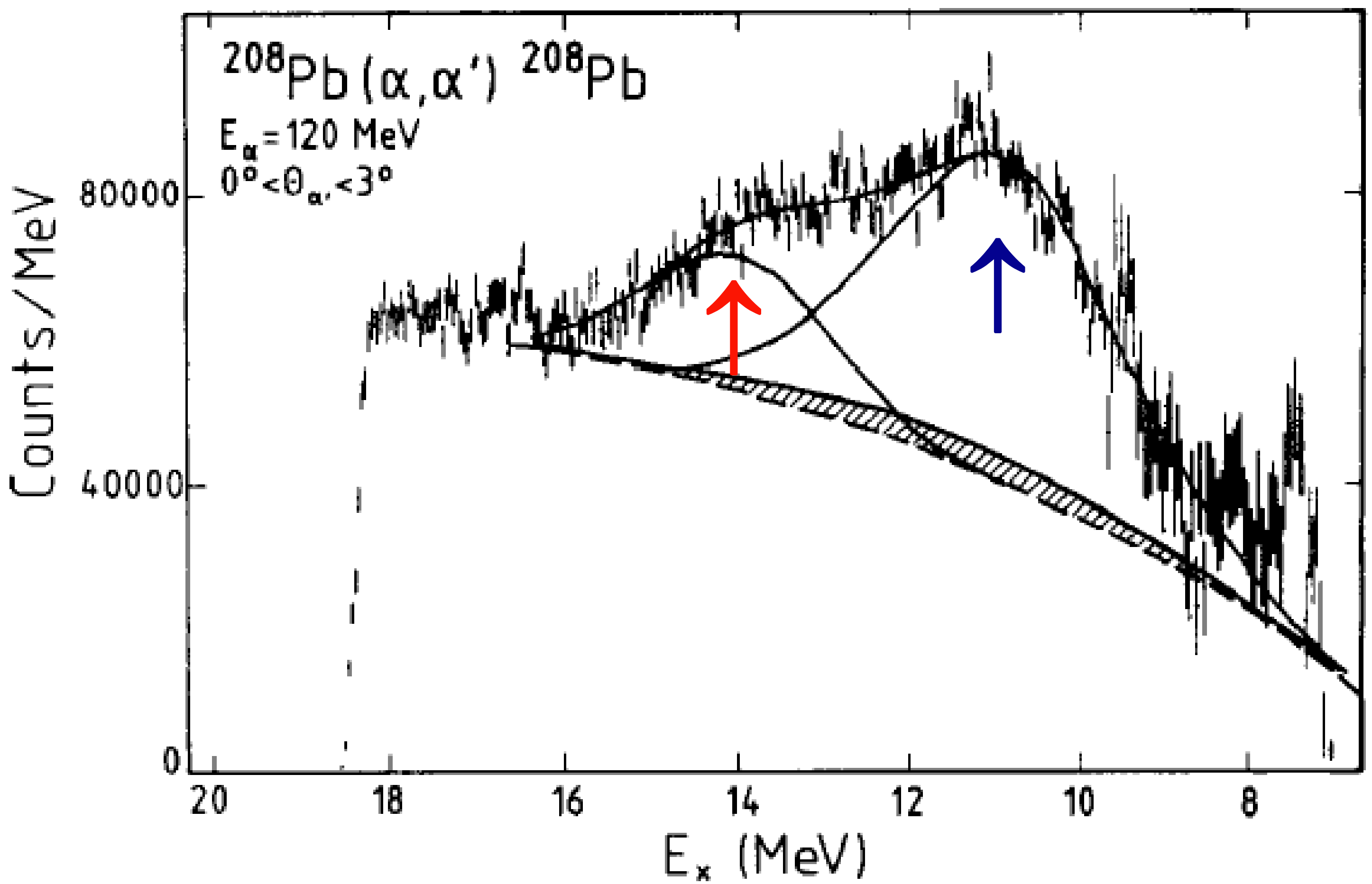

Difference of spectra

$0° < \theta_{\alpha'} < 3°$

$0° < \theta_{\alpha'} < 1.5°$

$1.5° < \theta_{\alpha'} < 3°$

Difference

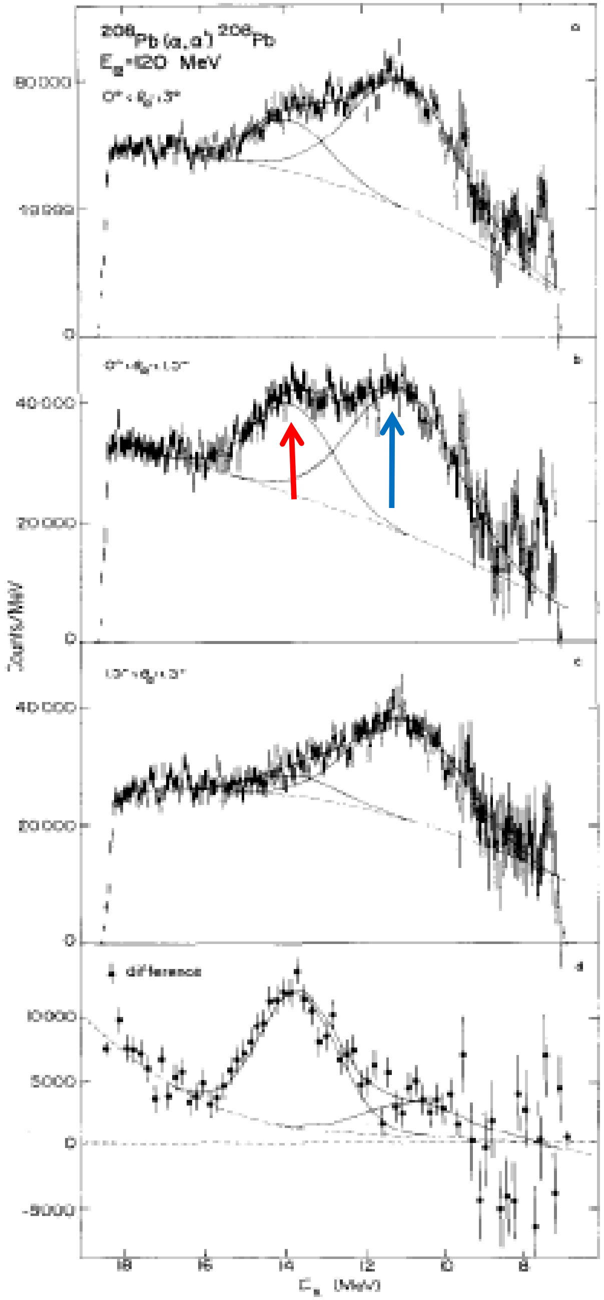

KVI

university of groningen

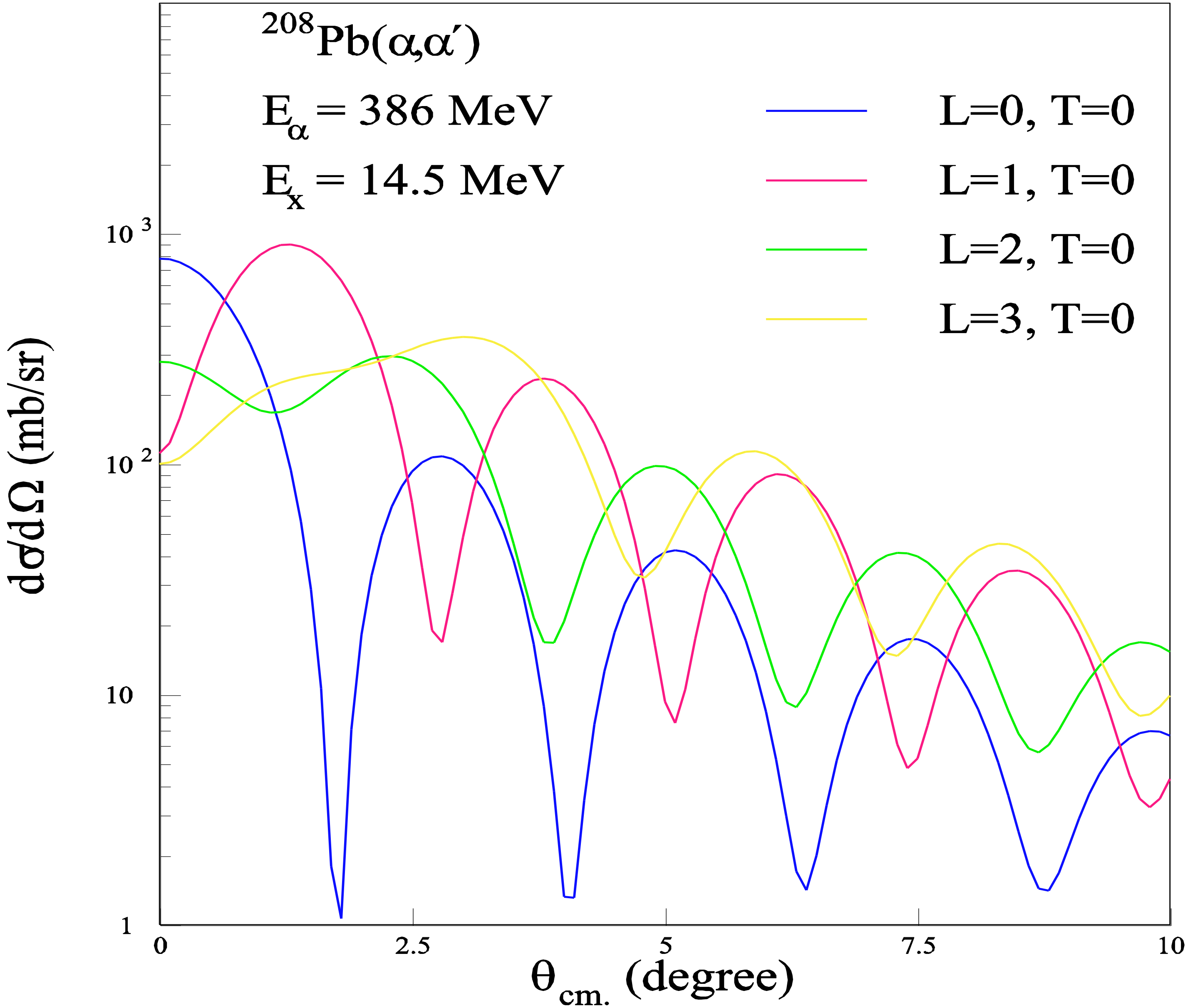

ISGMR, ISGDR

ISGQR, HEOR

100 % EWSR

At E_x= 14.5 MeV

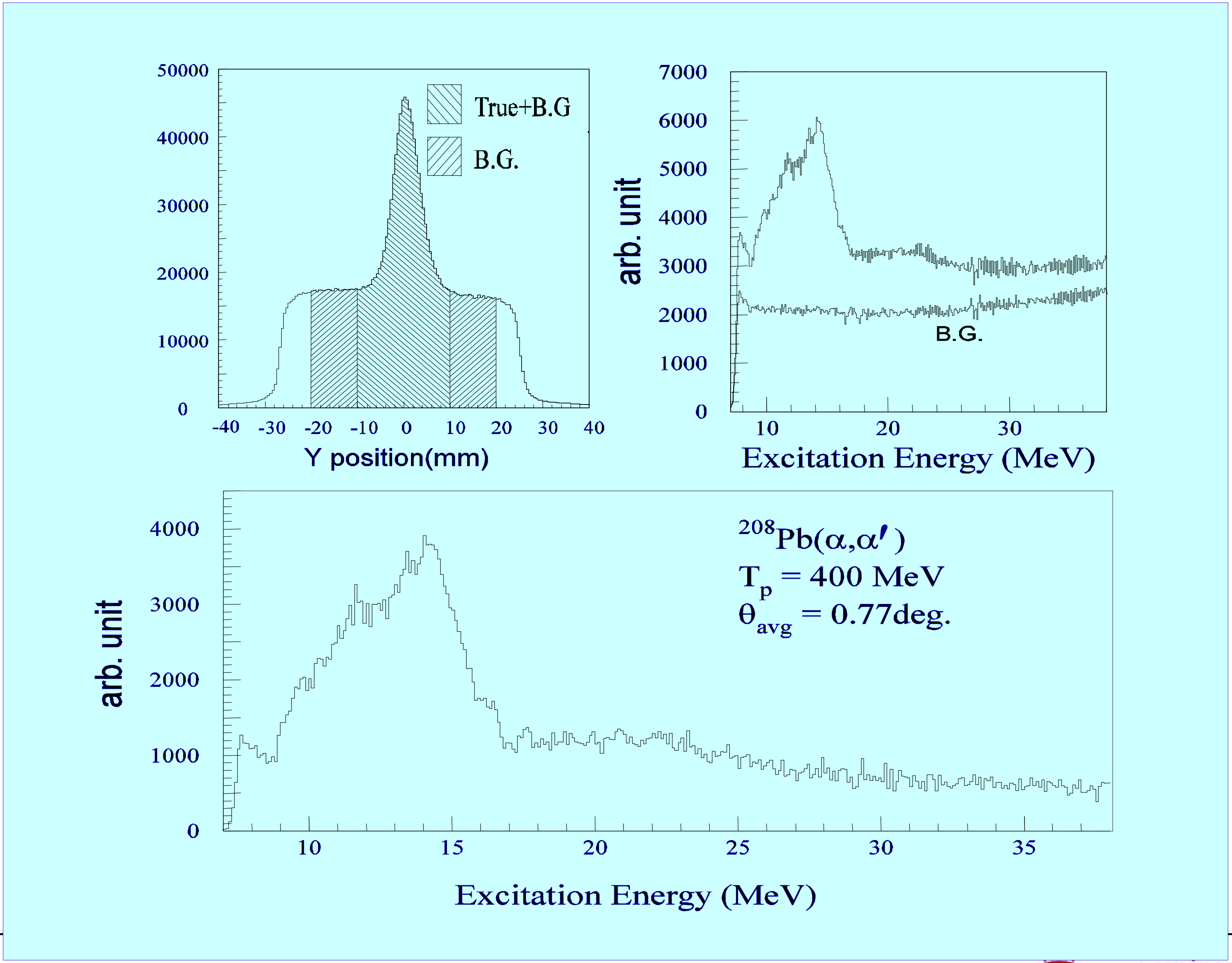
50000
40000
30000
20000
10000
0
True+B.G
B.G.
-40 -30 -20 -10 0 10 20 30 40
Y position(mm)
7000
6000
5000
4000
3000
2000
1000
0
arb. unit
B.G.
10 20 30
Excitation Energy (MeV)
4000
3000
2000
1000
0
arb. unit
$^{208}Pb(\alpha,\alpha')$
$T_p = 400$ MeV
$\theta_{avg} = 0.77$deg.
10 15 20 25 30 35
Excitation Energy (MeV)

Multipole decomposition analysis (MDA)

$$\left(\frac{d^2\sigma}{d\Omega dE}(\vartheta_{c.m.},E)\right)^{\exp.} = \sum_L a_L(E)\left(\frac{d^2\sigma}{d\Omega dE}(\vartheta_{c.m.},E)\right)_L^{calc.}$$

$$\left(\frac{d^2\sigma}{d\Omega dE}(\vartheta_{c.m.},E)\right)^{\exp.} : \text{Experimental cross section}$$

$$\left(\frac{d^2\sigma}{d\Omega dE}(\vartheta_{c.m.},E)\right)_L^{calc.} : \text{DWBA cross section (unit cross section)}$$

$a_L(E)$: EWSR fraction

a. ISGR (L<15)+ IVGDR (through Coulomb excitation)

b. DWBA formalism; single folding ⇒ transition potential

$$\delta U_L(r,E) = \int d\vec{r}'\,\delta\rho_L(\vec{r}',E)[V(|\vec{r}-\vec{r}'|,\rho_0(r')) + \rho_0(r')\frac{\partial V(|\vec{r}-\vec{r}'|,\rho(r'))}{\partial\rho_0(r')}]$$

$$U(r) = \int d\vec{r}'V(|\vec{r}-\vec{r}'|,\rho_0(r'))\rho_0(r')$$

Transition density

- **ISGMR Satchler, Nucl. Phys. A472 (1987) 215**

$$\delta\rho_0(r,E) = -\alpha_0[3 + r\frac{d}{dr}]\rho_0(r)$$

$$\alpha_0^2 = \frac{2\pi\hbar^2}{mA < r^2 > E}$$

- **ISGDR Harakeh & Dieperink, Phys. Rev. C23 (1981) 2329**

$$\delta\rho_1(r,E) = -\frac{\beta_1}{R\sqrt{3}}[3r^2\frac{d}{dr} + 10r - \frac{5}{3} < r^2 > \frac{d}{dr} + \varepsilon(r\frac{d^2}{dr^2} + 4\frac{d}{dr})]\rho_0(r)$$

$$\beta_1^2 = \frac{6\pi\hbar^2}{mAE}\frac{R^2}{(11 < r^4 > -(25/3) < r^2 >^2 - 10\varepsilon < r^2 >)}$$

- **Other modes Bohr-Mottelson (BM) model**

$$\delta\rho_L(r,E) = -\delta_L\frac{d}{dr}\rho_0(r)$$

$$\delta_L^2 = (\beta_L c)^2 = \frac{L(2L+1)^2}{(L+2)^2}\frac{2\pi\hbar^2}{mAE}\frac{< r^{2L-2} >}{< r^{L-1} >^2}$$

Uchida *et al.*,
Phys. Lett. B557 (2003) 12
Phys. Rev. C69 (2004) 051301

(α,α′) spectra at 386 MeV

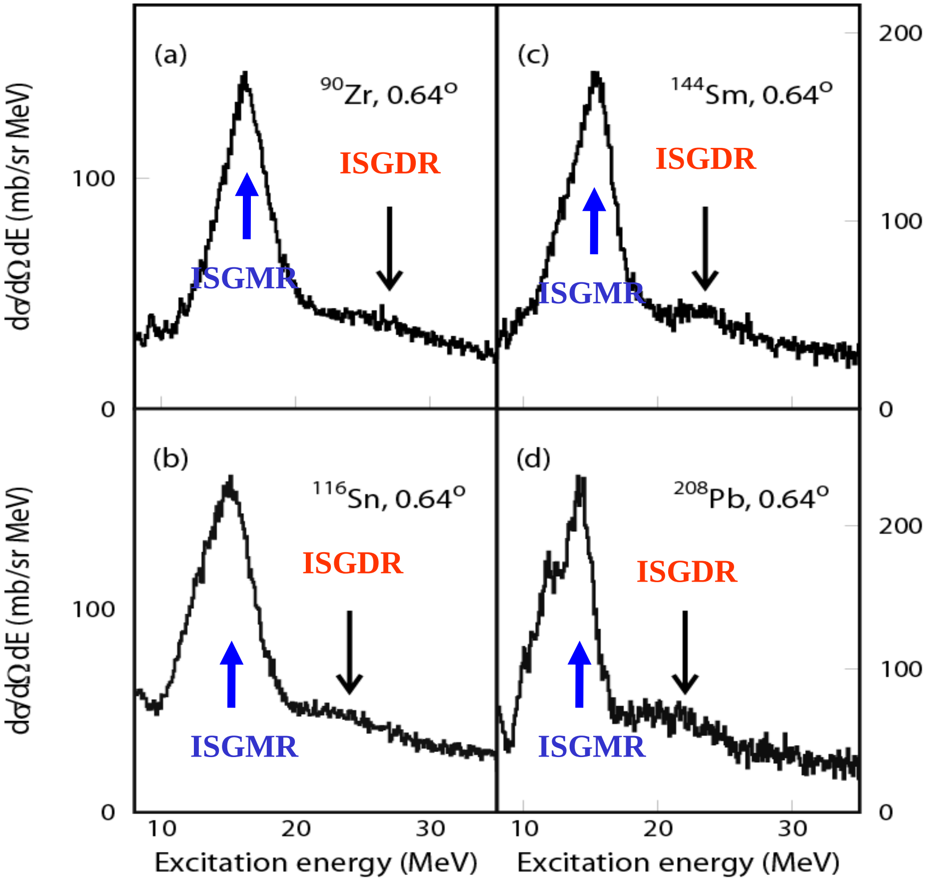

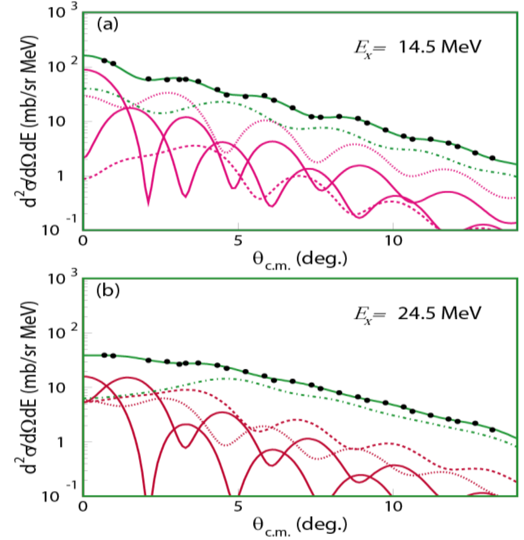

^{116}Sn

MDA results for *L=0* and *L=1*

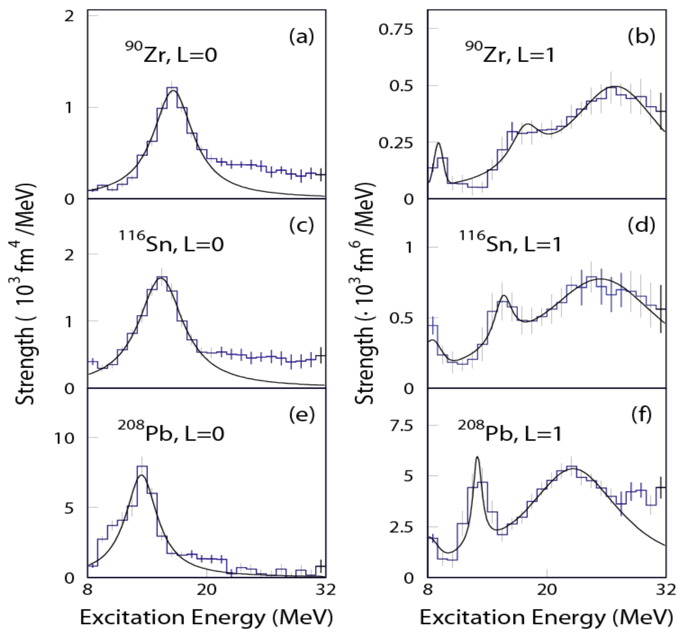

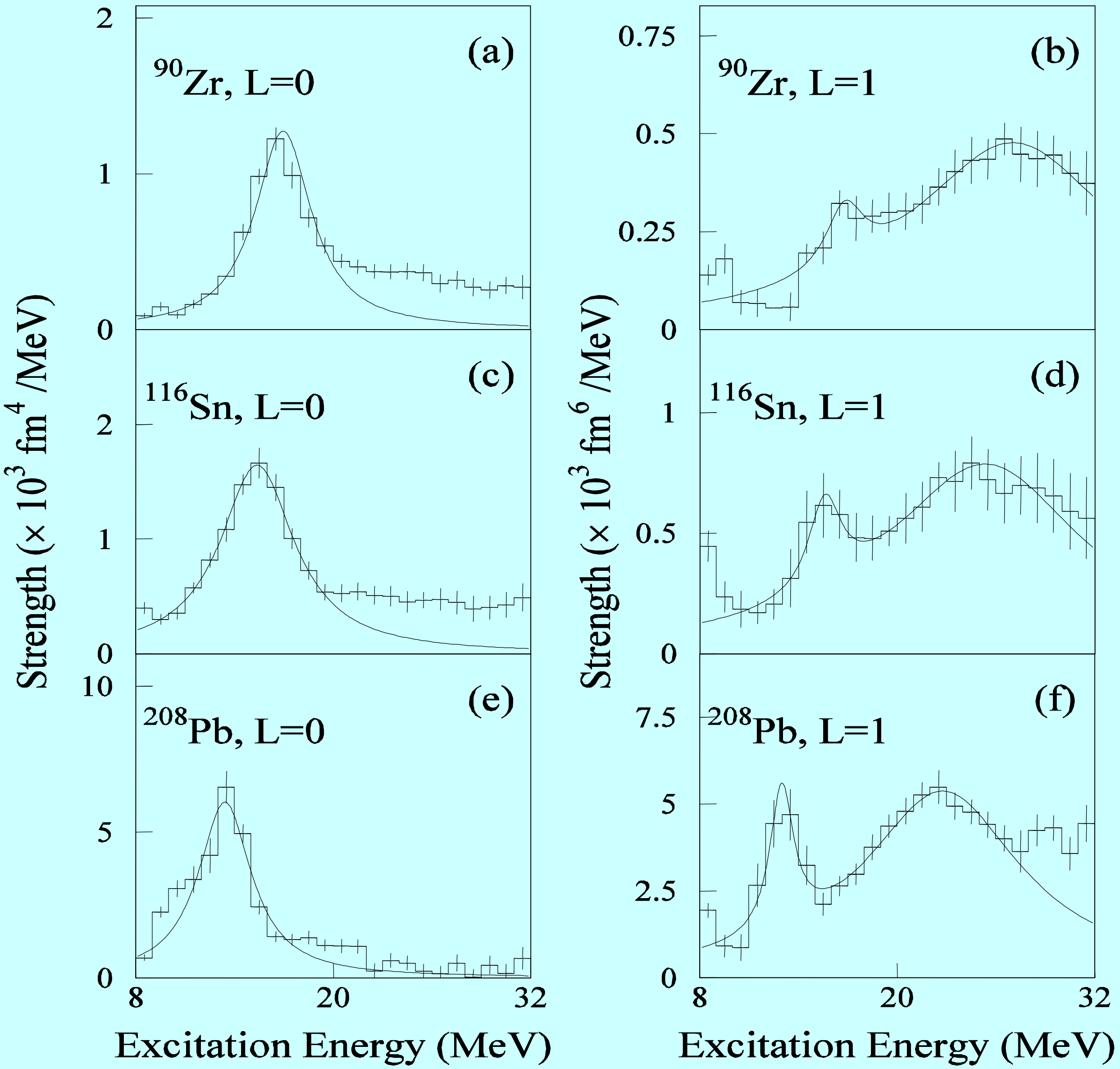

Strength (× 10³ fm⁴ /MeV)
Strength (× 10³ fm⁶ /MeV)
(a)
⁹⁰Zr, L=0
(b)
⁹⁰Zr, L=1
(c)
¹¹⁶Sn, L=0
(d)
¹¹⁶Sn, L=1
(e)
²⁰⁸Pb, L=0
(f)
²⁰⁸Pb, L=1
Excitation Energy (MeV)
Excitation Energy (MeV)

In HF+RPA calculations,

$$K_{nm} = \left[9\rho^2 \frac{d^2(E/A)}{d\rho^2} \right]_{\rho=\rho_0}$$

Nuclear matter

***E/A*: binding energy per nucleon**

K_A: incompressibility

ρ : nuclear density

ρ_0 : nuclear density at saturation

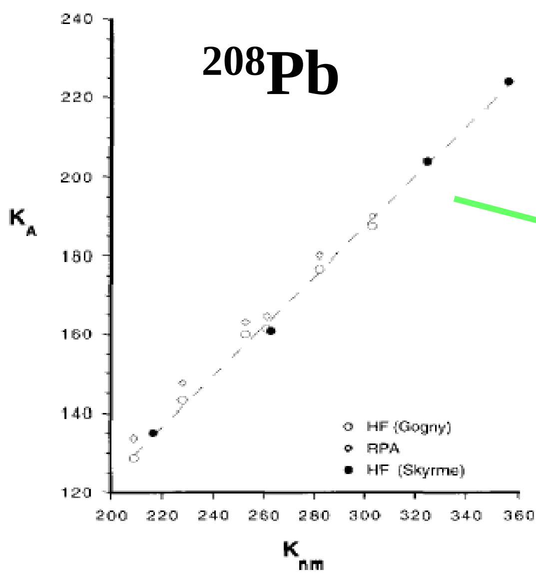

K_A is obtained from excitation energy of ISGMR & ISGDR

$$K_A = 0.64 K_{nm} - 3.5$$

J.P. Blaizot, Nucl. Phys. A591 (1995) 435

From GMR data on ^{208}Pb and ^{90}Zr,

$K_\infty = 240 \pm 10$ MeV

[See, *e.g.*, G. Colò *et al.*, Phys. Rev. C 70 (2004) 024307]

This number is consistent
with both ISGMR and ISGDR Data
and
with non-relativistic and relativistic calculations

Isoscalar GMR strength distribution in Sn-isotopes obtained by Multipole Decomposition Analysis of singles spectra obtained in ^{A}Sn(α,α′) measurements at incident energy 400 MeV and angles from 0º to 9º

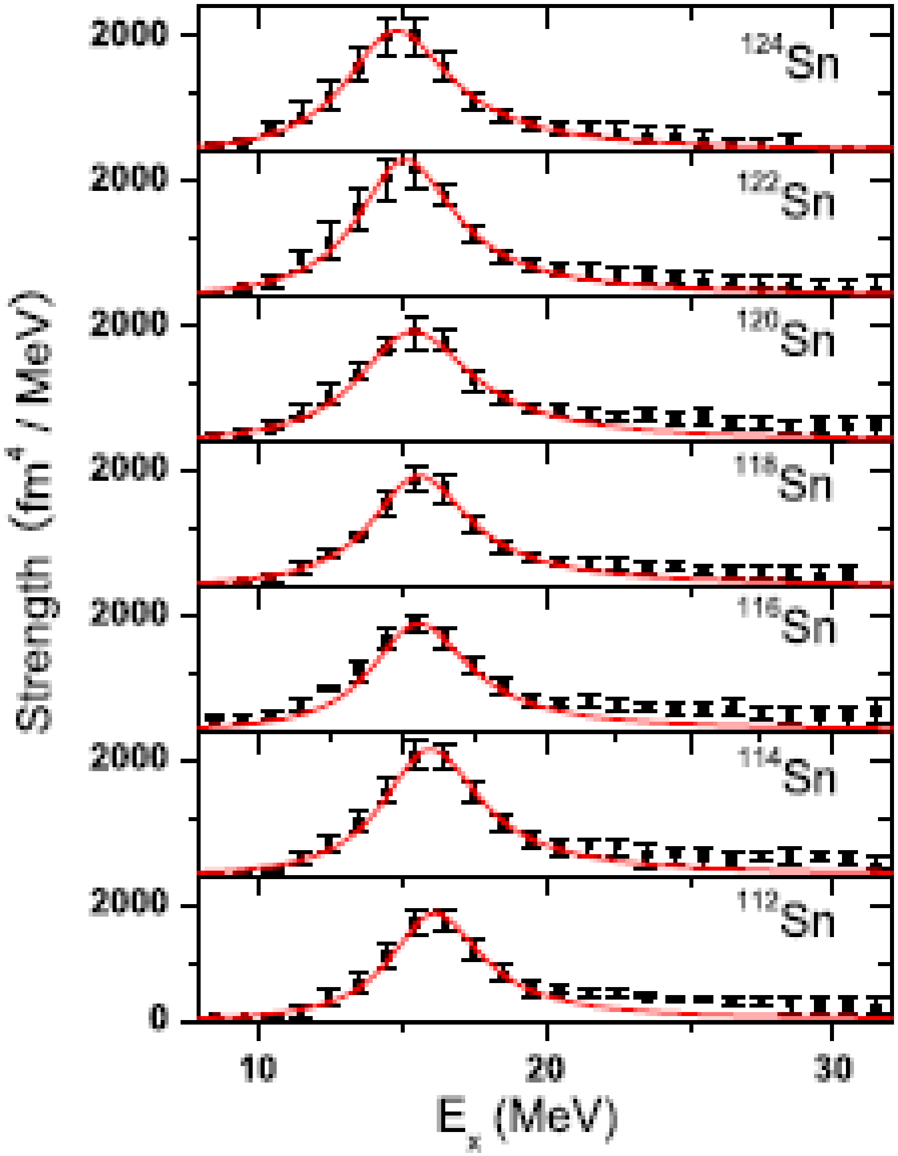

$$K_A \sim K_{vol}(1 + cA^{-1/3}) + K_\tau((N - Z)/A)^2 + K_{Coul} Z^2 A^{-4/3}$$

$$K_A - K_{Coul} Z^2 A^{-4/3} \sim K_{vol}(1 + cA^{-1/3}) + K_\tau((N - Z)/A)^2$$

$$\sim \text{Constant} + K_\tau((N - Z)/A)^2$$

We use K_{Coul} = - 5.2 MeV (from Sagawa)

$(N - Z)/A$

^{112}Sn – ^{124}Sn: 0.107 – 0.194

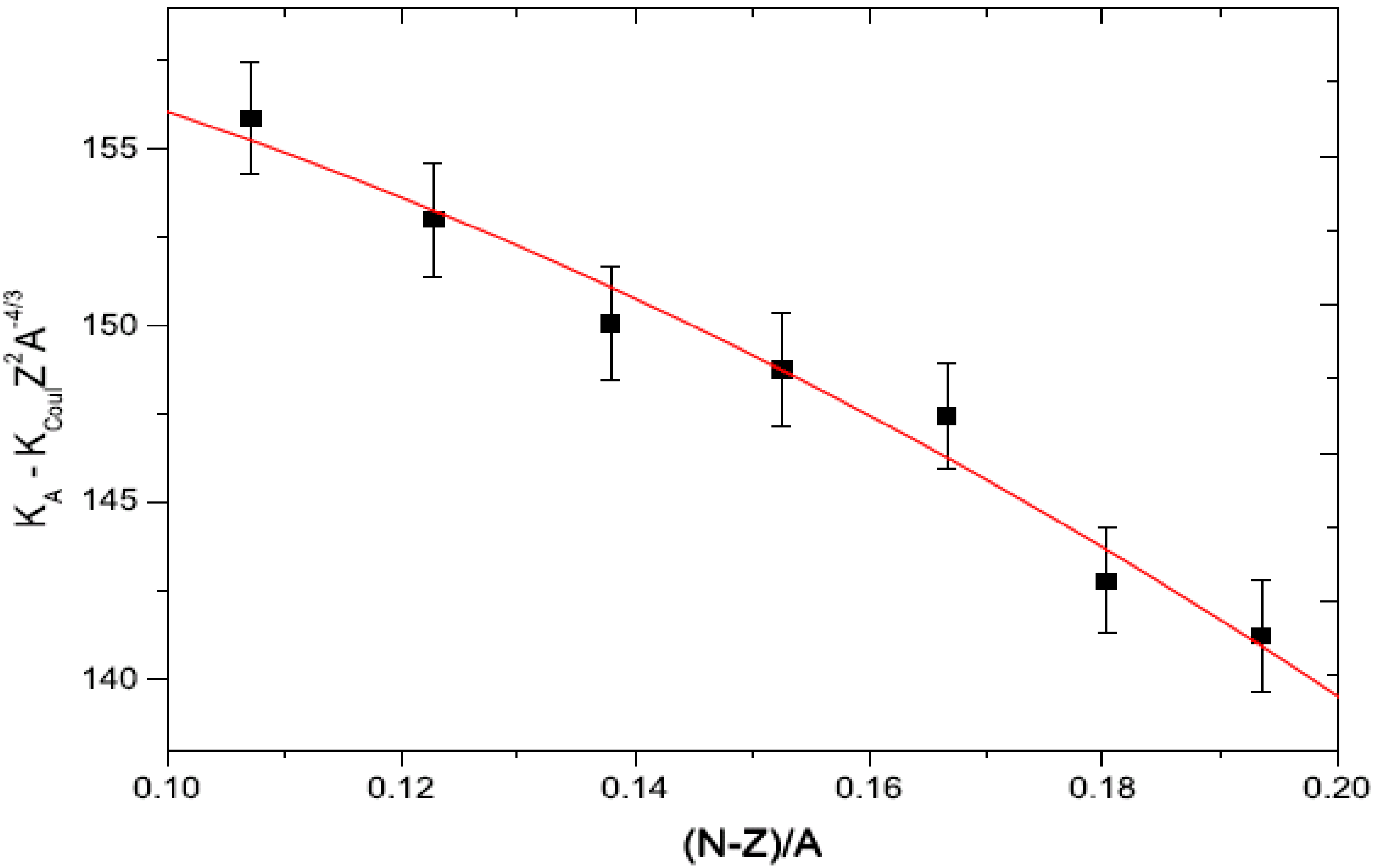

Sn isotopes ⇒ $K_\tau = -550 \pm 100$ MeV

Monopole strength Distribution

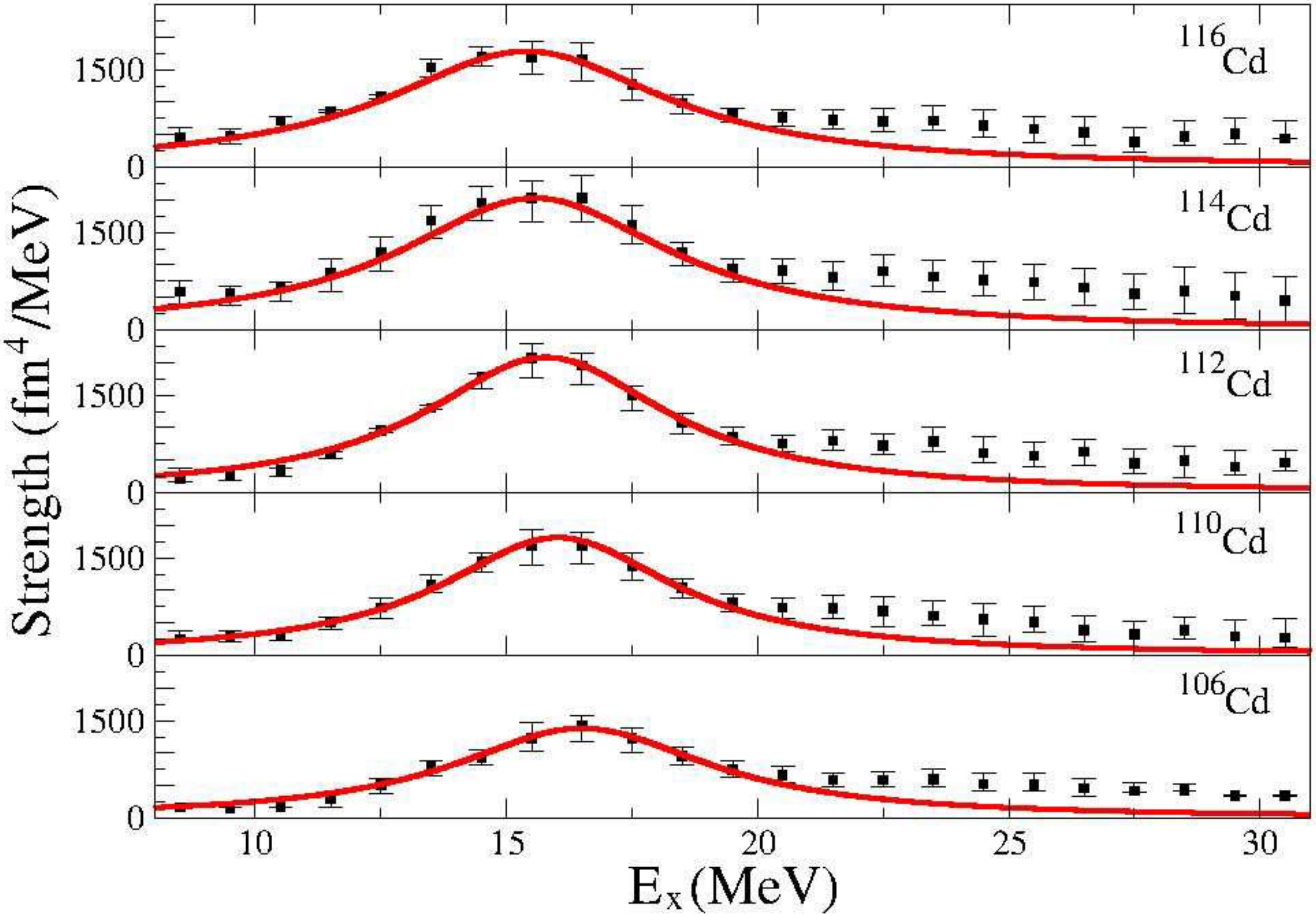

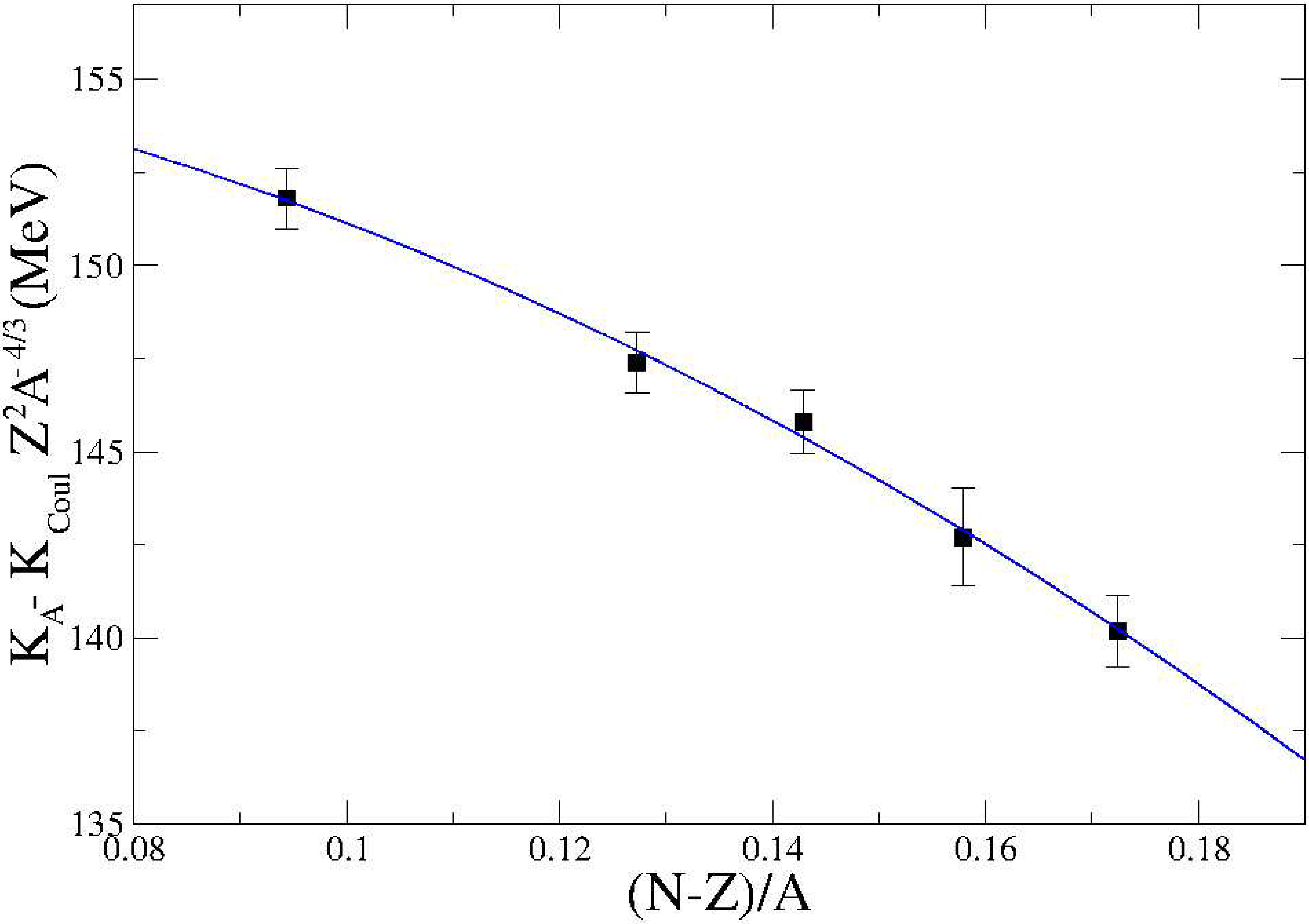

Cd isotopes ⇒ $K_\tau = -555 \pm 75$ MeV

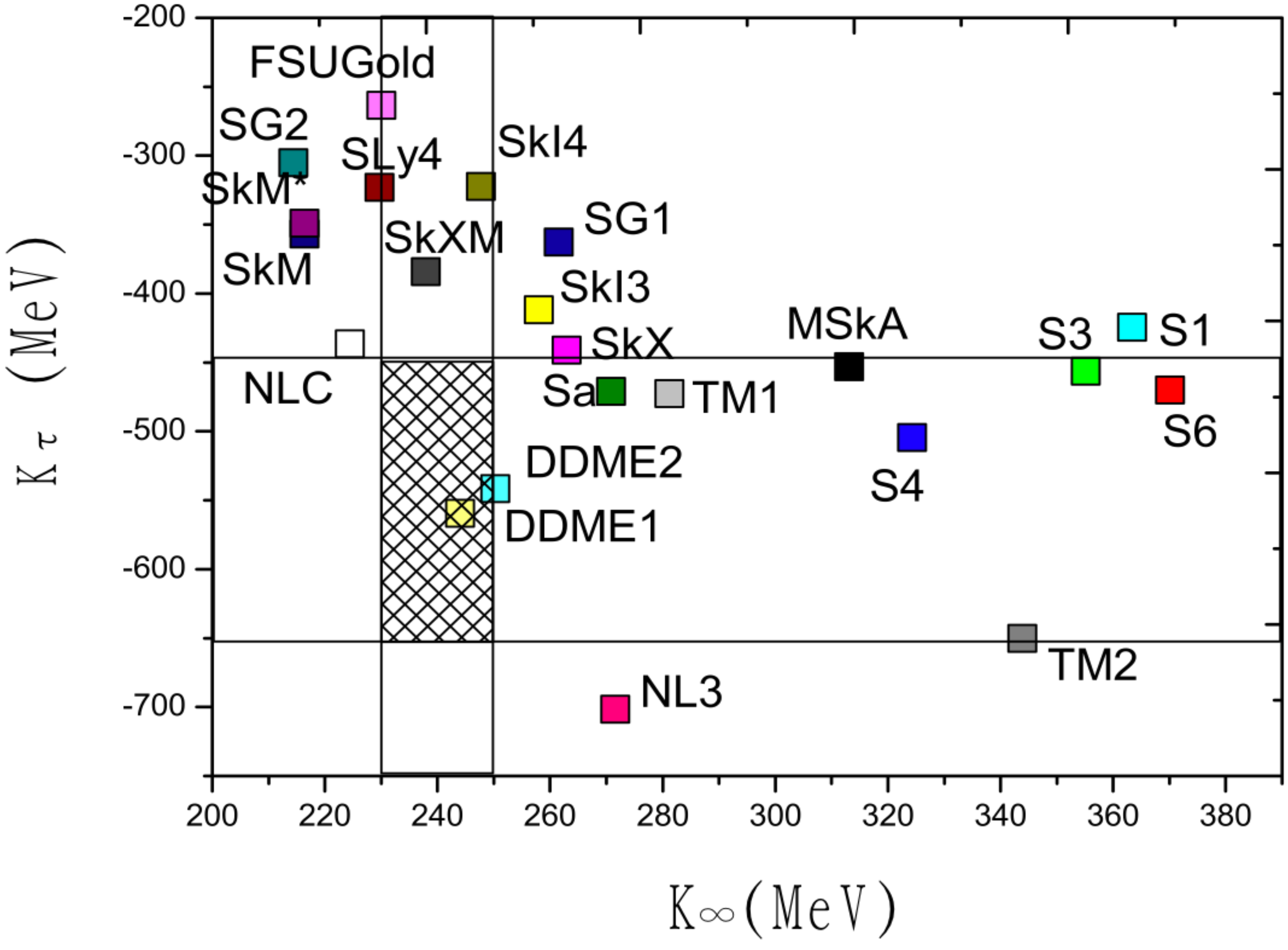

Data from H. Sagawa *et al*., Phys. Rev. C **76** (2007) 034327

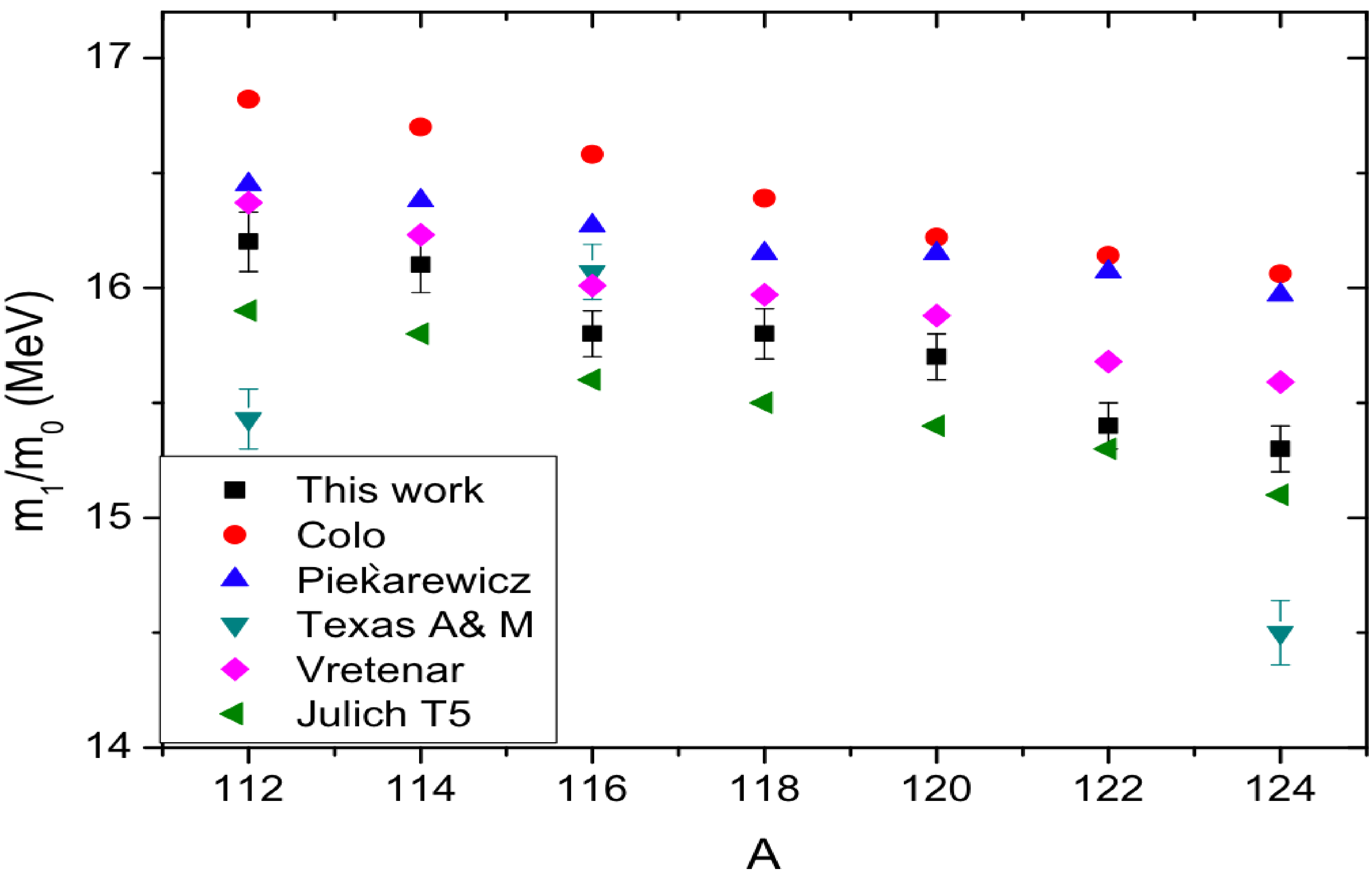

17
16
15
14
m_1/m_0 (MeV)
112
114
116
118
120
122
124
A
This work
Colo
Piekarewicz
Texas A& M
Vretenar
Julich T5

Colò *et al*.: Non-relativistic RPA (without pairing) reproduces ISGMR in ^{208}Pb and ^{90}Zr.

Piekarewicz: Relativistic RPA (FSUGold model) reproduces g.s. observables and ISGMR in ^{208}Pb, ^{144}Sm and ^{90}Zr [K_∞ = 230 MeV]

Vretenar: Relativistic mean field (DD-ME2: density-dependent mean-field effective interaction).

[K_∞ = 240 MeV]. Possibly agreement is fortuitous since strength distributions are not much different from those by Colò *et al*. and Piekarewicz.

Tselyaev *et al*.: Quasi-particle time-blocking approximation (QTBA) (T5 Skyrme interaction)

[K_∞ = 202 MeV?!]

Softness of Sn-nuclei is still unresolved

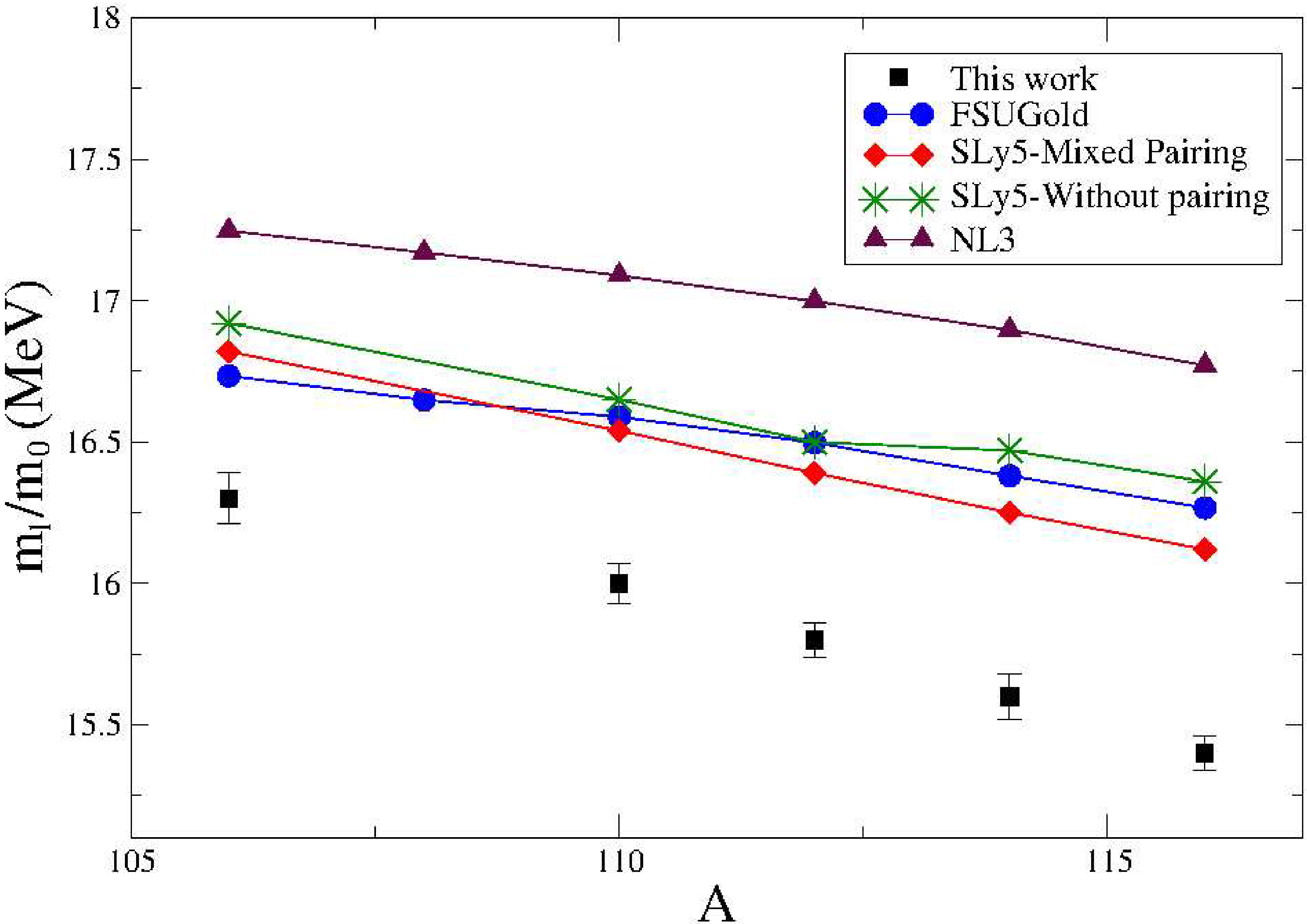

RRPA: FSUGold [K_∞ = 230 MeV]; SLy5 [K_∞ = 230 MeV]; NL3 [K_∞ = 271 MeV]

Splitting of the ISGMR under deformation

K projection of *J* on symmetry axis is good quantum number in deformed nuclei

Coupling of ISGMR with *K*=0 component of ISGQR

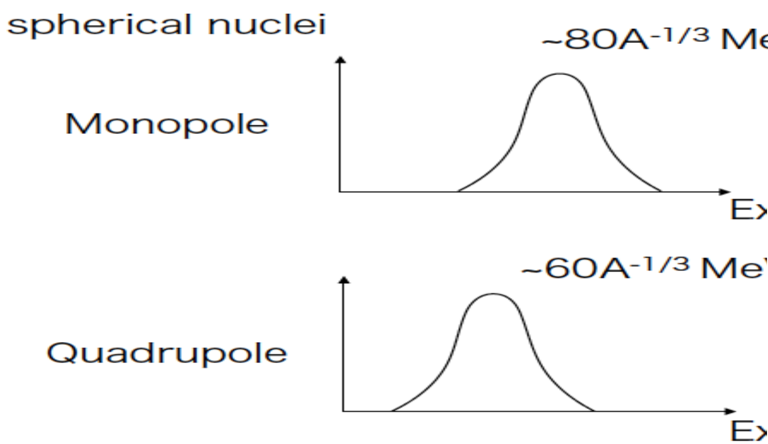

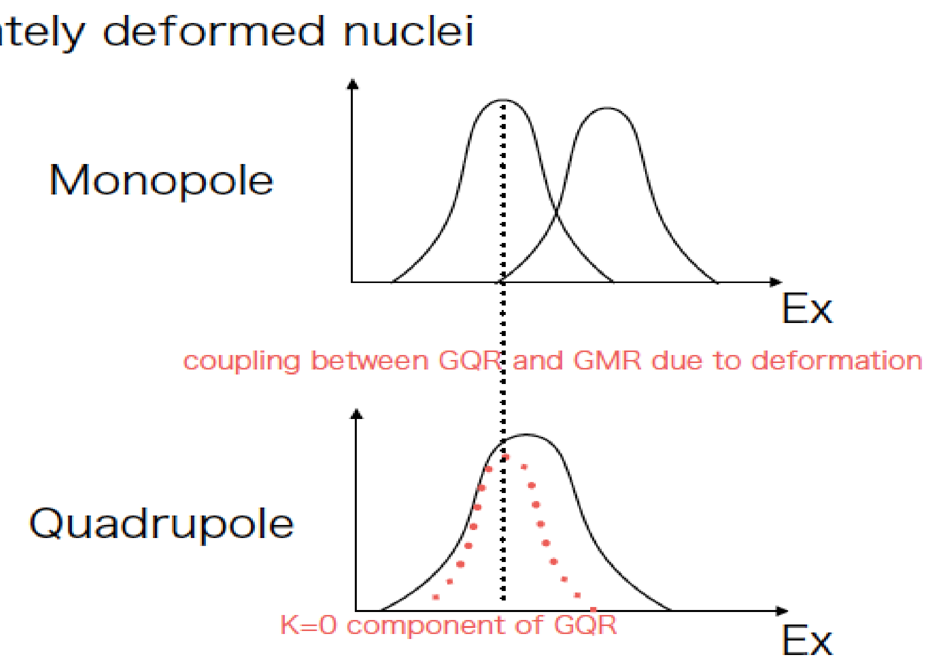

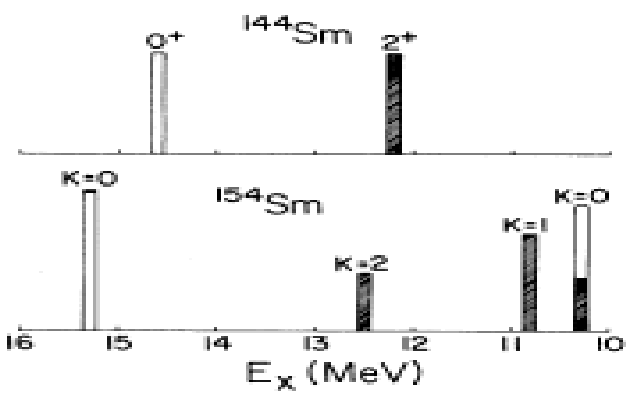

Isoscalar Giant Resonances in Nd isotopes: QRPA calculations

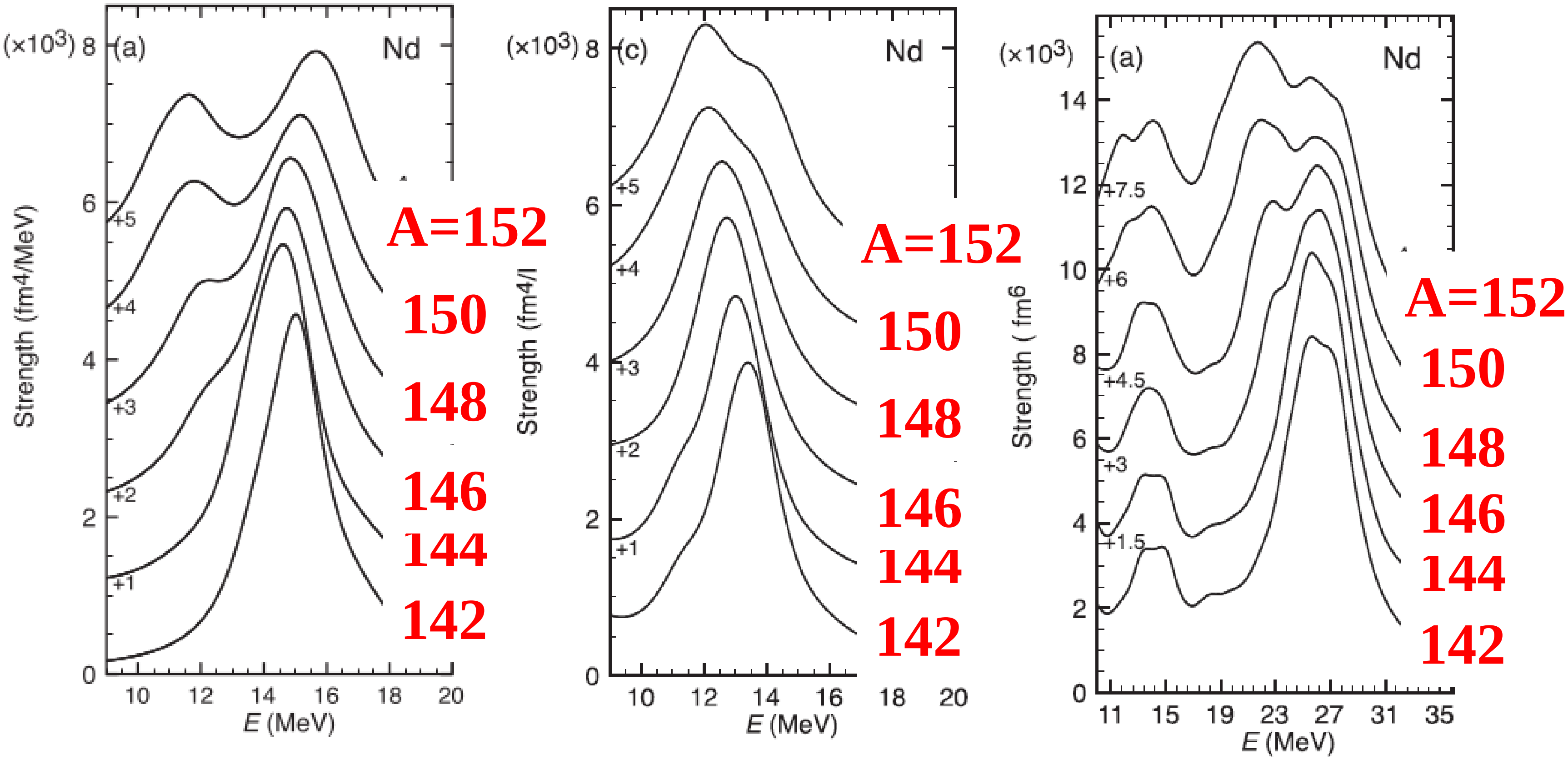

ΔL = 0; ISGMR ΔL = 2; ISGQR ΔL = 1; ISGDR

K. Yoshida and T. Nakatsukasa, Phys. Rev. C 88 (2013) 034309

Effect of deformation on Isoscalar Giant Resonances: Sm isotopes

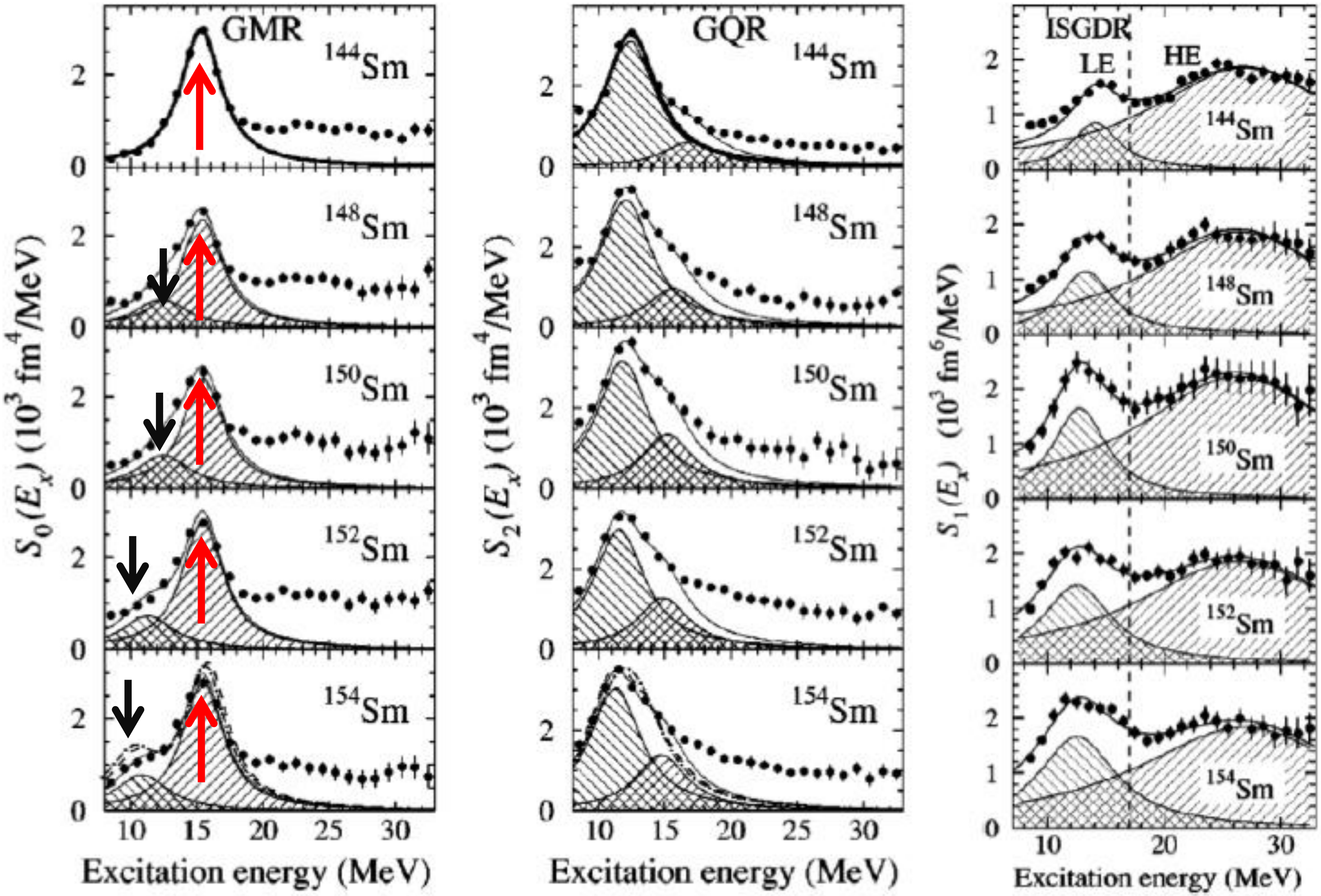

^{144}Sm

$\beta_2 = 0.0881$ (13)

^{148}Sm

^{150}Sm

^{152}Sm

^{154}Sm

$\beta_2 = 0.339$ (3)

ΔL = 0; ISGMR *ΔL* = 2; ISGQR *ΔL* = 1; ISGDR

M. Itoh *et al*., Phys. Rev. C 68 (2003) 064602

Decay of Giant Resonances

Decay of giant resonances

- **Width of resonance**

  $\Gamma, \Gamma^{\uparrow}, \ \Gamma^{\downarrow} \ (\Gamma^{\downarrow\uparrow}, \Gamma^{\downarrow\downarrow})$

  - **$\Gamma^{\uparrow}$: direct or escape width**
  - **$\Gamma^{\downarrow}$: spreading width**

    $\Gamma^{\downarrow\uparrow}$: pre-equilibrium, $\Gamma^{\downarrow\downarrow}$: compound

- **Decay measurements**

  ⇒ Direct reflection of damping processes

  Allows detailed comparison with theoretical calculations

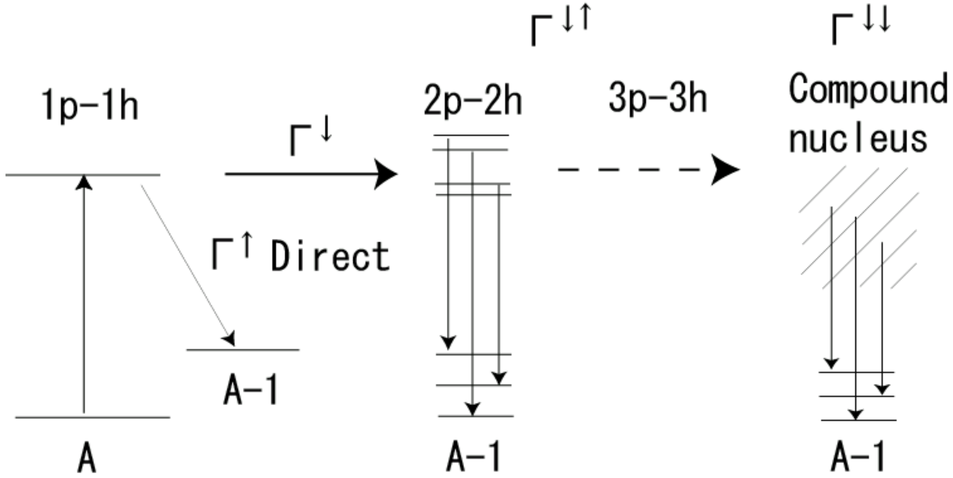

Excitation of ISGDR in ^{208}Pb

- In ^{208}Pb located around 22 MeV and width of 4 MeV
- *L=1* angular distribution peaks close to a scattering angle of 3°
- Difficult to identify in nuclear continuum and rides on instrumental background

Singles ^{208}Pb(α,α′)
At E_{α} = 200 MeV ⇒

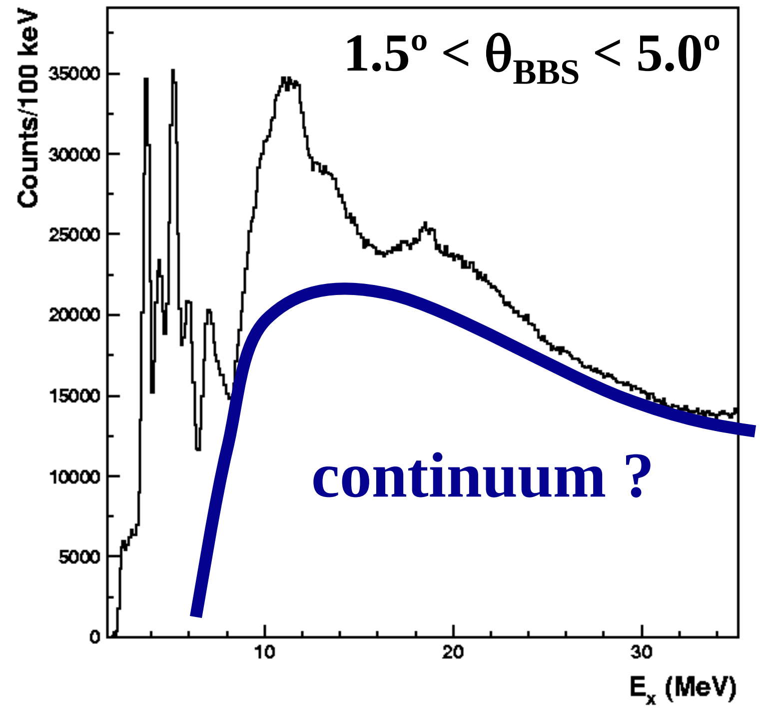

Microscopic structure of ISGDR

Transition operator

$$O^{L=1} = \sum_i r_i^1 Y_0^1 + \frac{1}{2}\sum_i r_i^3 Y_0^1 + \ ...$$

Spurious center of mass motion **Overtone**

***$3\hbar\omega$* excitation (overtone of c.o.m. motion)**

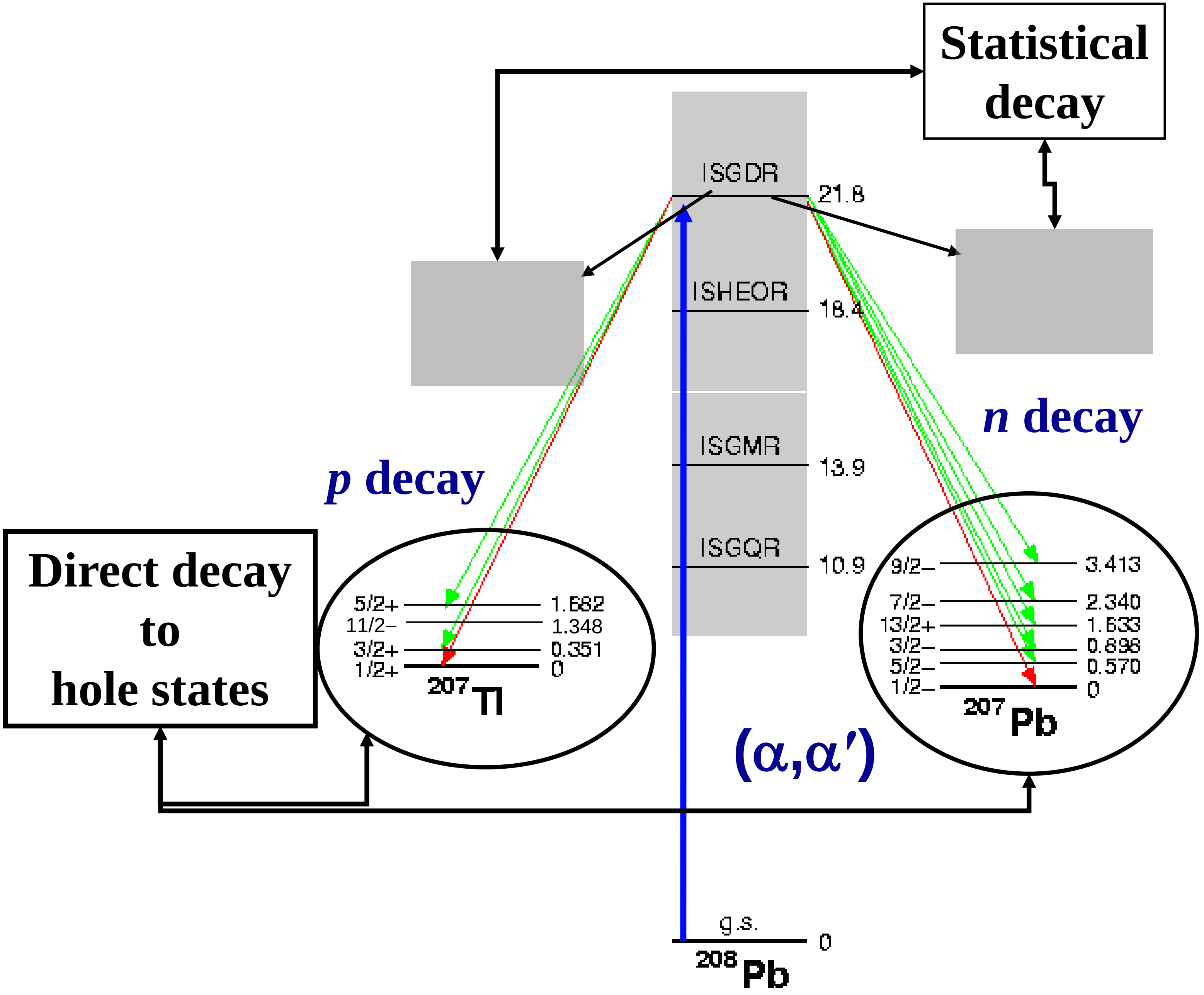
Statistical decay
ISGDR
21.8
ISHEOR
18.4
ISGMR
13.9
ISGQR
10.9
n decay
p decay
Direct decay to hole states
5/2+ 1.682
11/2– 1.348
3/2+ 0.351
1/2+ 0
207Tl
9/2– 3.413
7/2– 2.340
13/2+ 1.633
3/2– 0.898
5/2– 0.570
1/2– 0
207Pb
(α,α′)
g.s.
0
208Pb

Si-ball
16 Si-detectors at
10 cm from the target
total solid angle: 1 sr

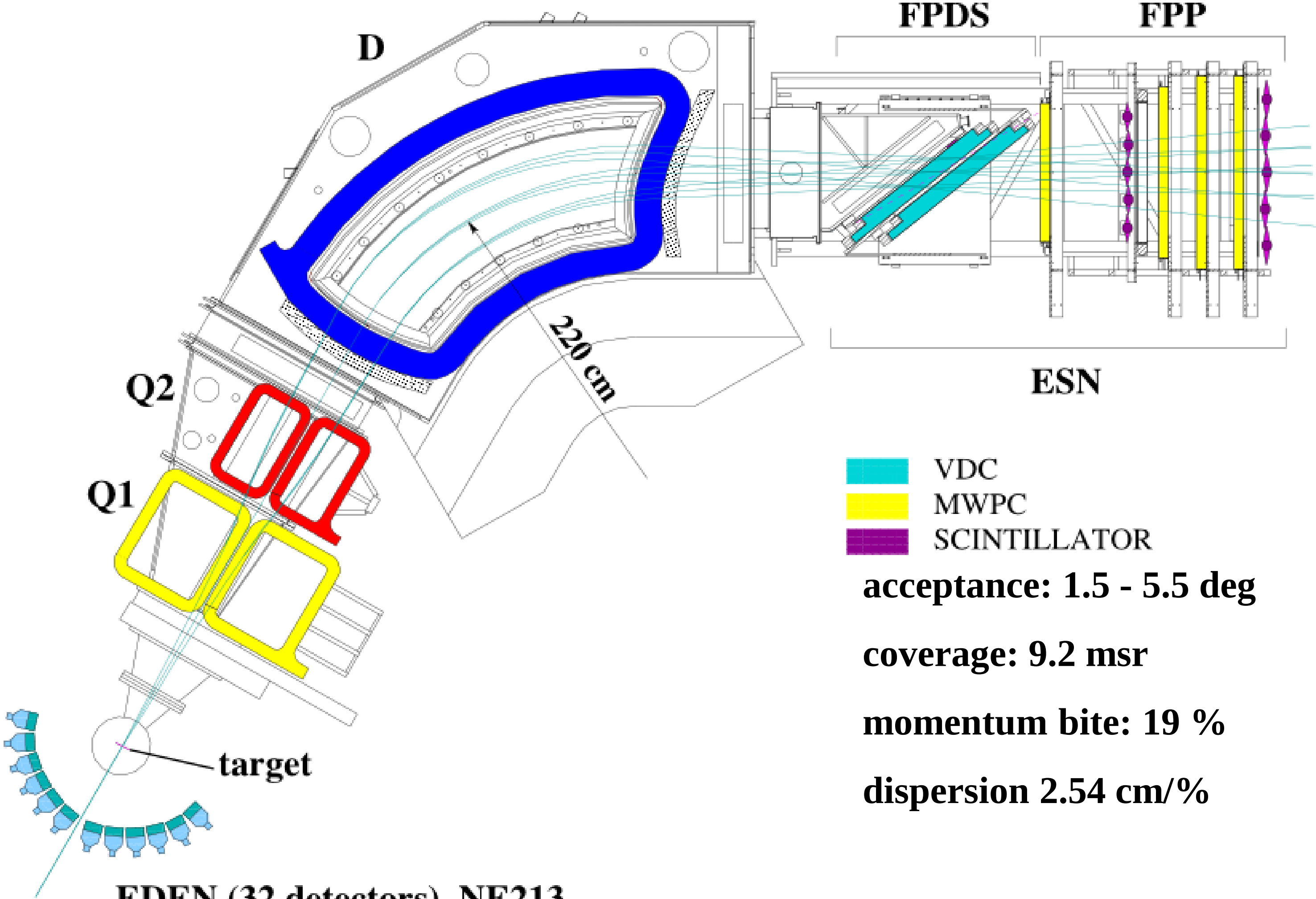

acceptance: 1.5 - 5.5 deg

coverage: 9.2 msr

momentum bite: 19 %

dispersion 2.54 cm/%

EDEN (32 detectors), NE213

total solid angle: 0.37 sr

KVI Big-Bite Spectrometer (BBS)

Proton-decay detection

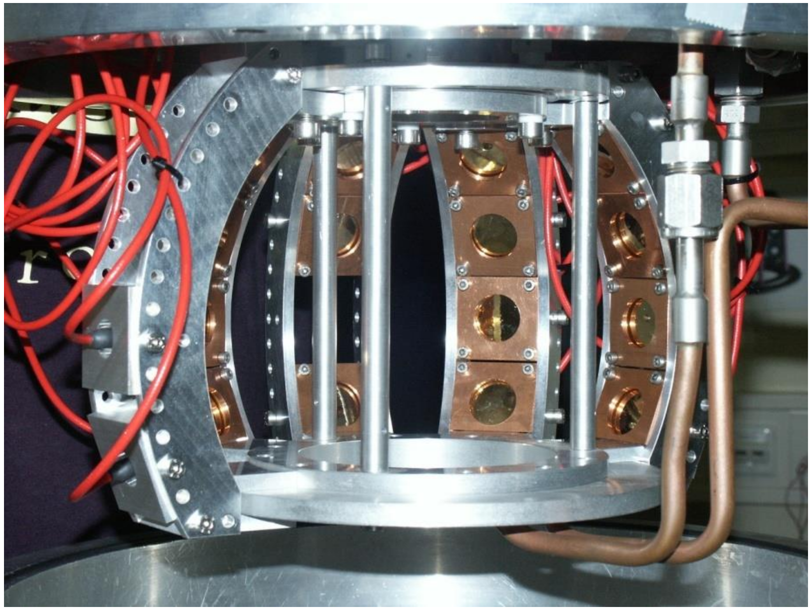

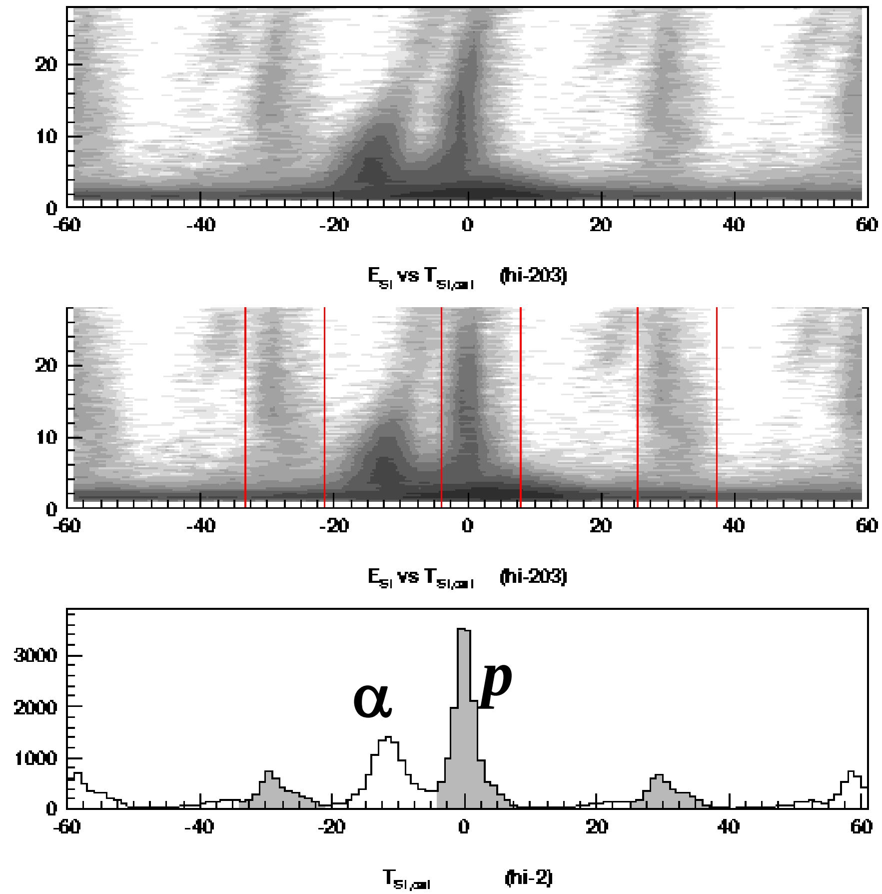

α-*p* separation using rise time of signal Si(Li)

Neutron-decay detection

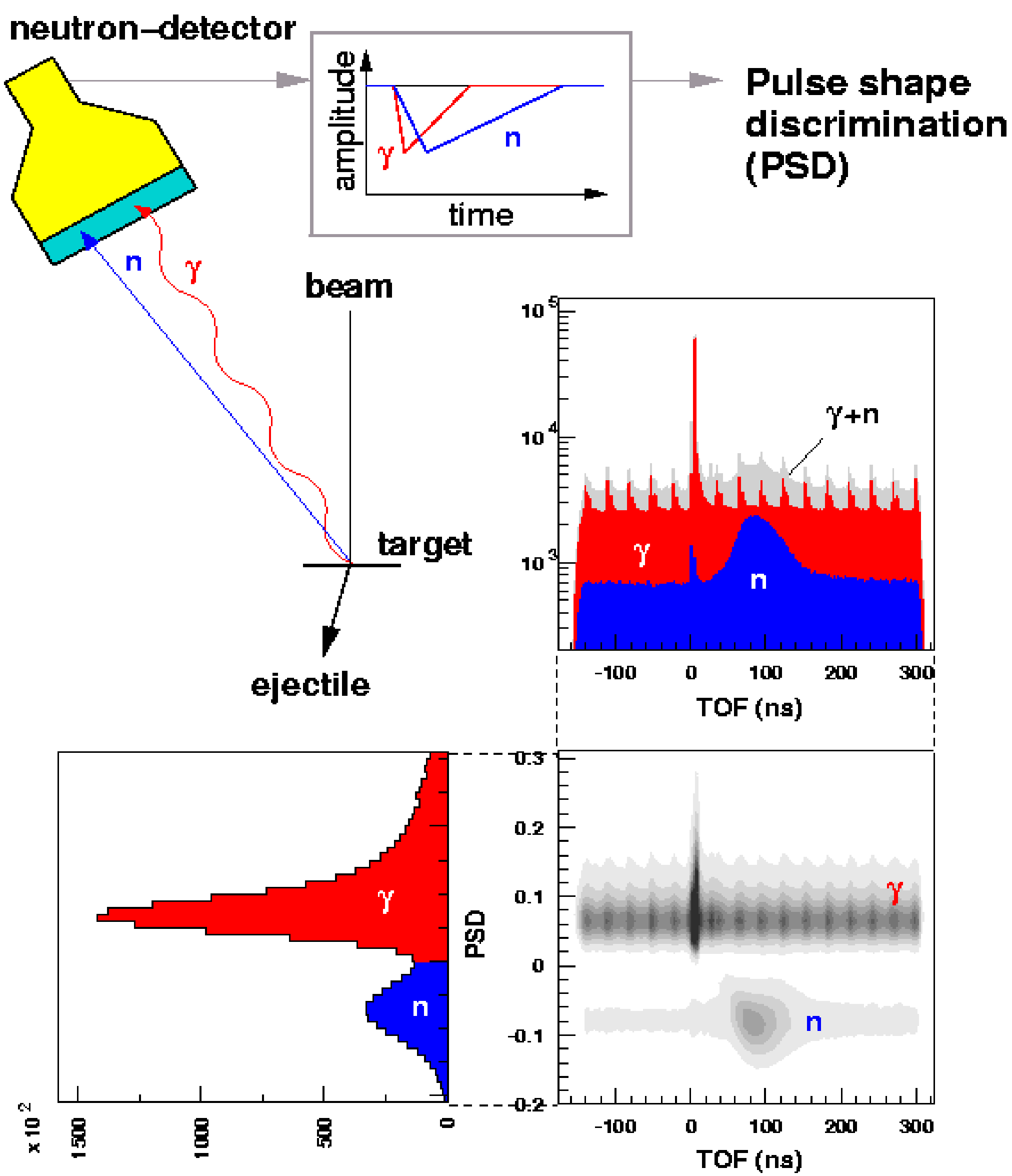

$^{208}Pb(\alpha,\alpha'\ p\ \text{or}\ n)$

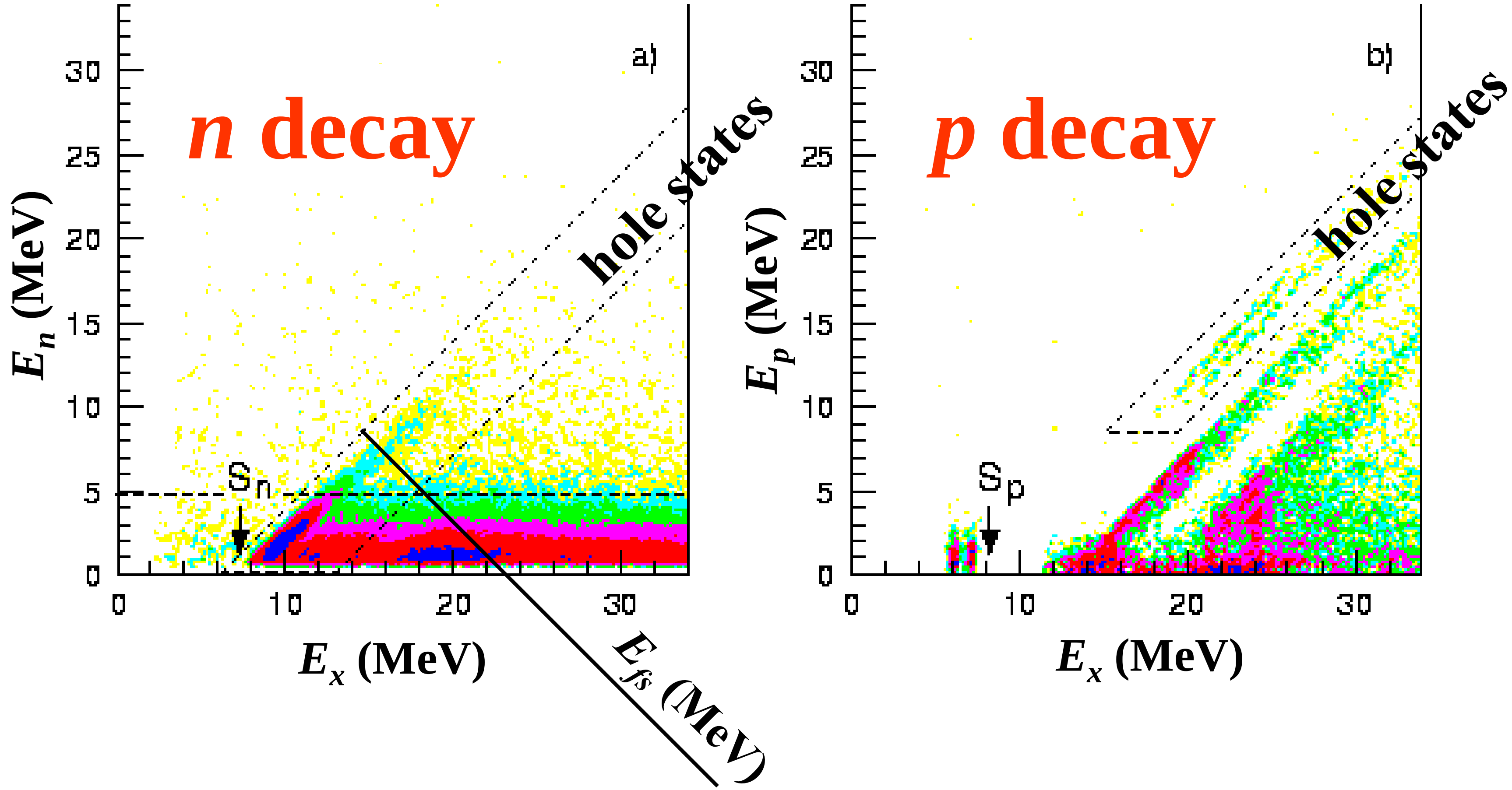

^{208}Pb(α,α′) followed by *p* decay

Decay to hole states in ^{207}Tl; branching ratios predicted by Gorelik *et al.*

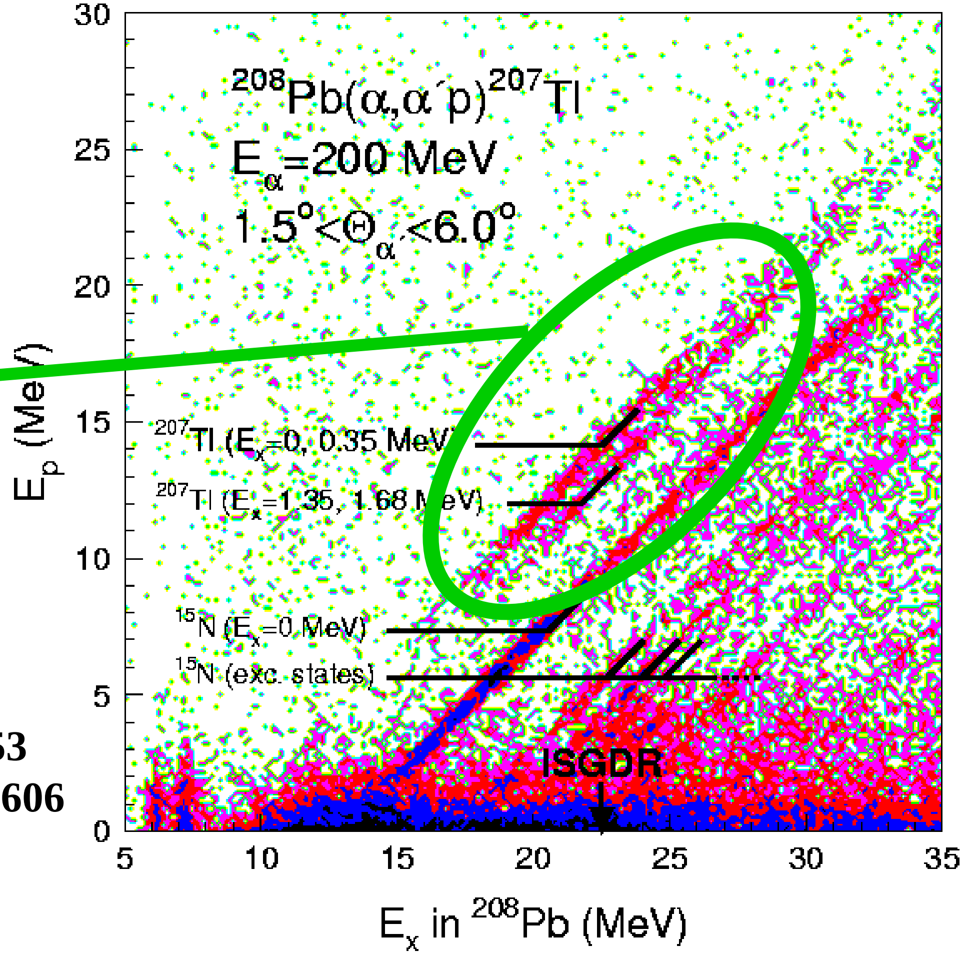

M. Hunyadi *et al*., Phys. Lett. B576 (2003) 253
M. Hunyadi *et al*., Phys. Rev. C75 (2007) 014606

Branching ratios for decay

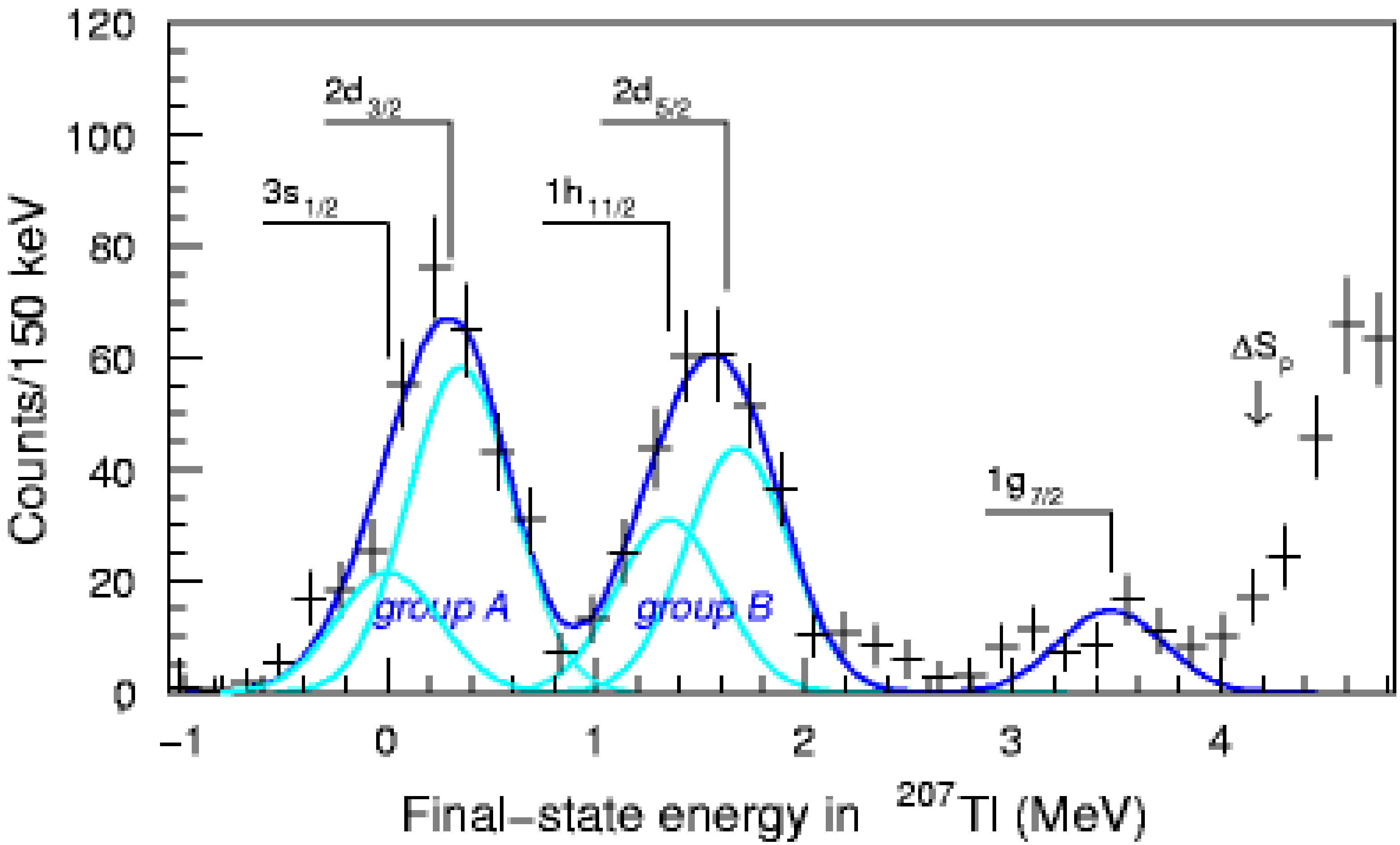

ISGDR in ^{208}Pb in *p* decay

E_x = 22.1 ± 0.3 MeV
L = *1* transition

gated on hole states

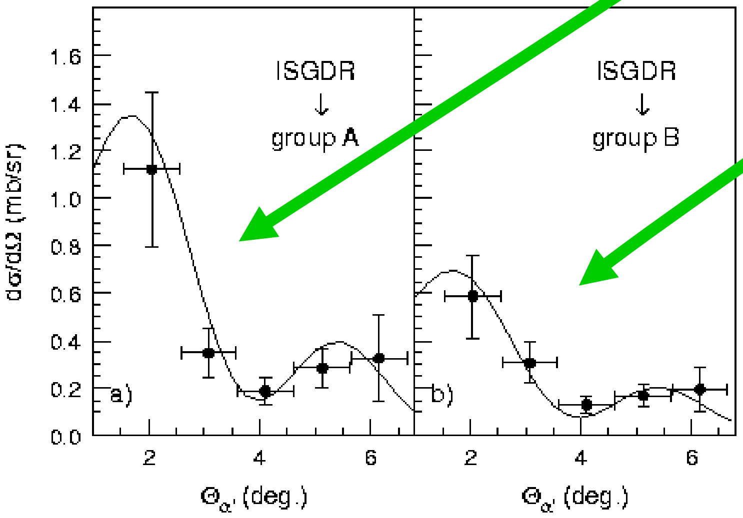

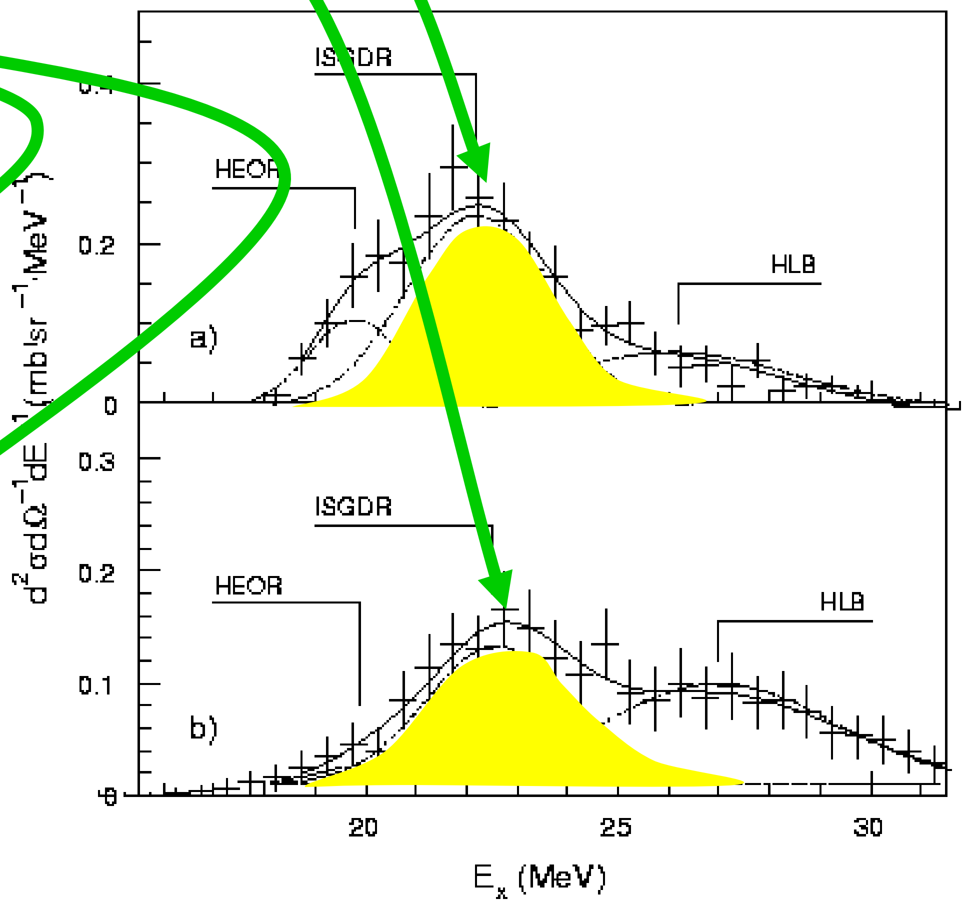

Branching ratios for decay

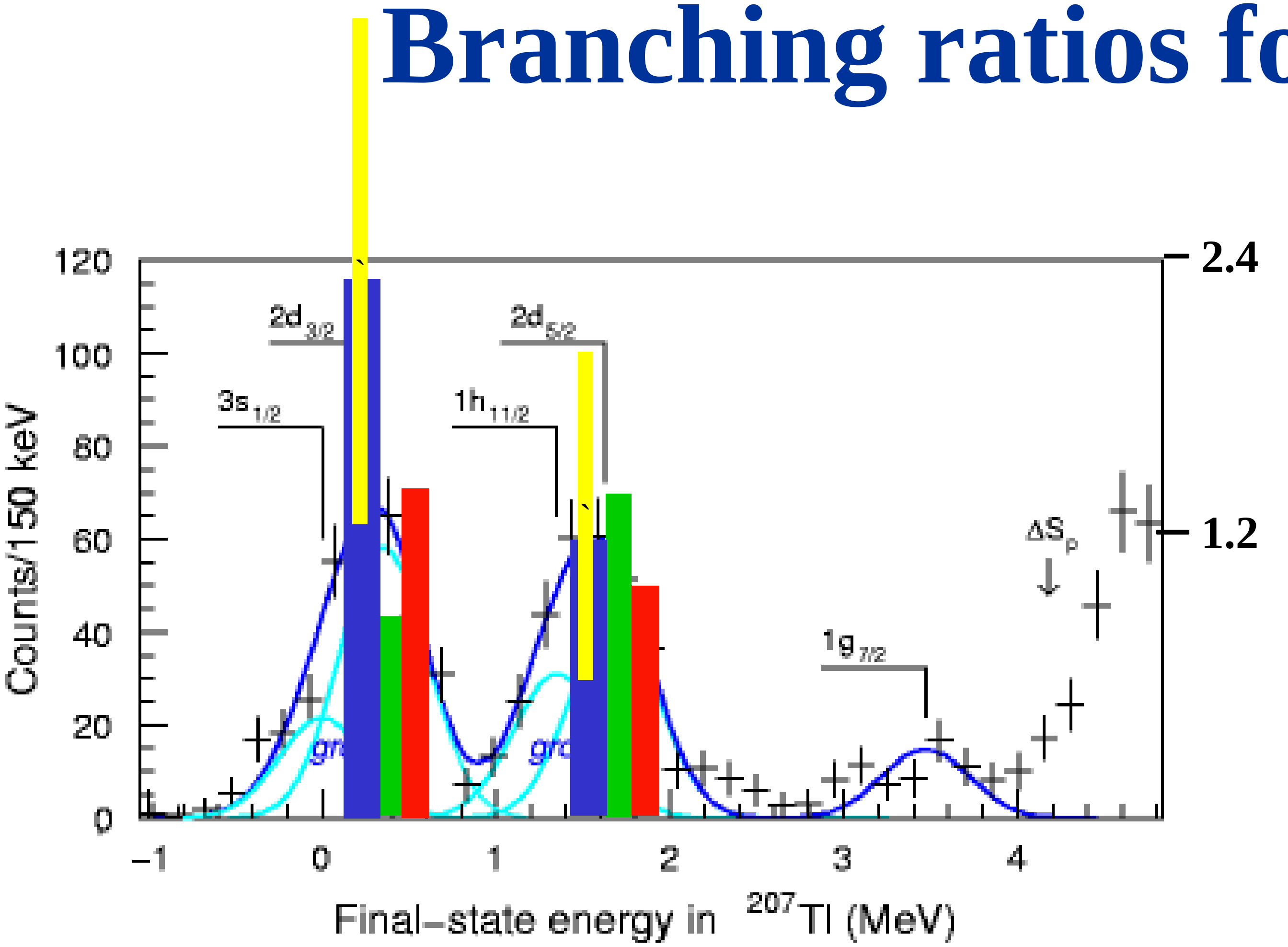

This work

M.L. Gorelik *et al.*, PRC 62 (2000) 047301;

Continuum RPA; Landau-Migdal Parameters: f^{ex}, f'; Smearing parameter Δ energy-dependent

M.L. Gorelik *et al.*, PRC 69 (2004) 054322

$1/2^+ + 3/2^+$	2.6%	(S~0.56) 1.45%	2.3 ± 1.1
$11/2^- + 5/2^+$	1.9%	(S~0.56) 1.04%	1.2 ± 0.7

Overtone of the ISGQR? [$r^4 Y_2$]

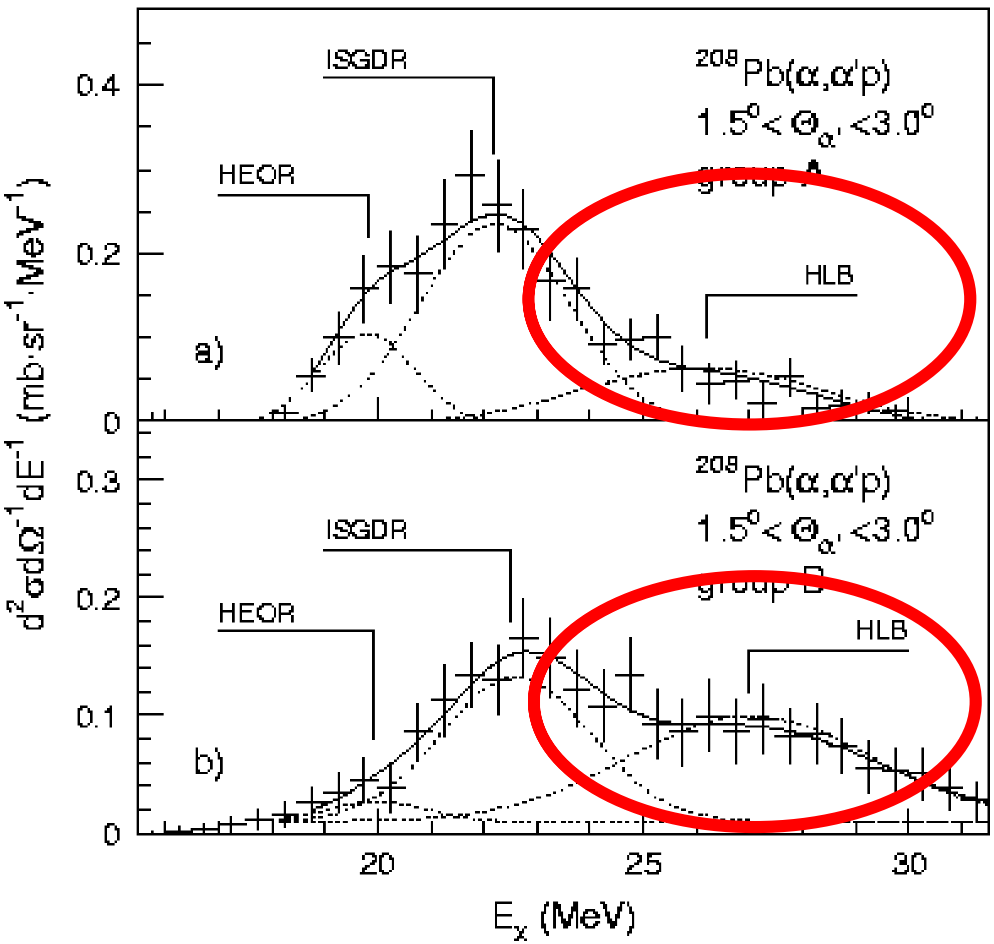

E_x = 26.9 ± 0.7 MeV

Muraviev and Urin
Bull. Acad. Sci. USSR
Phys. Ser. 52 (1988) 123
E_x = 28.3 MeV

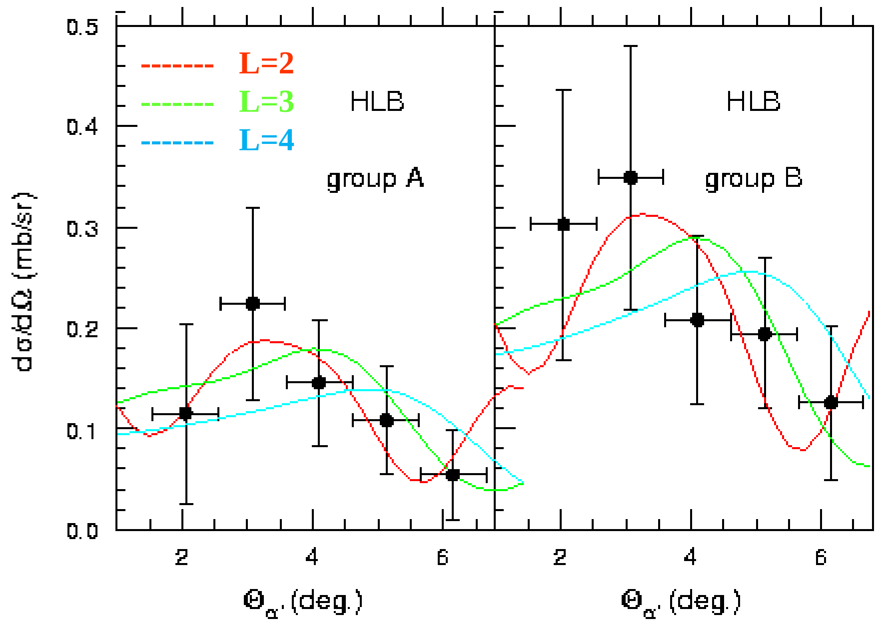

^{208}Pb(α,α′) followed by *n* decay

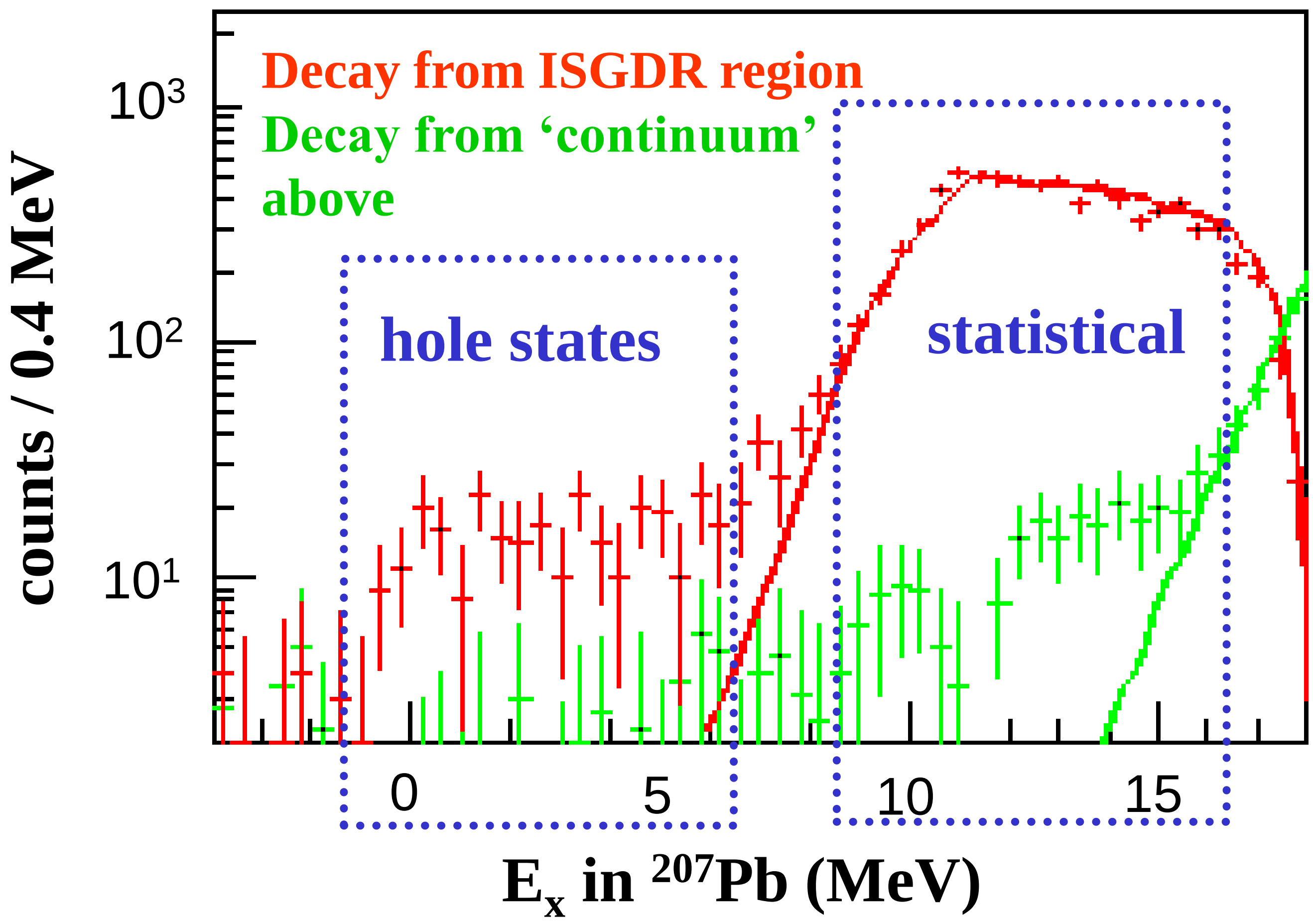

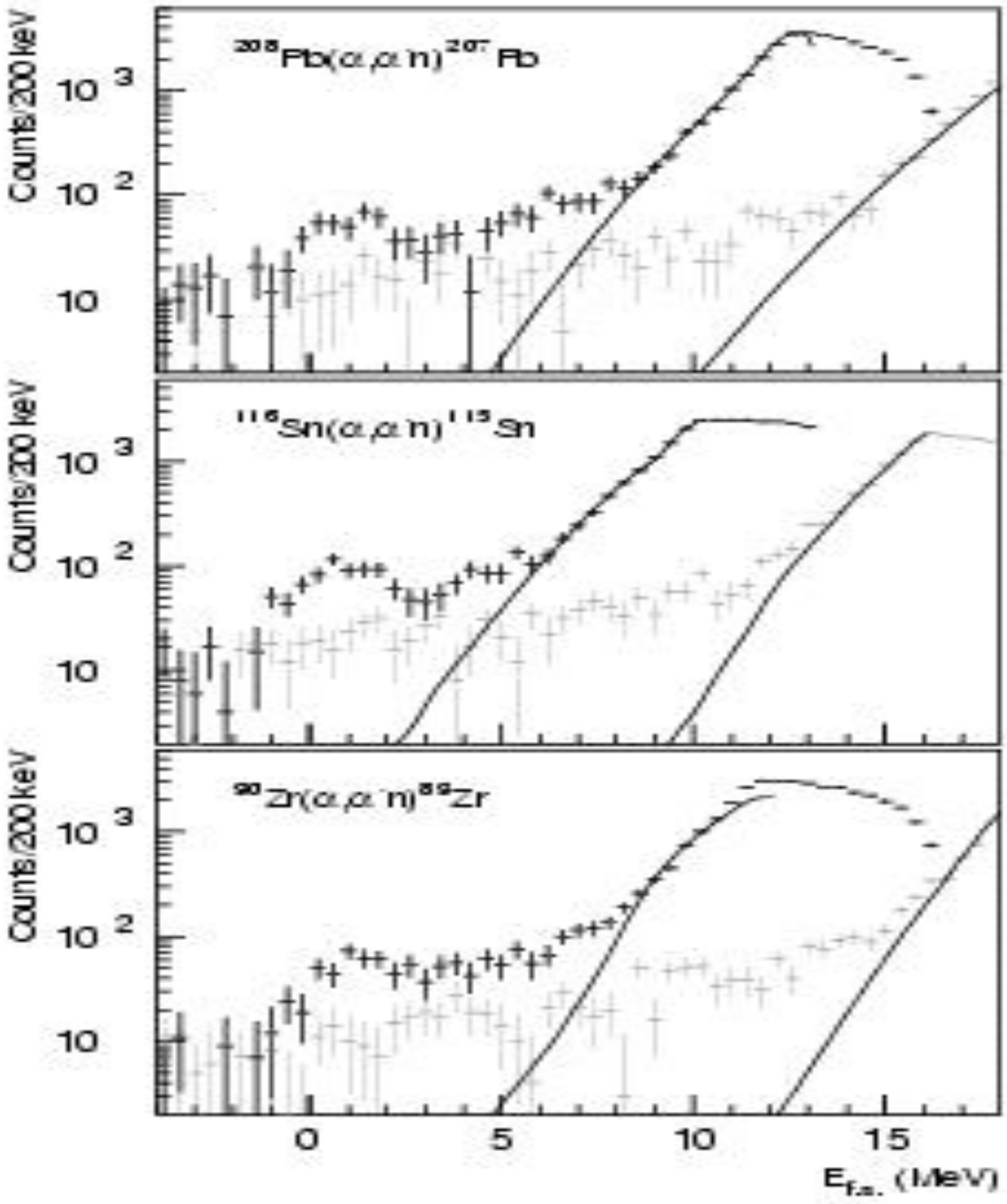

Counts/200 keV
^{208}Pb(α,α'n)^{207}Pb
^{116}Sn(α,α'n)^{115}Sn
^{90}Zr(α,α'n)^{89}Zr
10
10 2
10 3
0
5
10
15
E$_{f.s.}$ (MeV)

Branching ratios for the direct neutron-decay channel

From the simplified MDA of angular distributions ⇒

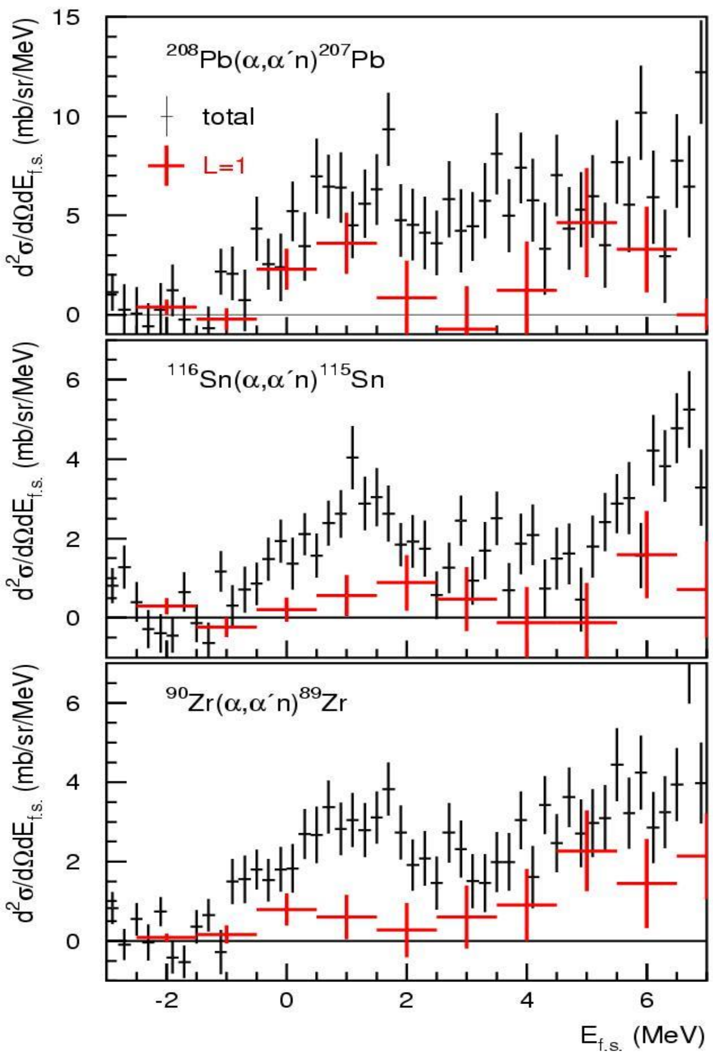

Br (Exp.)	Br (CRPA)
10.5 ± 5.6 %	11.46 %
5.1 ± 0.7 %	10.85 %
4.8 ± 0.9 %	16.8 %

Final-state spectra in ^{207}Pb obtained from neutron decay of
(a) continuum underlying ISGMR in ^{208}Pb and
(b and c) ISGMR proper.
(b) Fit with 100% statistical
(c) Fit with 60% statistical

l_j	E_x (MeV)	$\Gamma_j^{\uparrow}$ (keV), expt.	$\Gamma_j^{\uparrow}$ (keV), theory
$p_{1/2}$	0	140 ± 35	5
$i_{13/2}$	1.630		6
$f_{5/2}$	0.570	70 ± 15	92
$p_{3/2}$	0.890	50 ± 10	8
$f_{7/2}$	2.340	165 ± 40	174

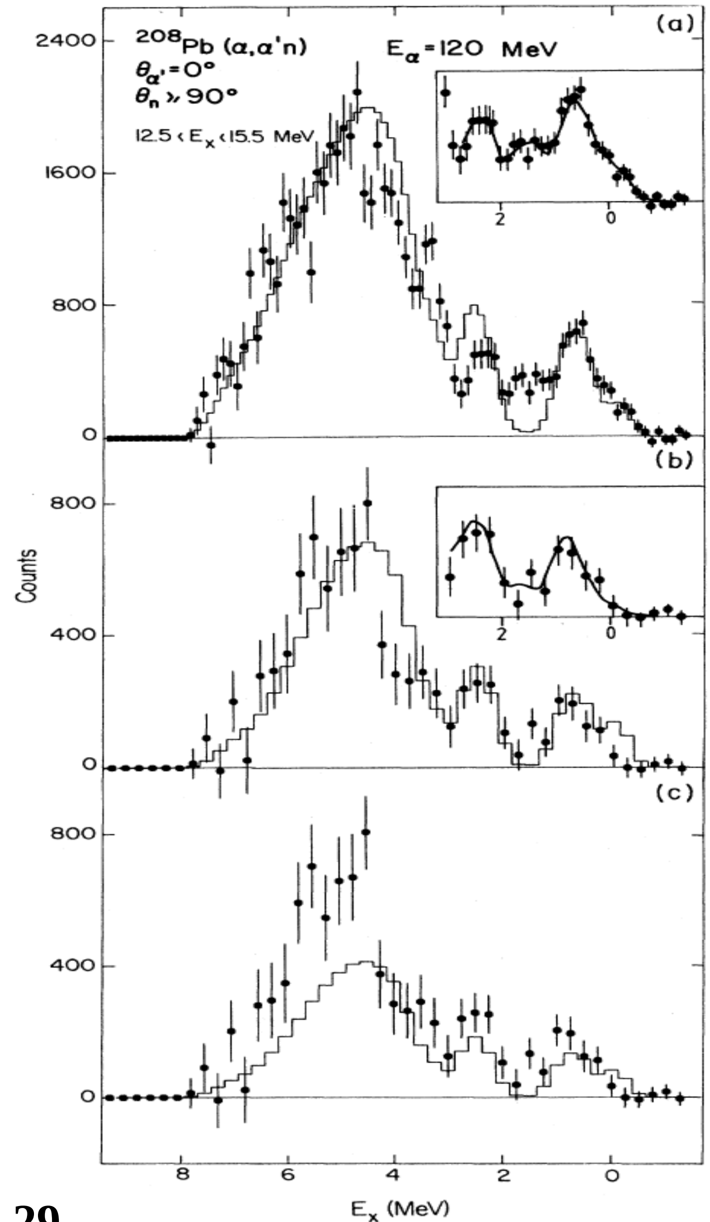

Γ_{tot} = 2.9 MeV; $\Gamma^{\uparrow}$ = 425 keV ≈ 15% Direct decay

S. Brandenburg *et al.*, Nucl. Phys. A466 (1987) 29

Data analysis: Proton decay

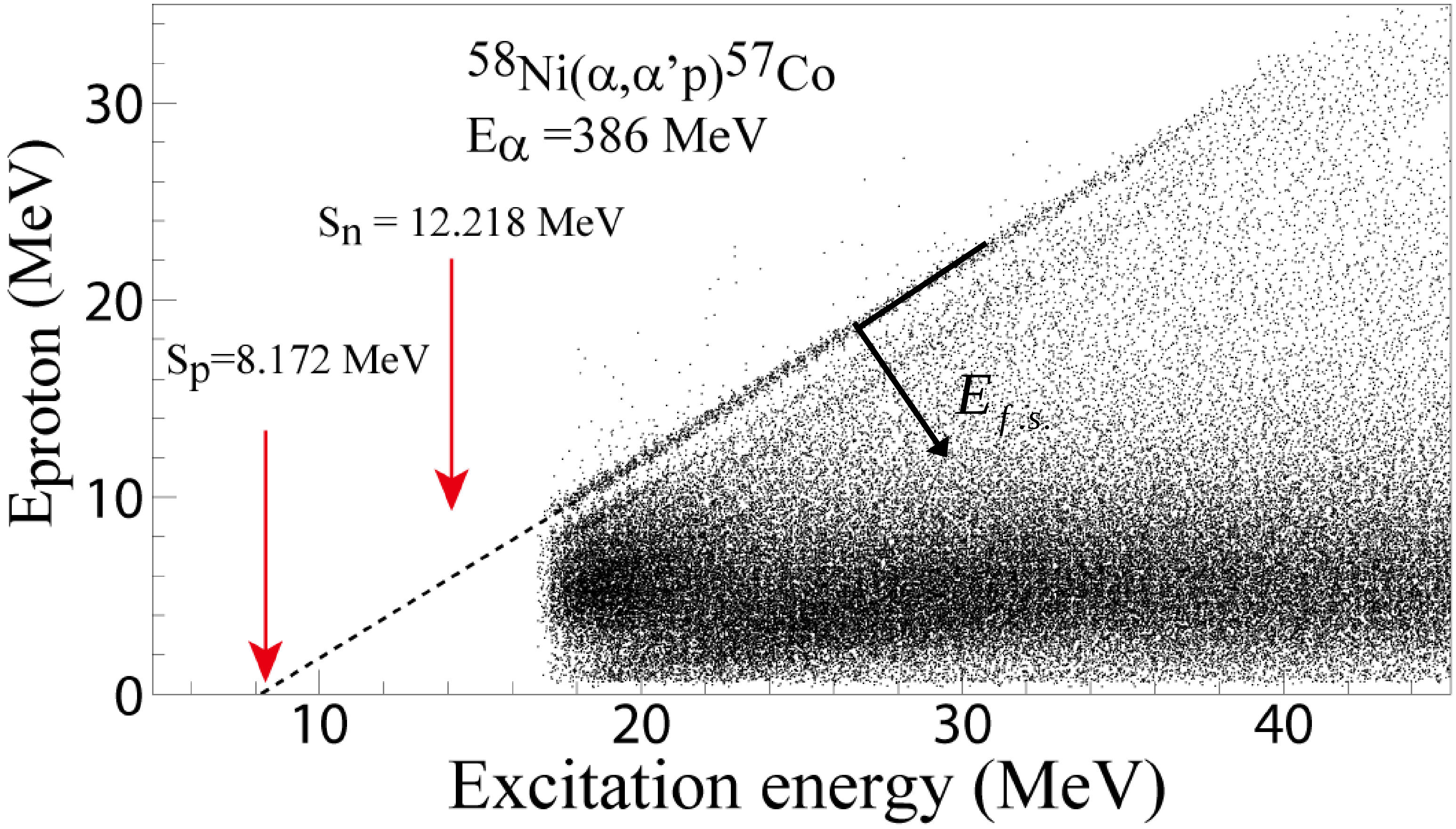

Final-state energy

$$E_{f.s.} = E_X - E_p - S_p$$

Experimental results

M. Hunyadi *et al.*, Phys. Rev. C 80 (2009) 044317

Final-state energy spectra

Final-state energy spectra after subtracting statistical contribution

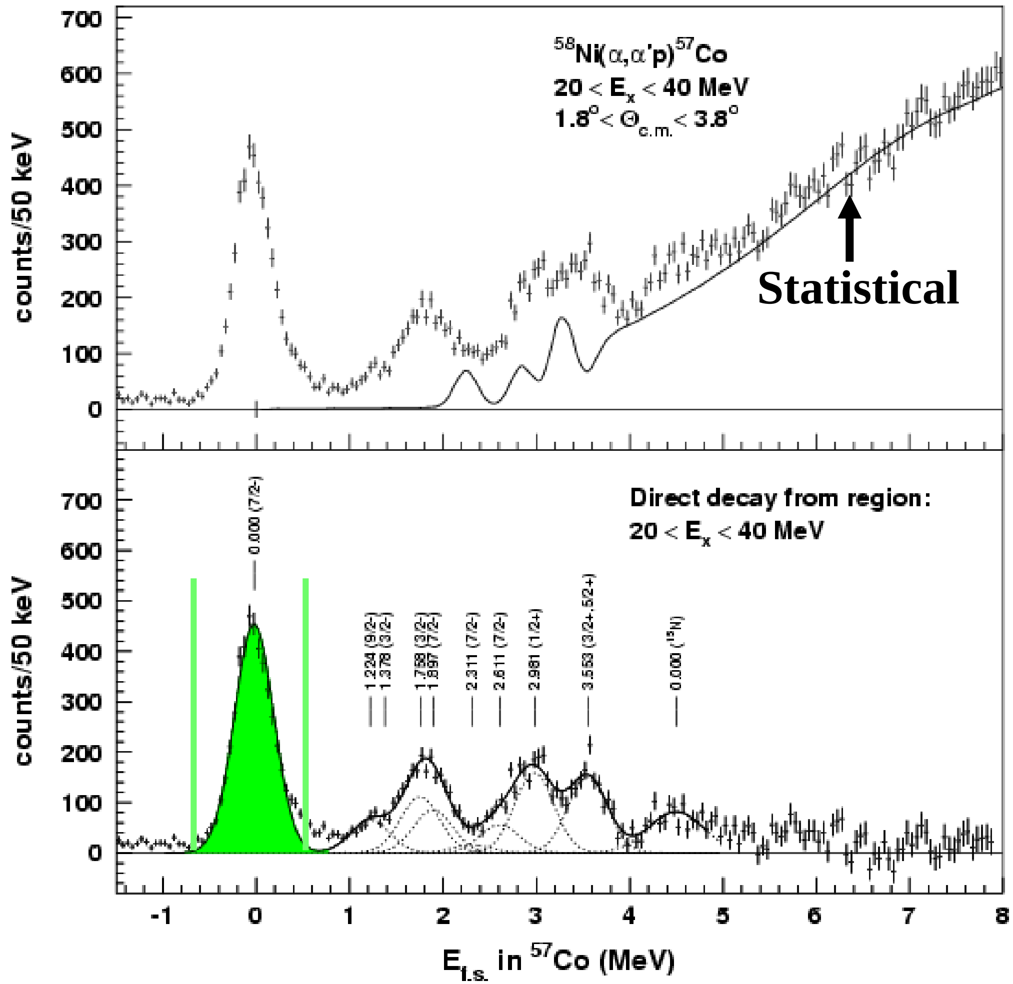

Experimental results

Difference of $E_{f.s.}$-spectra

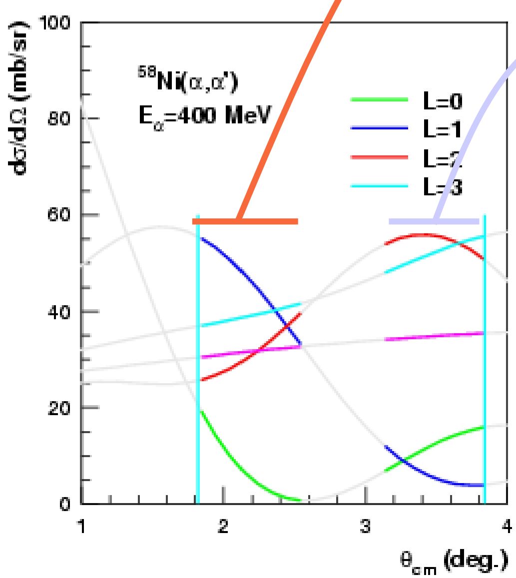

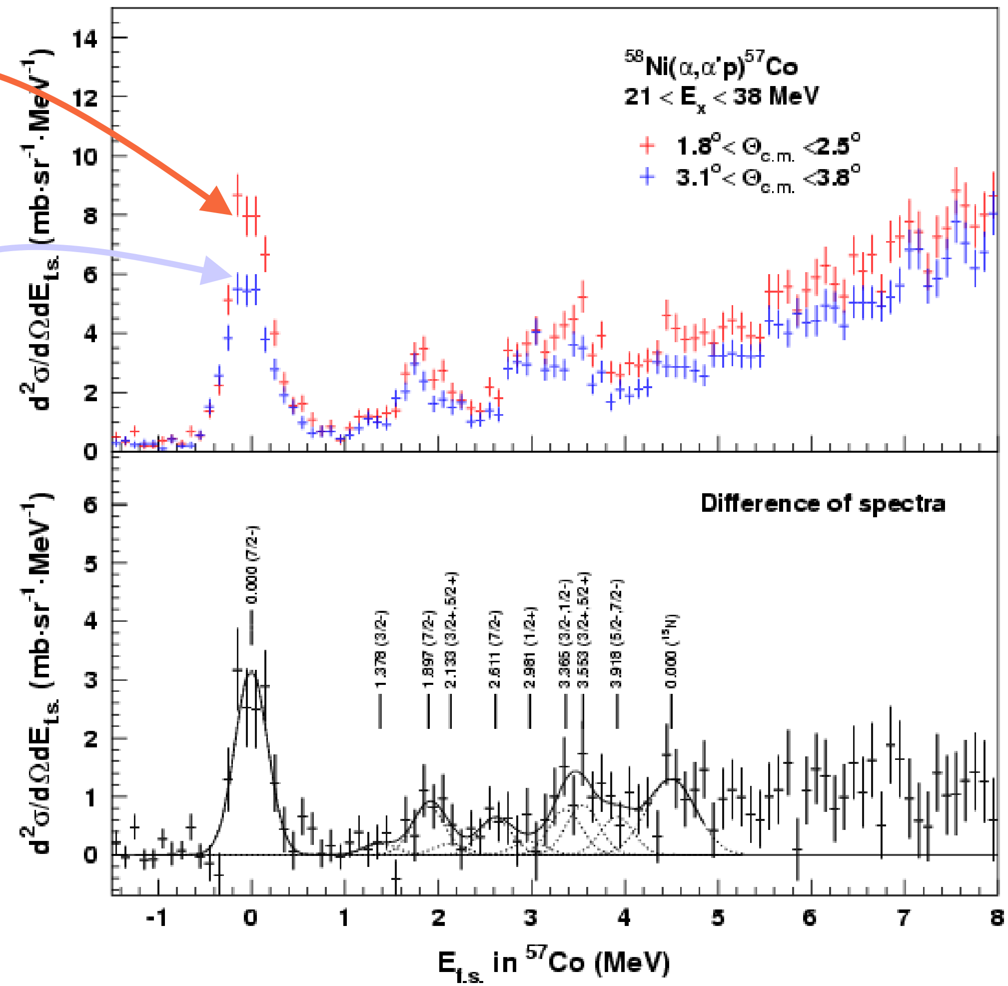

Strength distribution of ISGDR in ^{58}Ni

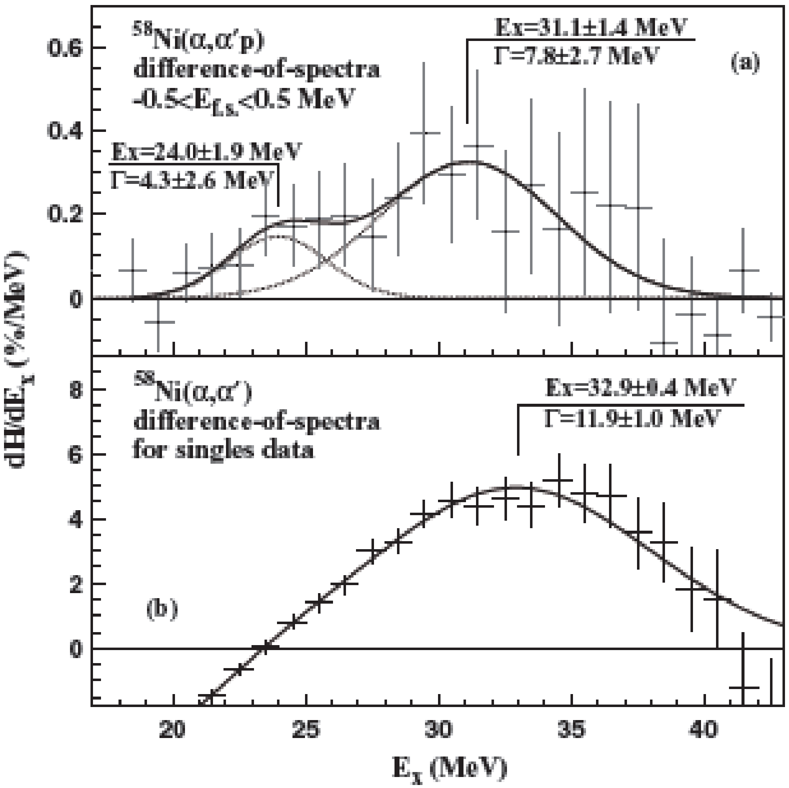

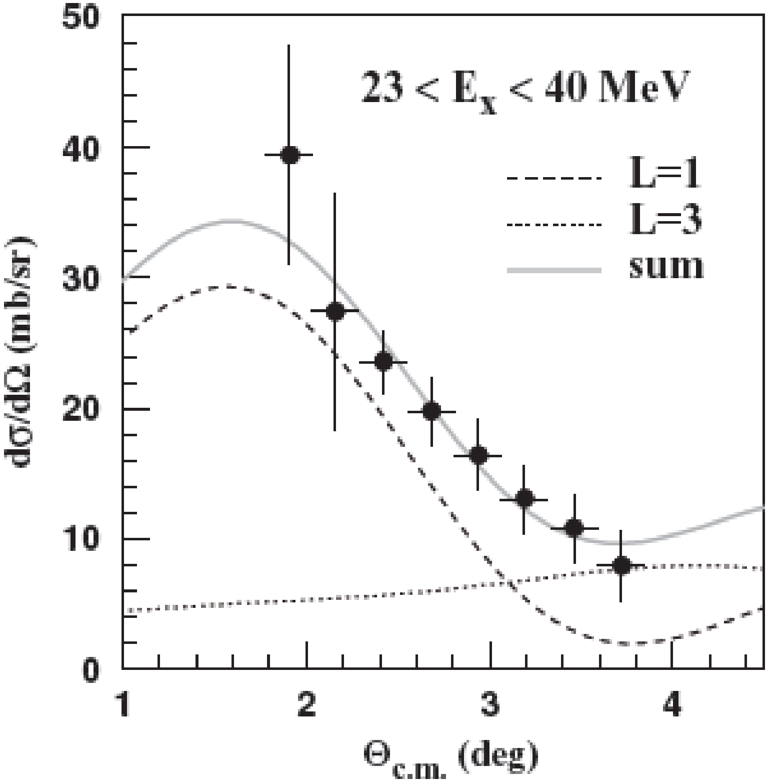

Spectra of *L = 1* strengths obtained with DOS method in percentage of isoscalar EWSR; a) coincidence data gated on g.s. decay and b) singles data.

Differential cross section of resonance structure fitted with *L* = 1 and *L* = 3 DWBA calculations.

Proton-decay branching ratios Normalized to 100%

	Exp. (%) (24-38 MeV)	Cal. (%) (15-40 MeV)
$7/2^-$	61.3 (with $5/2^-$)	47
$3/2^-$	7.9	3.1
$3/2^-$, $1/2^-$	9.9	2.2 (only for 1/2-)
$5/2^-$	3.2 ± 3.4	-
$1/2^+$	2.0 ± 4.2	13.4
$3/2^+$, $5/2^+$	15.9	34.3
Σ	100 %	100%

Calculations: M.L. Goerlik, I.V. Safonov, and M.H. Urin, Phys. Rev. C69 (2004) 054322

Conclusions!

- **There has been much progress in understanding ISGMR & ISGDR macroscopic properties**

  Systematics: E_x, Γ, %EWSR

  $\Rightarrow K_{\mathrm{nm}} \approx 240$ MeV

  $\Rightarrow K_\tau \approx -500$ MeV

- **Sn nuclei are softer than ^{208}Pb and ^{90}Zr.**
- **Recently, Microscopic Structure for a few nuclei**

  CRPA has some success in ^{208}Pb & ^{58}Ni but fails badly in ^{116}Sn & ^{90}Zr.

- **Possible observation quadrupole compression mode, i.e. overtone of ISGQR**

Gamma-Decay
Neutron-Skin Thickness
Pygmy Dipole Resonance

Setup at KVI

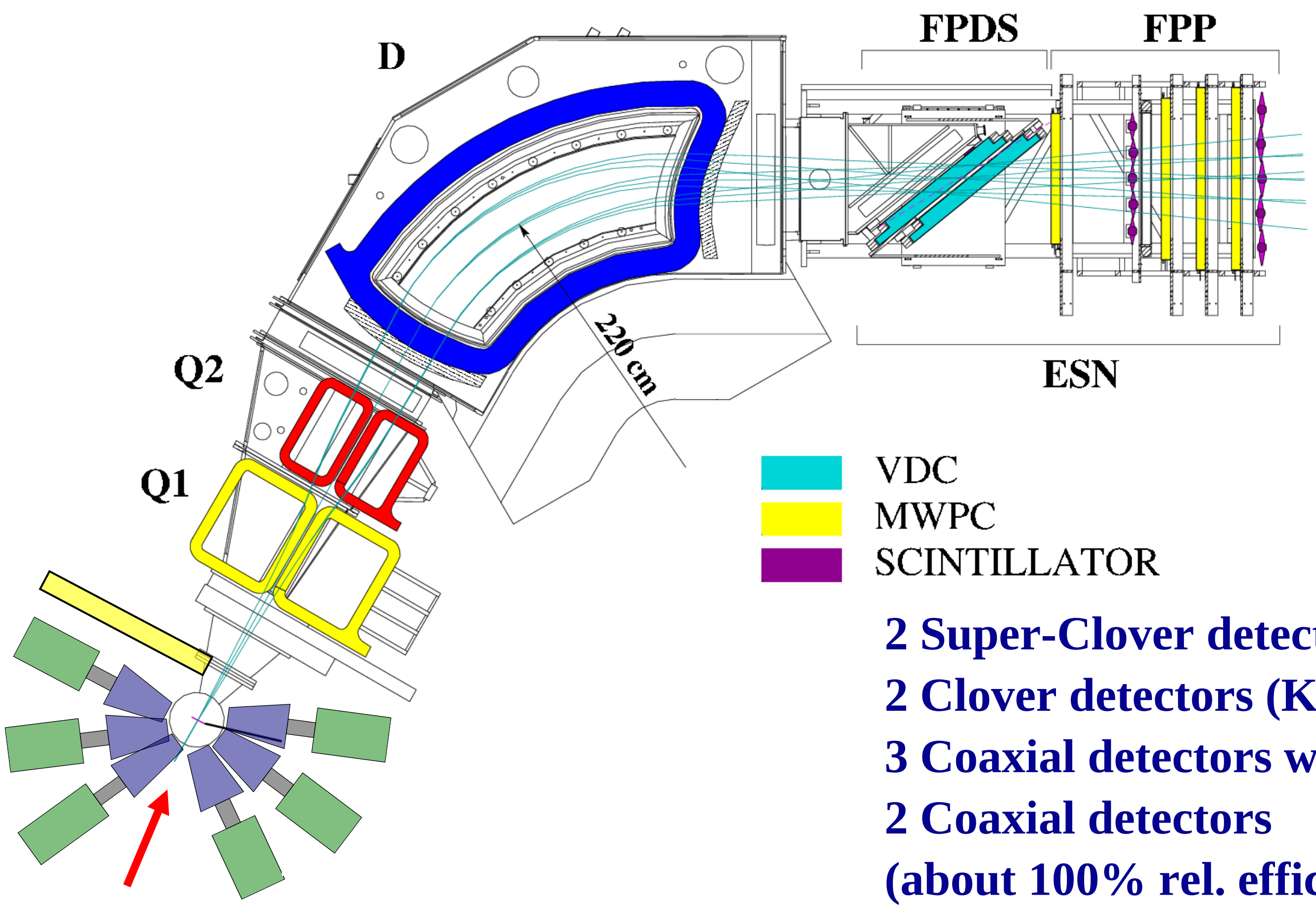

α beam

E_α = 136 MeV, θ_α = 3.5°

2 Super-Clover detectors (GSI)
2 Clover detectors (KVI)
3 Coaxial detectors with BGO
2 Coaxial detectors
(about 100% rel. efficiency each)
⇒ 0.5% absolute photo-peak efficiency

D. Savran *et al.*, Nucl. Inst. and Meth. Phys. Res. A 564 (2006) 267

ISGQR at 10.8 MeV

ISGMR at 13.8 MeV

Hatched area ⇒ IVGDR contribution (Coulomb + nuclear)

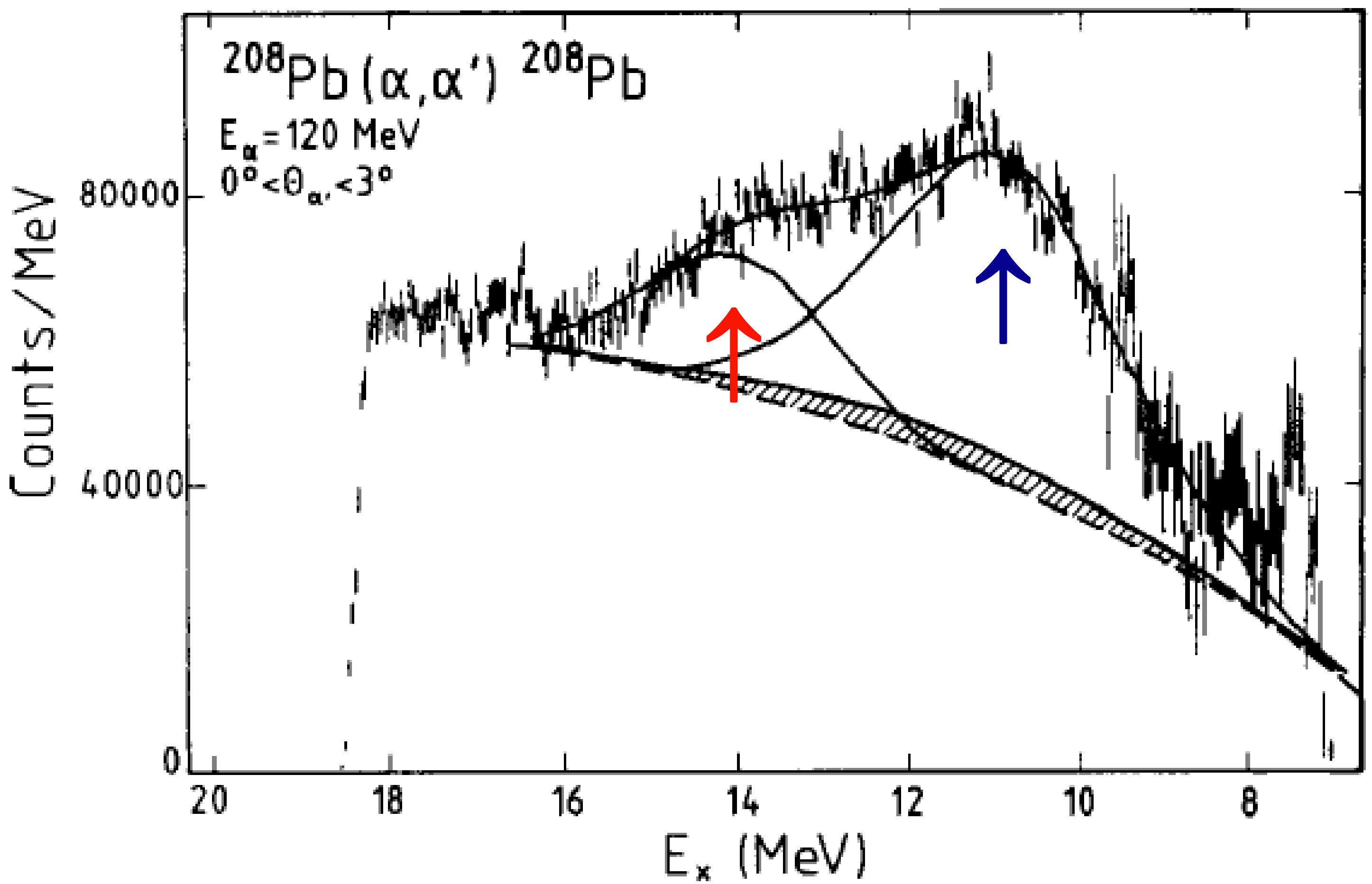

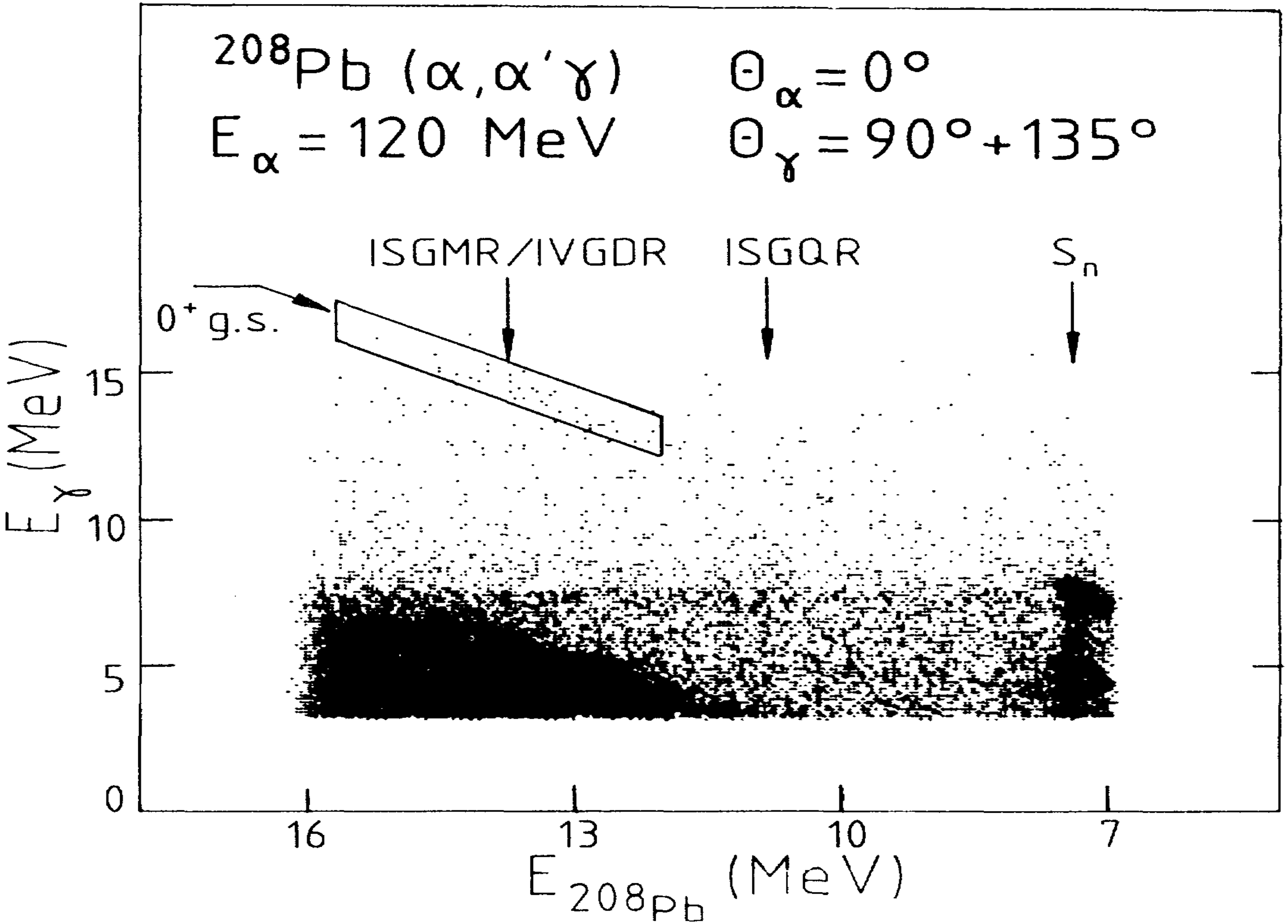

Two-dimensional spectrum showing inelastic α-scattering in coincidence with γ-decay

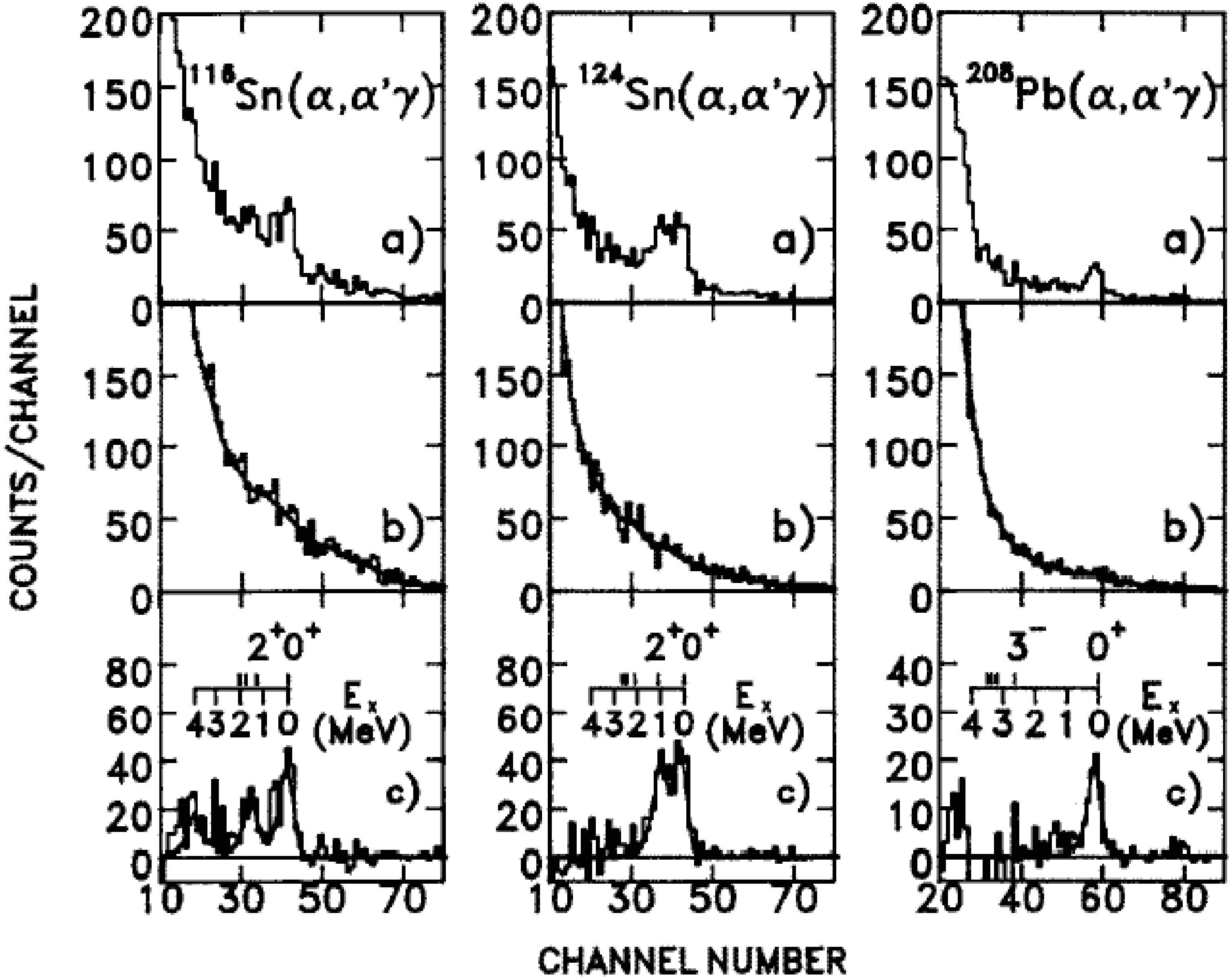

True
+
Random

Random

True

A. Krasznahorkay et al., Phys. Rev. Lett. 66 (1991) 1287

Isoscalar transition density in the Goldhaber-Teller model for excitation of IVGDR in inelastic α-scattering.

$$g_1^{10}(r) = g_1^{\mathrm{n}}(r) - g_1^{\mathrm{p}}(r) = \alpha_1 \gamma \left(\frac{N-Z}{A} \right) \left(\frac{\mathrm{d}\rho(r)}{\mathrm{d}r} + \frac{1}{3} c \frac{\mathrm{d}^2\rho(r)}{\mathrm{d}r^2} \right).$$

$$\frac{\Delta R_{\mathrm{PN}}}{R_0} = \frac{R_{\mathrm{n}} - R_{\mathrm{p}}}{\frac{1}{2}(R_{\mathrm{n}} + R_{\mathrm{p}})} = \gamma \frac{2(N-Z)}{3A}.$$

Here, γ is related to the proton and neutron central density distributions and thus to ΔR_{pn}. α_1 is deformation length obtained from TRK sum rule. Therefore, DWBA cross sections can be calculated as function of $\Delta R_{pn}/R_0$ for the Goldhaber-Teller model and similarly for the Steinwedel-Jensen model.

γ-decay branching ratios are known from photo-absorption experiments.

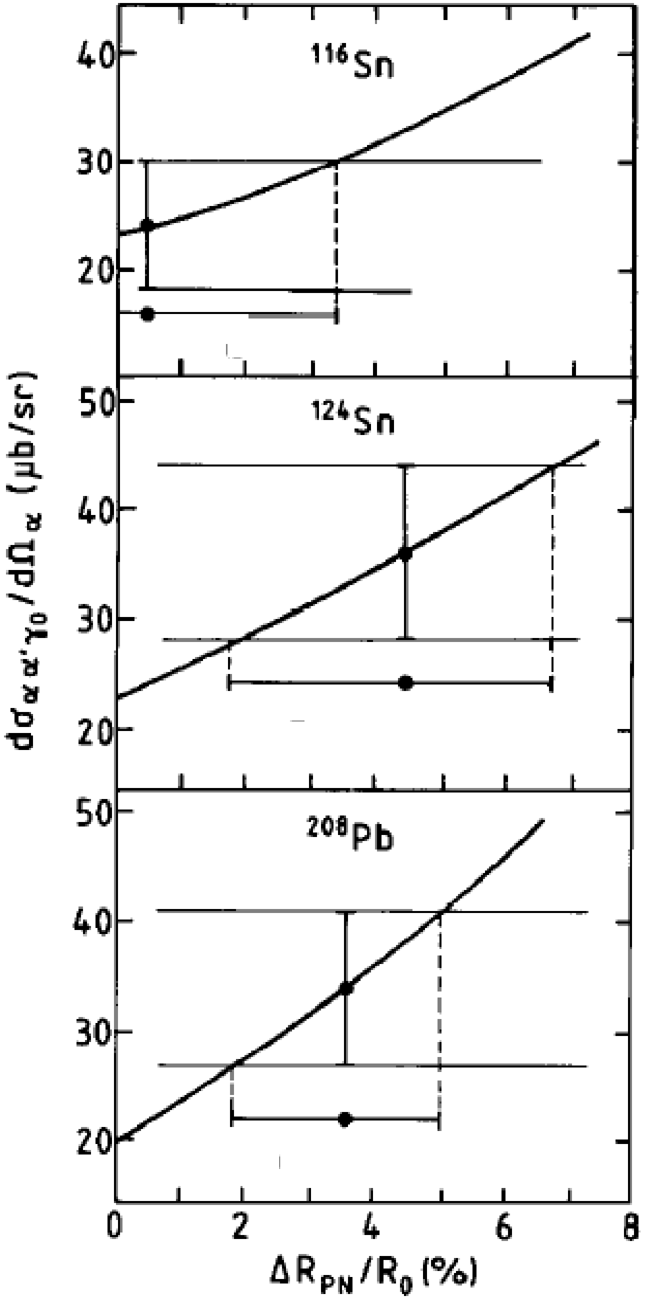

Full line is the calculated $\alpha\gamma_0$ coincidence cross section, averaged over the solid angle of the α-particle and integrated over the full γ-ray solid angle (4π) and over the *ΔE* energy range as function of $\Delta R_{pn}/R$.

The experimental $\alpha\gamma_0$ cross sections for the IVGDR are shown as full circles with vertical error bars. The deduced values for $\Delta R_{pn}/R$ with the associated uncertainty (full circles with horizontal error bars) are also indicated.

Isotope	Present work $\Delta R_{PN}/R_0$ (%)	Present work ΔR_{PN} (fm)	Batty et al. [2] ΔR_{PN} (fm)	Angeli et al. [6] ΔR_{PN} (fm)
^{116}Sn	0.5 ± 2.7	0.02 ± 0.12	0.15 ± 0.05	0.13
^{124}Sn	4.4 ± 2.4	0.21 ± 0.11	0.25 ± 0.05	0.22
^{208}Pb	$3.5^{+1.5}_{-1.6}$	0.19 ± 0.09	0.14 ± 0.04	0.22

^{140}Ce(α,α′γ) - coincidence matrix

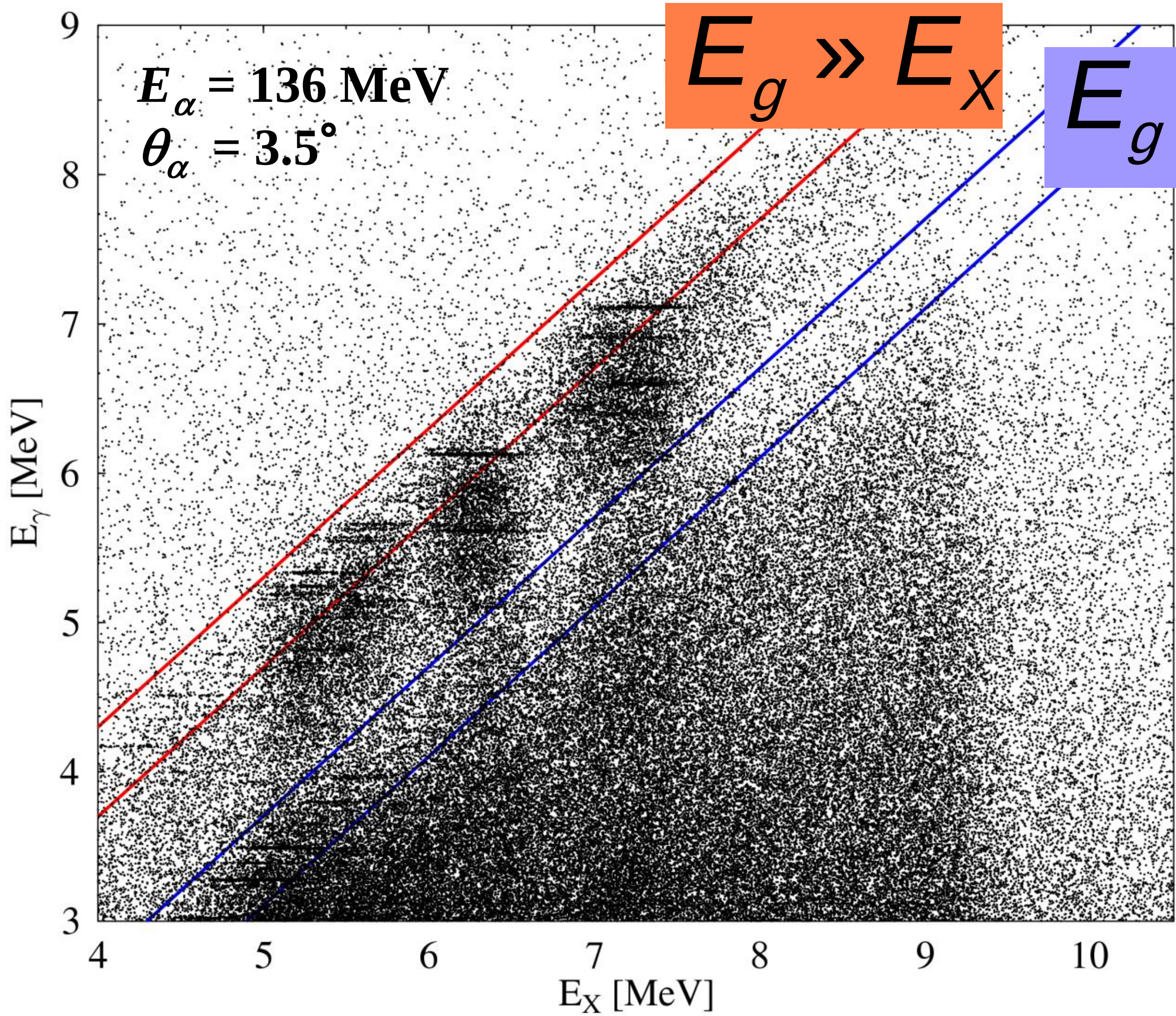

E_g » E_X

E_g » E_X - $E_{2_1^+}$

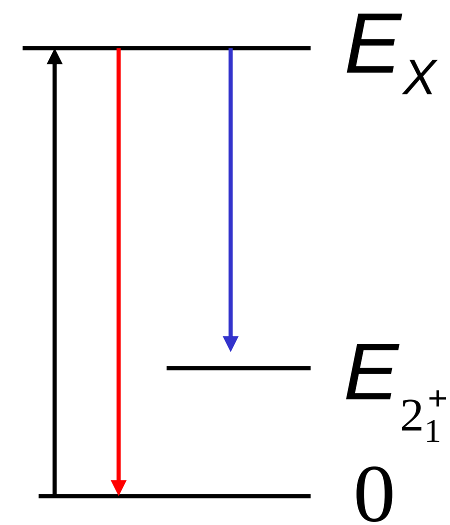

^{140}Ce(α,α′γ) vs. ^{140}Ce(γ,γ′)

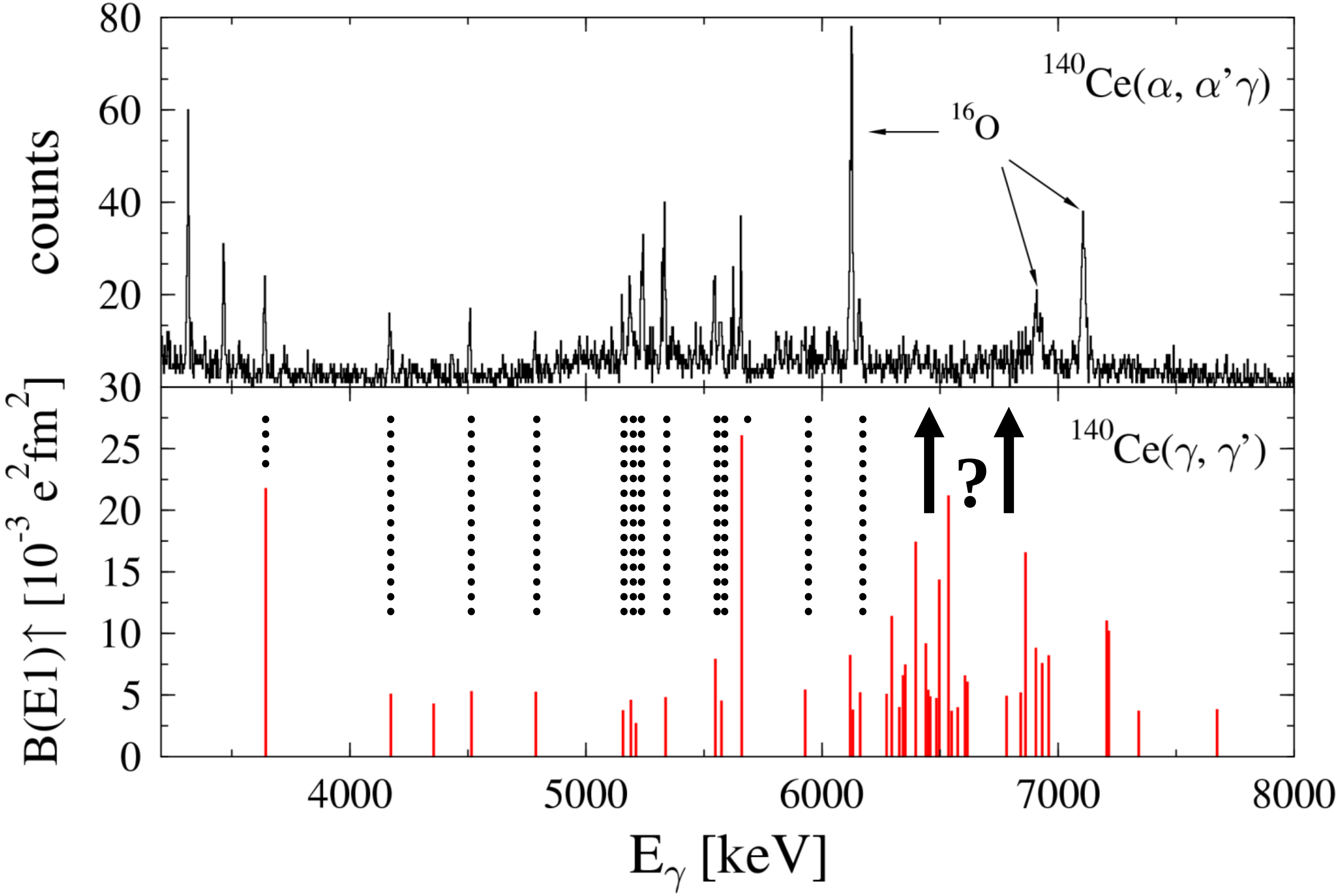

D. Savran *et al*., Phys. Rev. Lett. 97 (2006) 172502

Multipole assignment with α–γ angular correlation

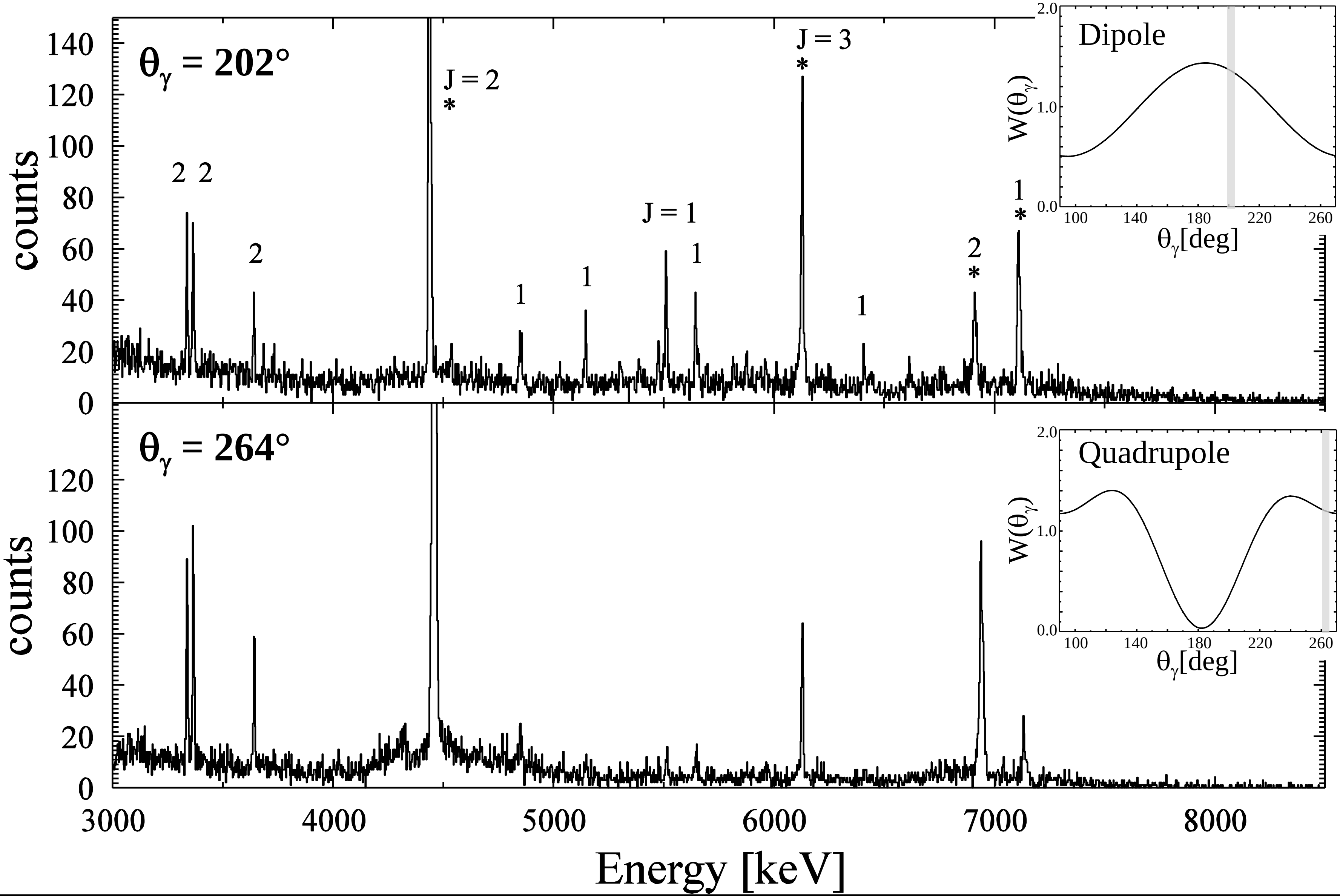

Multipole assignment with α-γ angular correlation

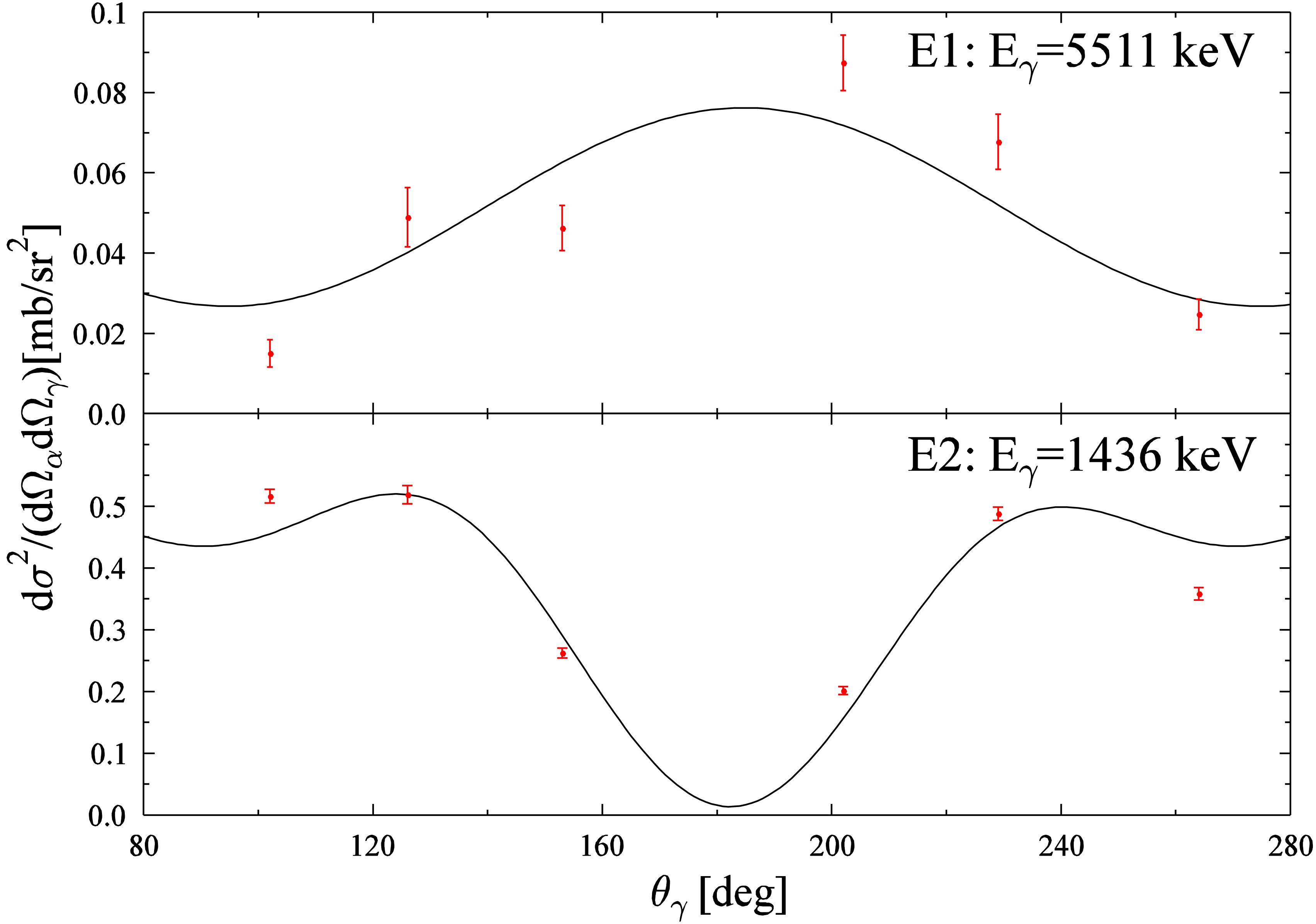

Comparison of (α,α′γ) with (γ,γ′) on ^{138}Ba

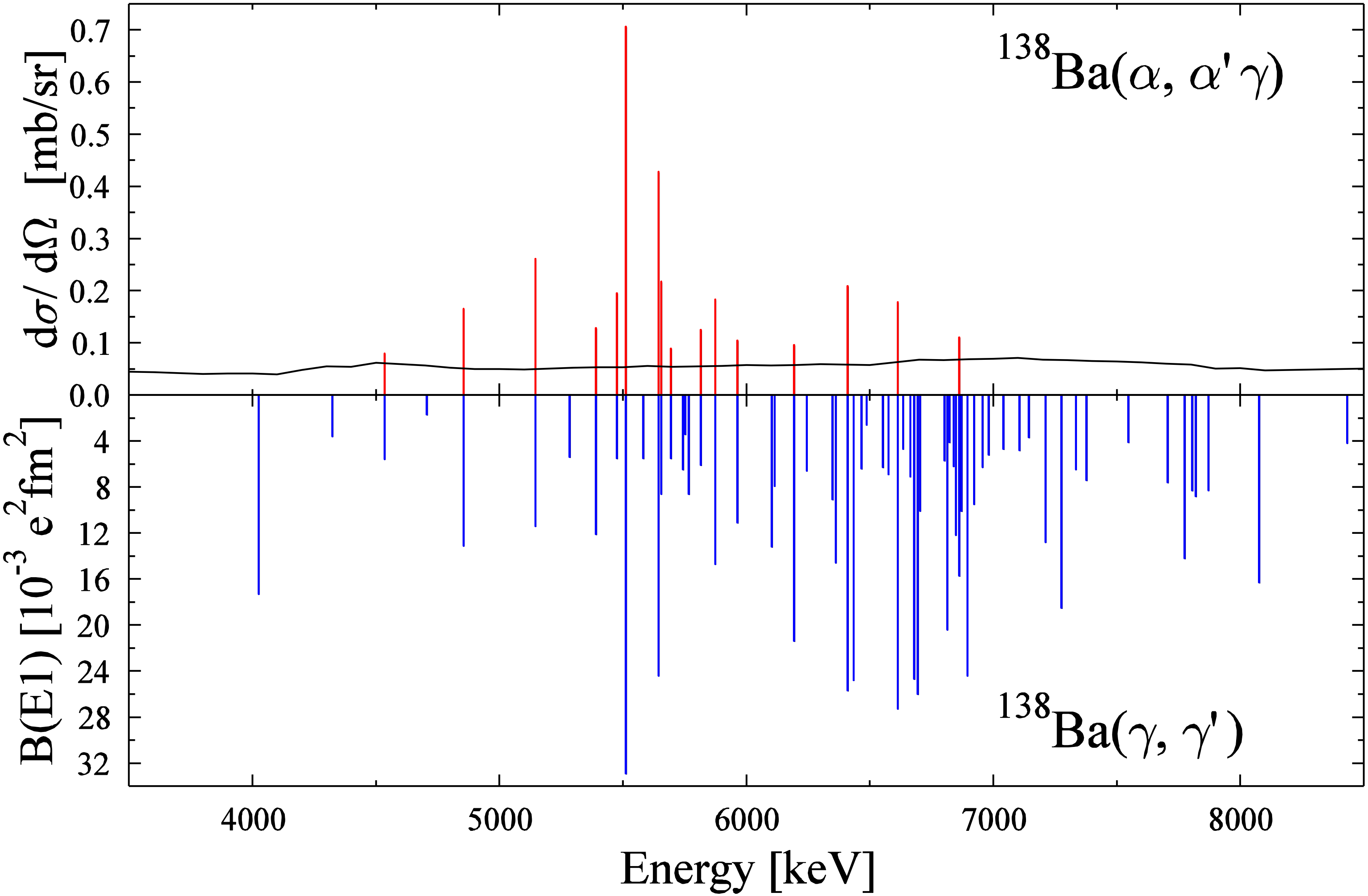

E1 strength distribution in ^{140}Ce, ^{138}Ba, ^{124}Sn, and ^{94}Mo

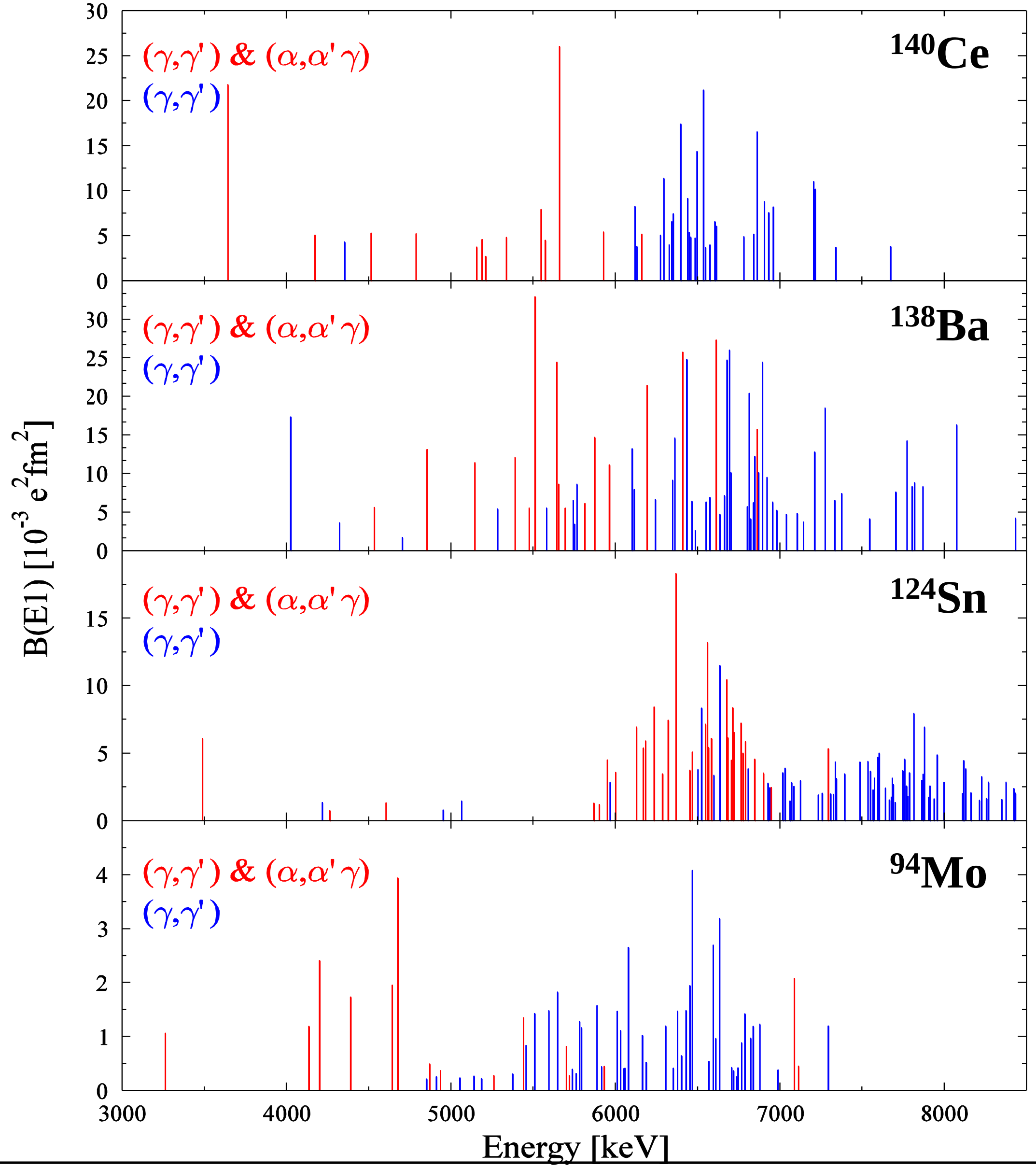

Systematics

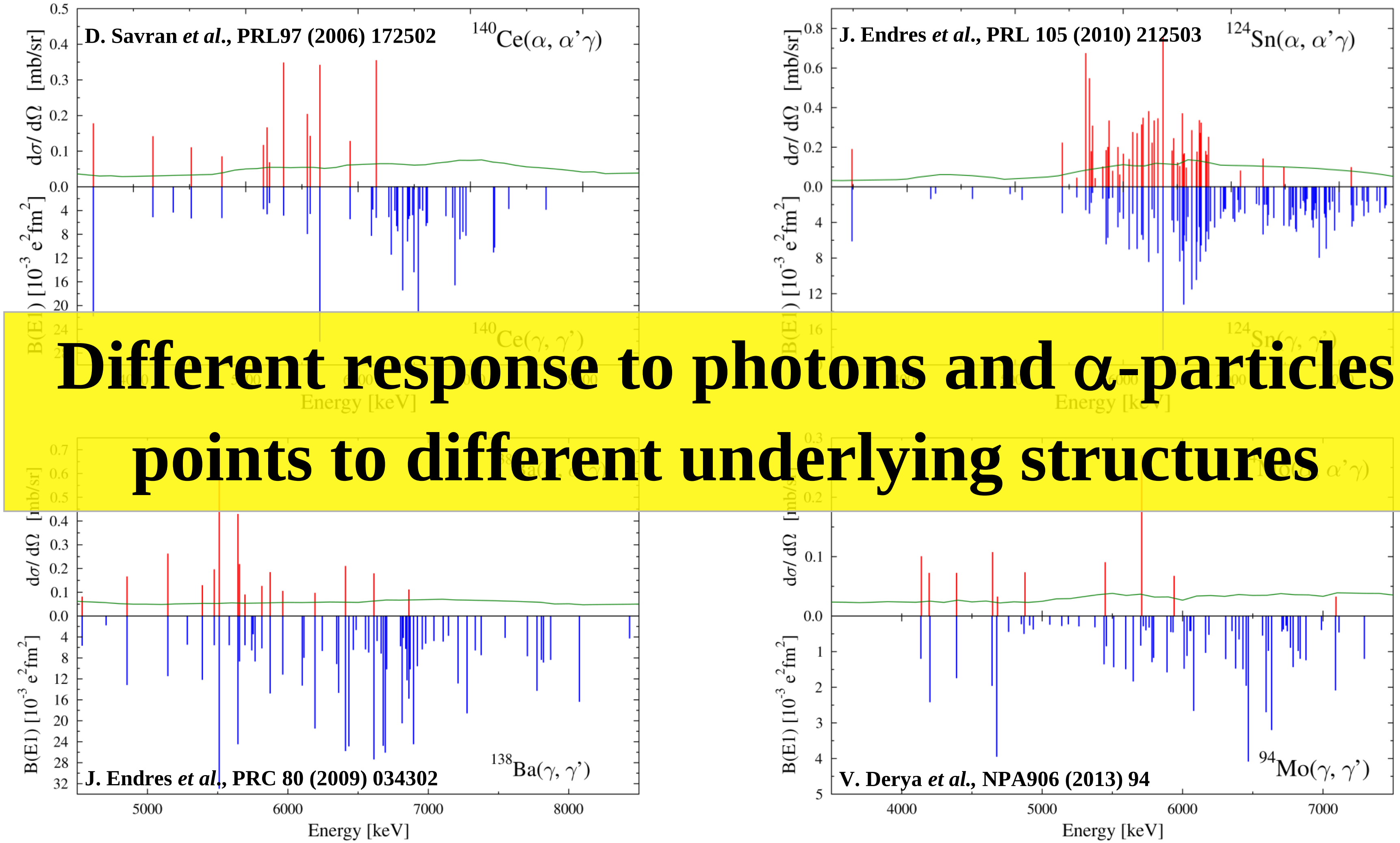

Different response to photons and α-particles points to different underlying structures

Identification of PDR structure in (α,α′γ)

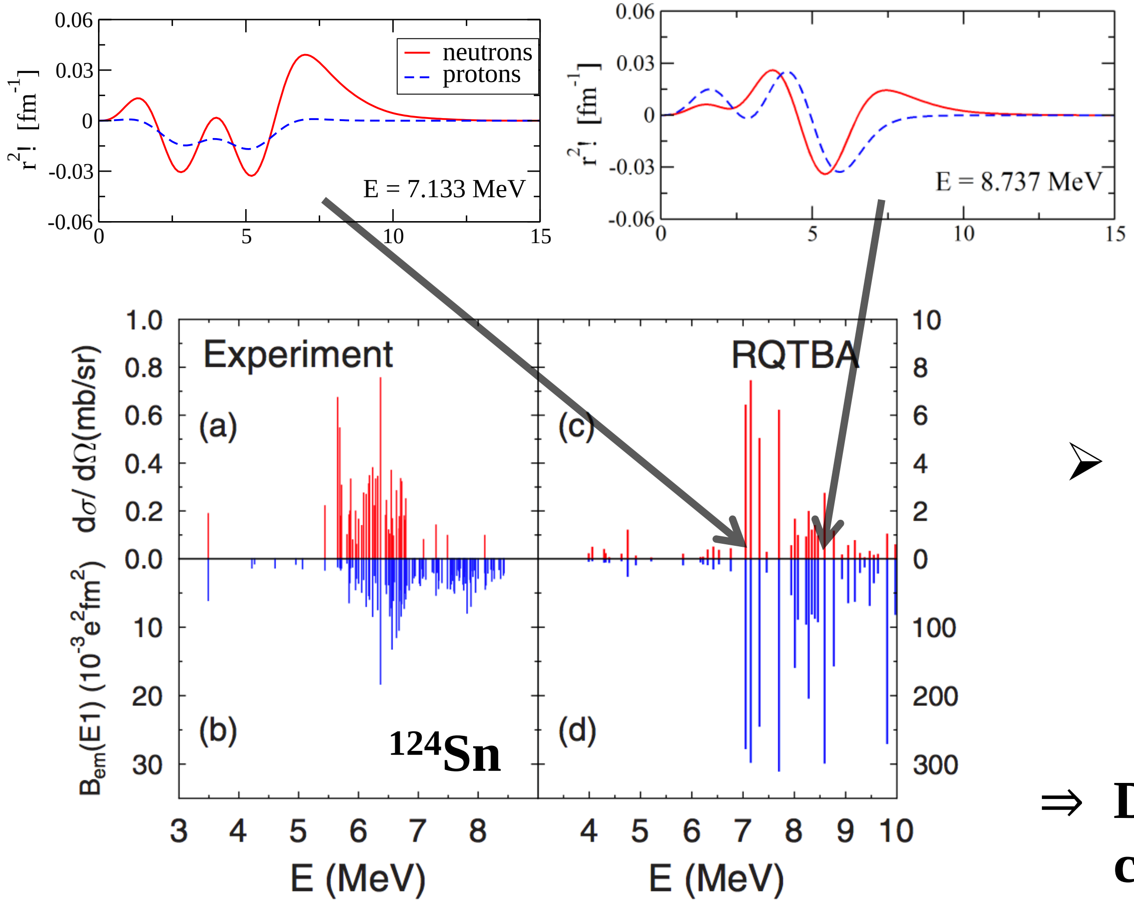

- **Good reproduction of experimental results using RQTBA transition densities + semi-classical reaction model**

⇒ **Different response to complementary probes allows identification of PDR structure**

J. Endres *et al.*, PRL 105 (2010) 212503
E. Lanza *et al.*, PRC 89 (2014) 041601(R)

The grey histogram corresponds to the total unresolved strength.

Top panel: Discrete level in α scattering

Centre panel: Discrete levels in ^{17}O scattering

Bottom panel: photon scattering

L. Pellegri *et al.*, Phys. Lett. B738 (2014) 519

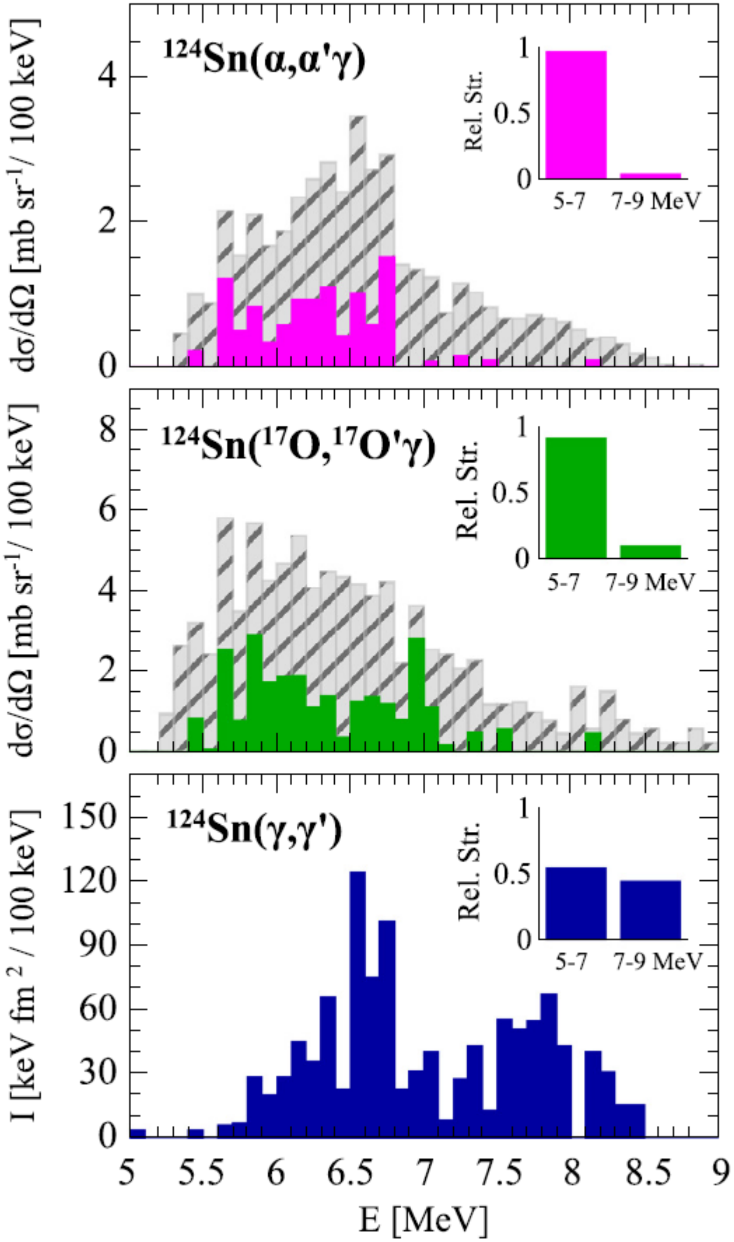

Future Prospects

Outlook

Radioactive ion beams will be available at energies where it will be possible to study excitation of ISGMR and ISGDR

RIKEN, FAIR, SPIRAL2, NSCL, EURISOL

Determine ISGMR and ISGDR in unstable Sn nuclei.

A = 106 to 134 possible

⇒ A more precise determination of K_τ

Nuclear structure studies with reactions in inverse kinematics

- **Possible at GSI/FAIR, RIKEN, GANIL**
  (beam energies of 50-100 MeV/u are needed!)

Approach
measure the recoiling alphas

(α,α′)

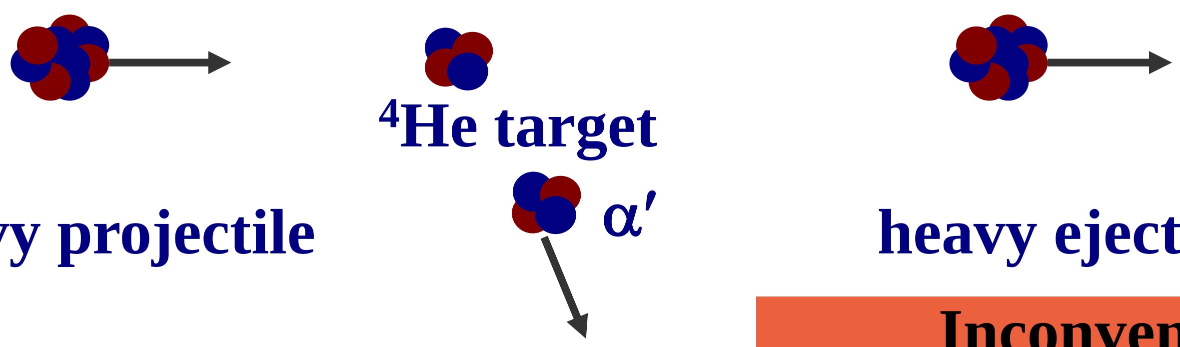

Inconvenience:
difficulty to detect the low-energy alphas

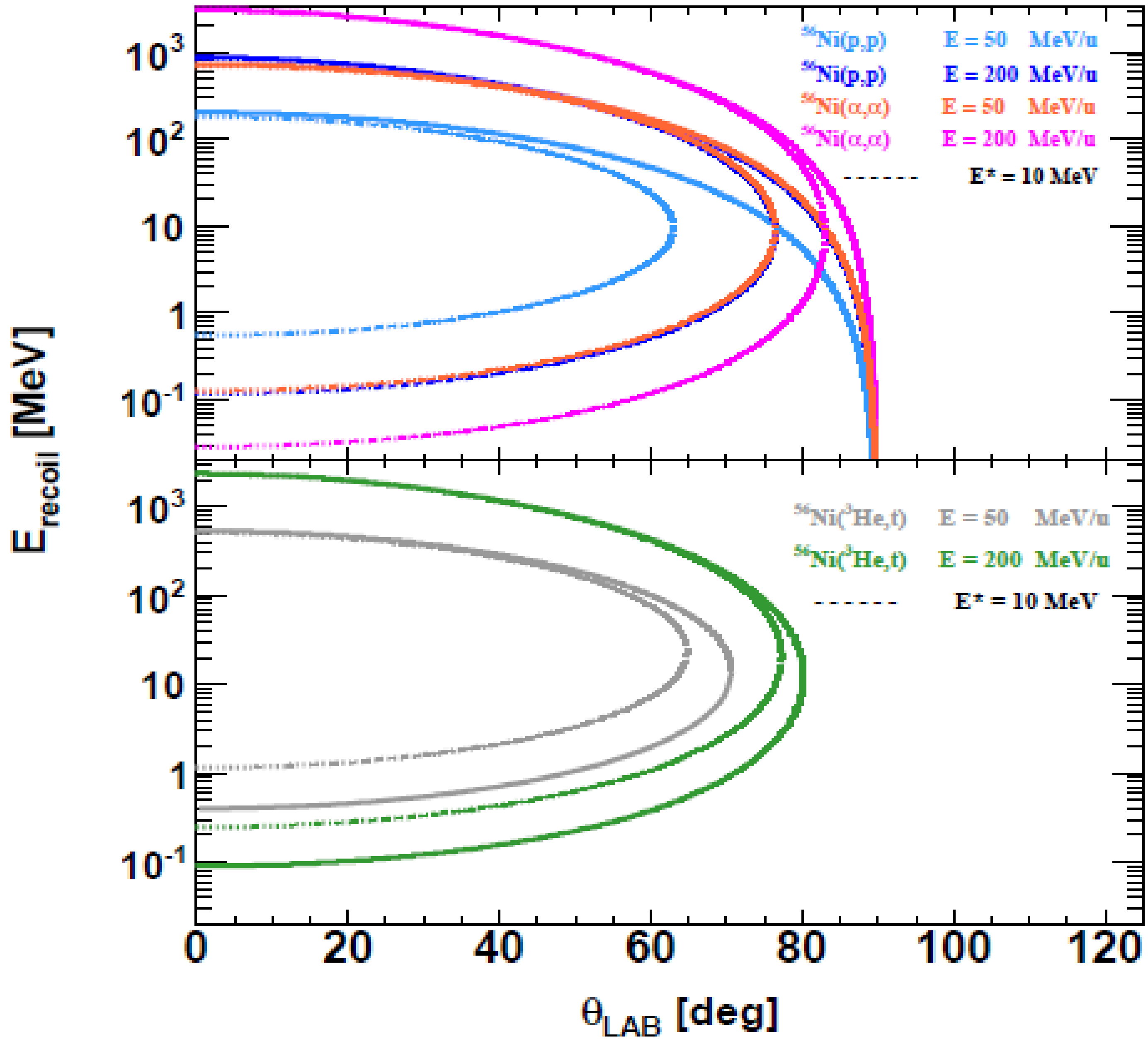

56Ni(p,p) E = 50 MeV/u
56Ni(p,p) E = 200 MeV/u
56Ni(α,α) E = 50 MeV/u
56Ni(α,α) E = 200 MeV/u
E* = 10 MeV
56Ni(3He,t) E = 50 MeV/u
56Ni(3He,t) E = 200 MeV/u
E* = 10 MeV
E_recoil [MeV]
θ_LAB [deg]

Nuclear structure studies with reactions in inverse kinematics
Challenges with exotic beams

- **Inverse kinematics**

^{56}Ni(α,α′)^{56}Ni*
α = Target
^{56}Ni = Projectile
at 50 MeV/u

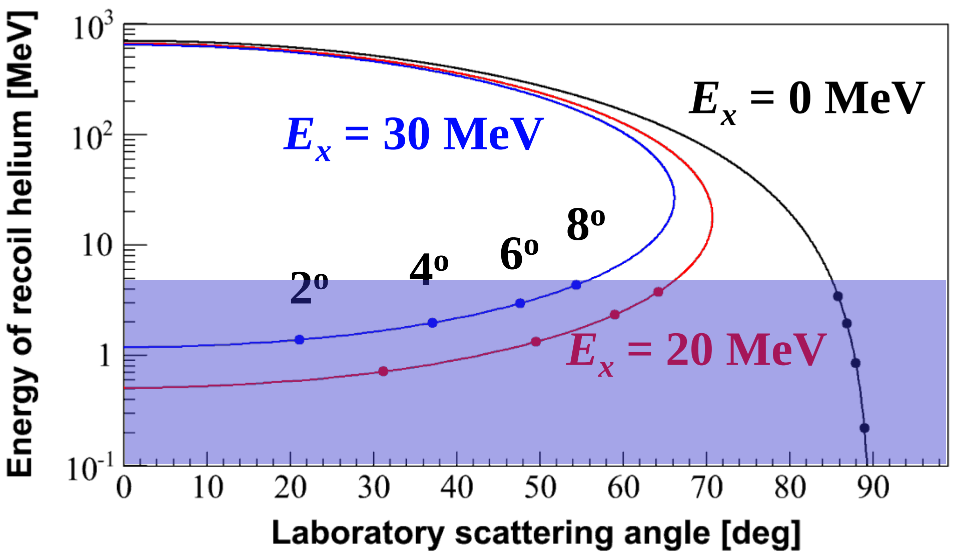

- **Intensity of exotic beams is very low (~10^4 – 10^5 pps)**
- **To get reasonable yields thick target is needed**
- **Very low energy (~ sub MeV) recoil particle will not come out of the thick target**

Active target

A gas detector where the target gas also acts as a detector

- **Good angular coverage**
- **Effective target thickness can be increased without much loss of resolution**
- **Detection of very low energy recoil particle is possible**

MAYA active-target detector at GANIL

Schematic view of MAYA active target detector

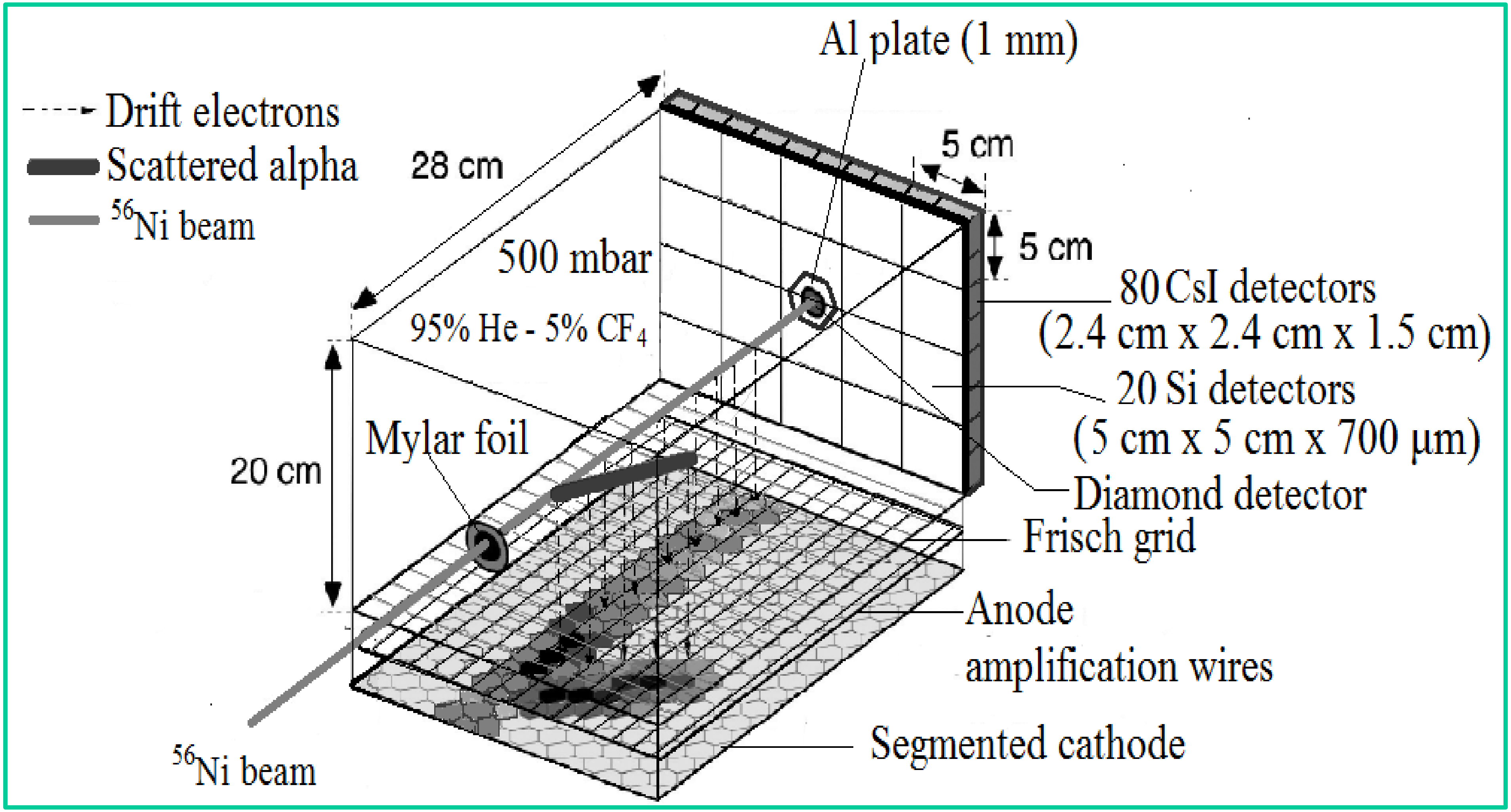

GSI Storage Ring

Experimental Storage Ring

Luminosity:
$10^{26} – 10^{27}$ cm^{-2}s^{-1}

EPJ Web Conf. 66, 03093 (2014)

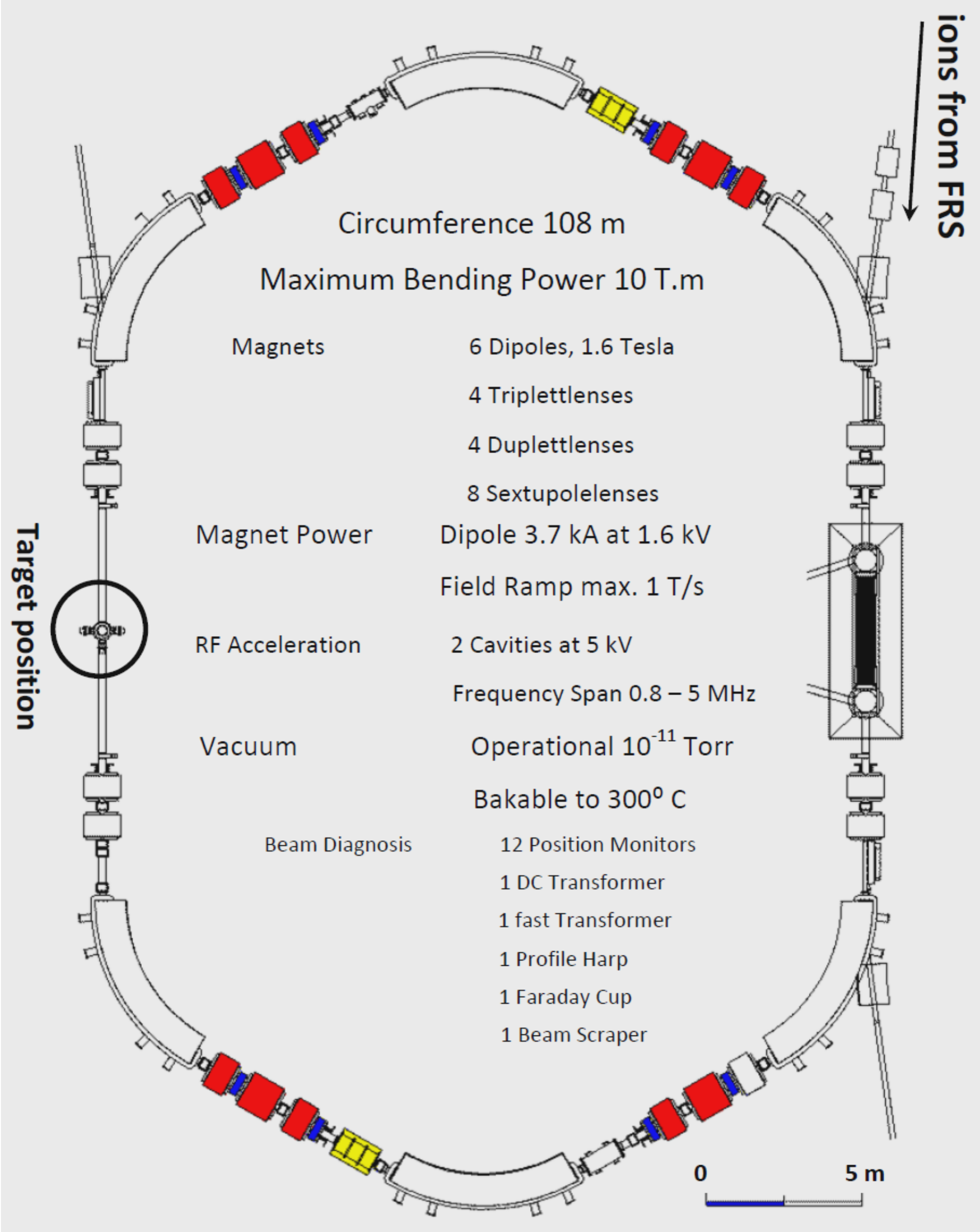

Advantages and disadvantages of storage-ring experiments

Advantages:

Large intensities in the ring

Little energy loss in the target

No target window (no background)

High resolution of the beam (cooling)

Forward focusing for high-energy particles

Low-energy threshold

Disadvantages:

Ultra high vacuum

Very small recoil energies for low q

Thin targets

Detection system @ FAIR

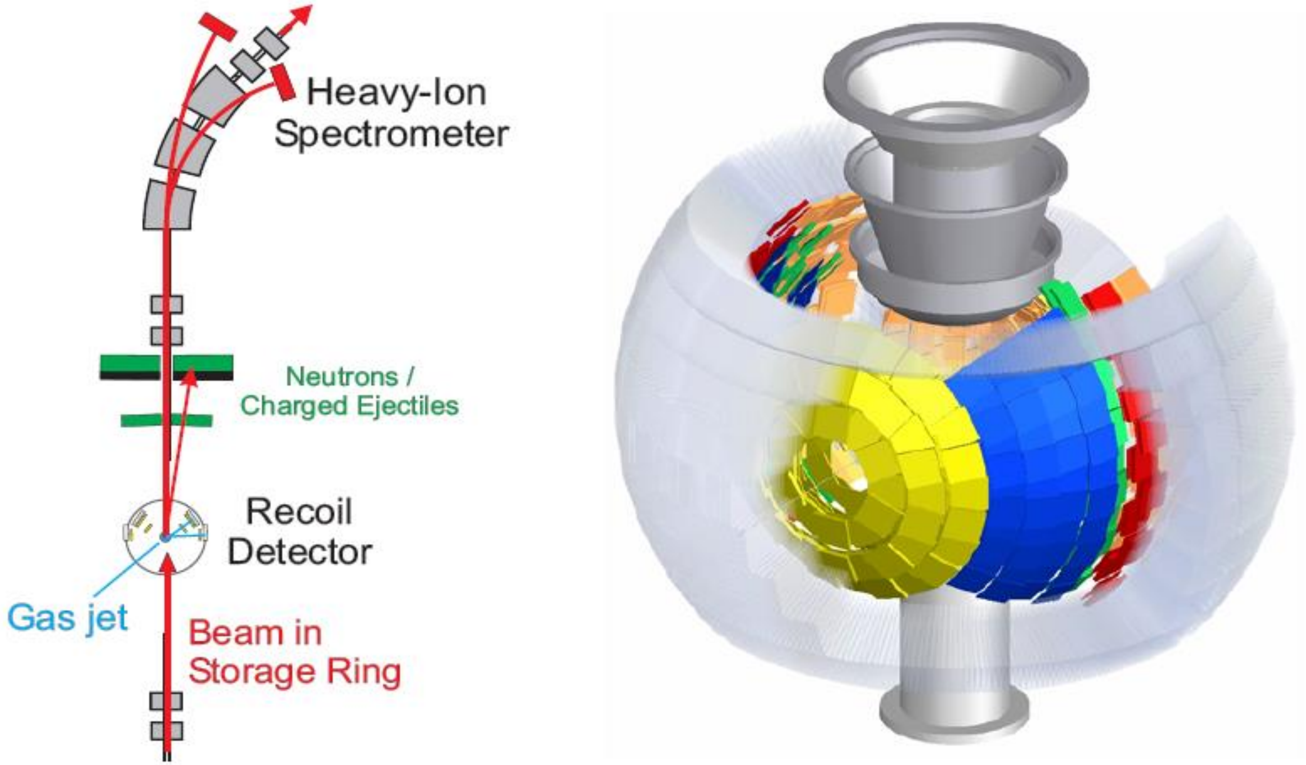

Figure 1: *Schematic view of the EXL detection systems. Left: Set-up built into the NESR storage ring. Right: Target-recoil detector surrounding the gas-jet target.*

Use of EXL recoil detector has been under evaluation

Thank you for your attention